2015

On the Development of Analytical Methodologies to Interrogate the Lipid Dynamics and Phase Transition Resulting from the Reduction of Stimuli-responsive Vesicles

James Edward Winter
Louisiana State University and Agricultural and Mechanical College

ON THE DEVELOPMENT OF ANALYTICAL METHODOLOGIES TO INTERROGATE THE LIPID DYNAMICS AND PHASE TRANSITION RESULTING FROM THE REDUCTION OF STIMULI-RESPONSIVE VESICLES

A Dissertation

Submitted to the Graduate Faculty of the
Louisiana State University and
Agricultural and Mechanical College
in partial fulfillment of the
requirements for the degree of
Doctor of Philosophy

in

The Department of Chemistry

by
James Edward Winter
B.S., The University of Georgia, 2010
A.S., Dalton State College, 2008
December 2015

This dissertation is dedicated to my parents:

My Mom, Connie Winter

My Dad, Larry Winter

Thank you for your enduring love, support, and encouragement

ACKNOWLEDGMENTS

One of my favorite hobbies is backpacking deep in the wilderness. Often, mid-way through a long venture, when the mental and physical challenges are at their greatest, when it is cold, raining, and there is a centimeter of standing water in my hiking boots, I stop and ask myself why I voluntarily do this in my spare time. While the sense of self-preservation is motivating enough to keep trudging on, nature's spectacle always offers reminder as to why. Hands down the best part of a long hike is its conclusion. This jubilation does not come from leaving the wilderness and returning to civilization; it stems from a sense of conquering achievement – the adversity overcome, the mountains climbed, and the distance traveled. It is a great feeling! As I reflect over the last 5 years of my doctorial experience, as much is the same; it too is a great feeling of accomplishment.

I first want to especially thank Professor McCarley for opening his lab to me and being an excellent mentor over the years. When it came to selecting a research group, I wanted to make the most out of my time in graduate school and select a challenging research topic that I had very little knowledge about. I remember first meeting with Professor McCarley and being intimidated about the on-going research in his lab. Not having a firm background in organic chemistry or biology, this liposome project was what I was looking for, and it did not disappoint.

I also want to thank Dr. Weldeghiorghis and Dr. Treleaven for their guidance, education, and expertise in the NMR facility at LSU. Dr. Treleaven aided in configuring the experimental setup for the ^{31}P NMR liposomal phase studies in my research. He was also a mentor early on in my graduate years and had a positive impact on my scientific development. Moreover, the time spent working in the NMR faculty with both

Dr. Weldeghiorghis and Dr. Treleaven afforded numerous opportunities where I was able to gain instrumental and experimental experience with these instruments. For this, I am most grateful.

A special thanks to my fellow McCarley group members both past and present. This has been an amazing group of people to work with on a daily basis. Whenever there was a problem or an issue that needed attention, there was never any blaming nor was there a shortage of volunteers. I am also most appreciative of the organic chemists in the McCarley group for answering the countless synthetic chemistry questions and aiding me along the way.

To the my post-docs both past and present – Dr. Martin Loew, Dr. Quinn Best, and Dr. Eli Mitran, thank you for training and instilling in me the proper analytical and organic lab techniques.

To my colleagues in the Department of Chemistry at LSU – thank you for all that you do to make this department function on a daily basis.

To my committee members – Dr. Gilman, Dr. Murray, and Dean's representative Dr. Benton, thank you for taking your time to participate in both my general exam and thesis defense.

And to my family – thank you for your unwavering love and support.

TABLE OF CONTENTS

LIST OF TABLES

LIST OF FIGURES

LIST OF SCHEMES

LIST OF ABBREVIATIONS AND SYMBOLS

ANTS	8-Aminonapthalene-1,3,6-trisulfonic acid
B	NMR magnetic field
χ^2	Second-order susceptibility (SHG)
χ^3	Third-order susceptibility (SHG)
CSA	Chemical shift anisotropy
DCC	Dicyclohexylcarbodiimide
DDS	Drug delivery system
DLS	Dynamic light scattering
DOPC	1,2-Dioleoyl-*sn*-glycero-3-phosphatidylcholine
DOPG	1,2-Dioleoyl-*sn*-glycero-3-phosphatidylglycerol
DOPE	1,2-Dioleoyl-*sn*-glycero-3-phosphatidylethanolamine
DPA	Dipicolinic acid, pyridine-2,6-dicarboxylic acid
DPX	*p*-xylene-bis-pyridinium bromide
DSC	Differential scanning calorimetry
EDTA	Ethylenediaminetetraacetic acid
$FADH_2$	1,5-Dihydro-flavin adenine dinucleotide
GUV	Giant unilamellar vesicle
HEPES	*N*-2-hydroxyethylpiperazine-*N'*-2-ethanesulfonate
H_{II}	Inverted micelle hexagonal phase
hNQO1	Human NAD(P)H:quinone oxioreductase isozyme 1
HQ_{PA}	1,2,4-trimethylhydroquinone propionic acid
IMI	Intermembrane intermediate
I_{SHG}	Intensity of SHG signal

L_α	Lamellar liquid–crystal phase
L_β	Lamellar gel phase
LUV	Large unilamellar vesicle
MG	Malachite green
MLV	Multi-lamellar vesicle
MMP	Matrix metalloproteases
MPS	Mononuclear phagocyte system
NBS	*N*-Bromosuccinimide
NHS	*N*-Hydroxysuccinimide
NQO1	NAD(P)H:quinone oxidoreductase type 1
PA	Phosphatidic acid
PBS	Phosphate buffered saline
PC	Phosphatidylcholine
PDI	Polydispersion index
PE	Phosphatidylethanolamine
PEG	Poly–ethylene glycol
PG	Phosphatidylglycerol
POPE	1-Palmitoyl-2-dioleoyl-*sn*-glycero-3-phosphatidylcholine
POPE	1-Palmitoyl-2-dioleoyl-*sn*-glycero-3-phosphatidylethanolamine
PS	Phosphatidylserine
R_o	Radius of curvature
$\sigma_{11},\sigma_{22},\sigma_{33}$	^{31}P chemical shift tensors
$\Delta\sigma$	^{31}P NMR chemical shift linewidth
SHG	Second harmonic generation

SUV	Small unilamellar vesicle
t_{50}	Time required for 50% release of the encapsulated contents
TEA	Trimethylamine
TES	2-[2-hydroxy-1,1-bis(hydroxymethyl)ethyl)amino]ethanesulfonic acid
T_H	Lamellar-liquid crystal to inverted hexagonal phase transition temperature
THF	Tetrahydrofuran
T_M	Lamellar-gel to lamellar-liquid transition temperature
Q_{II}	Inverted cubic phase
Q_{PA}	1,2,4-trimethyl-quinone propionic acid
Q_{PA}-DOPE	1,2,4-trimethyl-quinone propionic acid–functionalized DOPE lipid
Q_{Br}-DOPE	1-Bromo-2,4-dimethyl-quinone propionic acid–functionalized DOPE lipid

ABSTRACT

The potential is great for liposome drug delivery systems that provide specific contents release at diseased tissue sites upon activation by upregulated enzymes; however, this potential will only come to fruition with mechanistic knowledge of the contents release process. NAD(P)H:quinone oxidoreductase type 1 (NQO1) is a target for reductively-responsive liposomes, as it is an enzyme upregulated in numerous cancer tissues and is capable of reducing quinone propionic acid (Q_{PA}) trigger groups to hydroquinones that self-cleave from dioleolylphosphatidylethanolamine (DOPE) liposome surfaces, thereby initiating contents release. This research targets the development of analytical methodologies to observe and characterize the dynamics and resulting phase change of the Q_{PA}-DOPE liposomal system. It is known that after reduction, Q_{PA}-DOPE vesicles aggregate and that the aggregation is correlated with release of their encapsulated contents. While postulated, the final phase identity of this system has not been identified as the conventional methods used to make this measurement are not capable of studying such a unique and dynamic system. Presented herein are the analytical methods, both developed and adapted, which have been used to investigate a liposomal system capable of redox stimulated contents release. The purpose of this work was to utilize these tools to (1) study the terminal phase identity of Q_{PA}-DOPE vesicles after reduction, (2) manipulate the Q_{PA}-DOPE liposomal system for triggerable inter-vesical fusion, and (3) investigate the liposome bilayer behavior post-reduction and pre-release. The findings of this work are presented and their significance discussed.

CHAPTER 1
INTRODUCTION

1.1 Research Goals and Aims

The goal of the research presented herein is a set of analytical methods capable of observing and characterizing the lipid dynamics and phase behavior of quinone propionic acid (Q_{PA}) functionalized 1,2-dioleolyl-*sn*-glycero-3-phosphatidylethanolamine (DOPE) lipid vesicles. The McCarley group has previously demonstrated lab that Q_{PA}-DOPE spontaneously forms liposomes when dispersed in water, and they are capable of encapsulating cargo inside their aqueous space.[1] Upon reduction and cleavage of the Q_{PA} head group from DOPE, the entrapped contents are released into the surrounding environment. Beyond this, our knowledge of the lipid moiety's properties, specifically its polymorphic phase behavior during this process, was shrouded by the then-existing limitations of analytical methods to measure with the potential non-traditional lipids, such as Q_{PA}-DOPE. To overcome this challenge and probe behavior before, during, and after reduction, new analytical methods had to be developed or those traditional ones needed to be adapted.

The therapeutic efficiency of conventional disease and cancer treatments is limited by the ability of the drug delivery method to specifically target the afflicted site without harming healthy tissues. Two primary objectives to improve cancer treatment therapies are: (1) increase the bioavailability of the anti-tumor agent at the tumor site, and (2) minimize the damage to healthy non-tumor cells. Liposomal drug delivery systems (DDS) have a demonstrated ability to bio-accumulate at tumor sites and passively deliver their encapsulated drugs at 7–10x higher concentrations relative to healthy tissue at non-tumor sites.[2] A new class of "stealth" liposomes developed in the

mid-1990s has improved intravenous circulation times, thereby allowing such needed concentrations. This 2nd generation of liposomes relies on surface modification of the bilayer, which hinders the body's immune response. However, this modification results in a decrease in the bioavailability of the encapsulated therapy agents inside the liposomes by hindering their diffusion through the bilayer.[3] An ideal liposomal DDS would provide site–specific drug delivery to a targeted tumor site and have long circulation times in the body. Such a system should not rely on passive leakage of its contents, but rather, active release of its entire payload at the targeted site upon being triggered to do so. To accomplish this, a new 3rd–generation of liposomal DDSs, which utilizes an endogenous chemical stimulus unique to cancer cells capable of triggering contents release, is needed.

An area gaining interest in the field of 3rd–generation liposomes is that of liposomal DDSs engineered to respond to enzymes upregulated in cancer cells.[4-6] The McCarley group has been investigating human NAD(P)H:quinone oxioreductase isozyme 1 (hNQO1) as an endogenous stimulus in cancer cells for novel therapy options. hNQO1 is upregulated in many solid tumors and is capable of catalyzing the $2e^-/2H^+$ reduction of a quinone to a hydroquinone.[7-10] The quinone–based responsive systems developed at LSU are based on a "trimethyl–locked" quinone bound as a protecting group to an amine.[11] Ong et al. in the McCarley group first reported a quinone trigger group bound to the amine group of DOPE (Q_{PA}-DOPE).[1] Upon reduction and cleavage of the quinone–capped head group from DOPE, the liposome releases its encapsulated contents into the surrounding medium (Scheme 1.1). From the results presented in this dissertation work, it is now definitively known that Q_{PA}-DOPE liposomes undergo a triggered phase change from a lamellar liquid–crystal (L_α) to an

inverted micelle hexagonal phase (H_{II}), which is the driving process for aggregation and contact–mediated release of the encapsulated contents after reduction. The chemically unique properties and behavior of Q_{PA}-DOPE liposomes (e.g., a redox–triggered change in surface charge, chemical structure, and polymorphic phase behavior, and tuned control over contents release) suggests this lipid system is a possible 3rd–generation liposomal DDS candidate.

Scheme 1.1. Q_{PA}-DOPE lipids spontaneously form liposomes having a lamellar liquid crystal phase (L_α) when dispersed in excess water and are capable of encapsulating materials in the entrapped volume (green). Upon introduction of a reducing agent capable of a $2e^-/2H^+$ reduction, the quinone-capped head groups on the outer leaflet (red) are reduced to a hydroquinone (blue). Formation of a lactone soon follows, which results in cleavage from the DOPE lipids in the outer leaflet (black). After a period of deformation of the bilayer, opposing bilayers aggregate and initiate a contact–mediated $L_\alpha \rightarrow H_{II}$ phase transition that results in the release of the encapsulated contents into the interstitial space surrounding the liposomes.

The second aim of this work is to manipulate the behavior of a Q_{PA}-DOPE containing liposomal system, using the knowledge gained from its behavior during and after reduction. Biological cells contain more than one type of lipid. Studying multi-component bilayers is an effective way to probe the nature of lipids and their role in a membrane. Understanding the role of a lipid in the $L_\alpha \rightarrow H_{II}$ process can give insight

into the biological fusion process of two opposed cells. Moreover, greater insight into how lipids behave and interact in multi–component bilayers can improve how scientists design liposomal DDSs. Reported in this work are lipid mixtures containing Q_{PA}-DOPE with increasing amounts of 1-palmitoyl-2-oleoyl-*sn*-glycero-3-phosphatidylethanolamine (POPE). The bicomponent bilayers are capable of releasing their encapsulated contents in dramatically less time than Q_{PA}-DOPE liposomes alone. Moreover, this lipid system is not dependent on lipid concentration and exhibits fusogenic properties.

The goal of this project is to improve the function of the Q_{PA}-DOPE system using the criteria outlined above. Investigating the unique water-lipid interface properties, bilayer packing effects, and polymorphic phase behavior of this lipid will provide novel insight into the dynamics of the phase change process brought about by a chemical modification of the surface. Furthering our understanding of the Q_{PA}-DOPE system and 3rd–generation liposomes alike are necessary to advance liposomal applications in this field. To this end, the overall goal of this work is to develop a robust strategy and exhaustive toolbox of analytical methods to probe the dynamic properties of Q_{PA}-DOPE in order to fully utilize its potential.

1.2 The Nature of Lipids

1.2.1 Defining Aqueous Phospholipid Dispersions

A lipid is an amphiphilic molecule consisting of (1) a polar head group bound to a (2) glycerol backbone that binds (3) the non-polar region consisting of one or more hydrocarbon chains (Figure 1.1). The physical properties of any lipid are dictated by the identity of the head group, as well as the length and degree of saturation of its acyl chain(s). Alec Bangham is credited with discovering that phospholipids form liposomes when dispersed in aqueous media.[12,13] Bangham had initially called these structures

"multi-lamellar smectic mesophases" or informally "banghasomes."[14] It wasn't until 1968 that the term "liposomes" was formally used to describe the spherical bilayers that Bangham had discovered.[15]

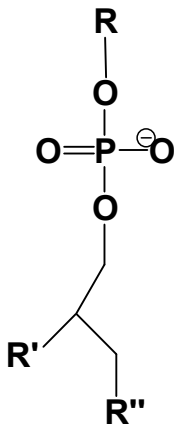

R = $(CH_2)_2NH^{3+}$ Phosphatidylethanolamine (PE)

R = $(CH_2)_2N^+(CH_3)_3$ Phosphatidylcholine (PC)

R = $C_2H_4(NH^{3+})COO^-$ Phosphatidylserine (PS)

R = $CH_2CH(NH^{3+})(OH)_2$ Phosphatidylglycerol (PG)

R = H Phosphatidic Acid (PA)

Figure 1.1. The structure of a phospholipid consists of 3 regions: a polar head group (R), a glycerol backbone, and non-polar hydrocarbon chains (R' and R''). The properties and phase behavior of a phospholipid are determined by its class (eg., PE, PC, PS, PG, PA) and the identity of the hydrocarbon chains denoted n:m where n is the chain length and m is the number of double bonds (degree of unsaturation).

In excess hydration, phospholipids will form an ordered structure of one of three basic phases: a lamellar gel (L_β), lamellar liquid–crystal (L_α), or inverted micelle hexagonal tubes (H_{II}), Figure 1.2.[16] Other phases, such as, inverted cubic (Q_{II}) and rhombic (R_h), are commonly referred to as intermembrane intermediates (IMIs), because these phases are short-lived intermediates of either liposome fusion or the $L_\alpha \rightarrow H_{II}$ phase transition.[17-24] Liposomes are further characterized by their size and lamellarity. A liposome can have one or more bilayers, termed as "unilamellar" or "multi-lamellar" vesicles, respectively.[25] The size of a unilamellar liposome is also denoted by referring to it as small (SUV, d < 100 nm), large (LUV, d = 100–1000 nm), giant (GUV, d > 1000 nm), Figure 1.3.[26]

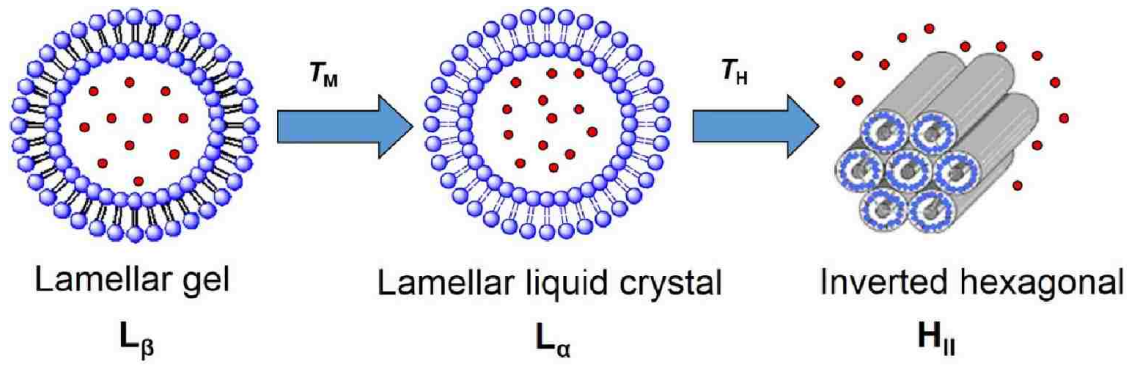

Figure 1.2. When hydrated in excess water, phospholipids spontaneously form one of three basic phases: lamellar gel (L_β), characterized by a rigid bilayer; lamellar liquid crystal (L_α), characterized by a fluid bilayer; or inverted hexagonal (H_{II}) characterized as inverted micelle tubes in an hexagonal packing arrangement. The free energy of these phases is a function of temperature. The temperature where a lipid undergoes a $L_\beta \rightarrow L_\alpha$ phase transition is denoted as T_M, while T_H is denoted as a $L_\alpha \rightarrow H_{II}$ phase transition.

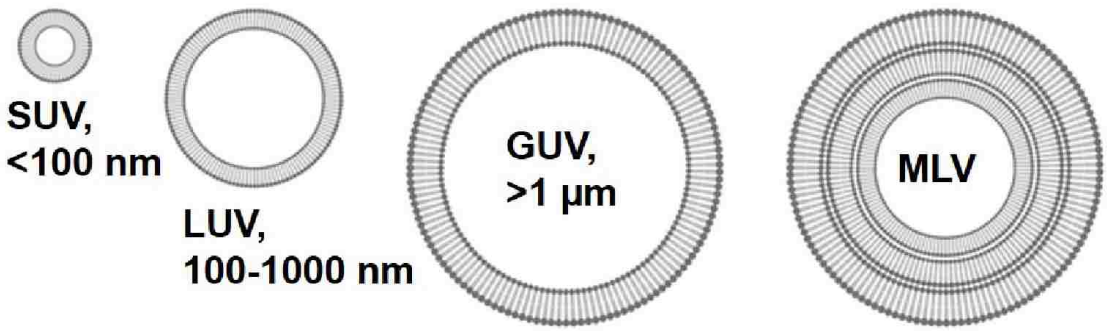

Figure 1.3. There are four subsets of a lamellar phase: small unilamellar vesicles (SUVs, d < 100 nm), large unilamellar vesicles (LUVs, d = 100–1000 nm), giant unilamellar vesicles (GUVs, d > 1000 nm), and multi-lamellar vesicles (MLVs). MLVs have a large dynamic range of diameters but can range from 100s of nm to 10s of μm in size.

1.2.2 Factors Determining Phase Behavior

Three properties dictate the free energy of a lipid's phase: (1) chain length and saturation, (2) head group identity, and (3) its environment.[27-29] Longer acyl chains and chains having increased degrees of unsaturation favor the H_{II} phase as they increase the area of the non-polar region.[28-30] A lower degree of saturation in a lipid's acyl chain(s) decreases hydrogen bonding between adjacent chains, lowers their packing

order, and favors the L_α phase.[28, 29, 31-34] The head group of a lipid also affects the phase of lipid, based on the charge and hydration of its non-polar region. Adjacent anionic lipids undergo charge repulsion and require a larger radius of curvature relative to zwitterionic lipids.[27,34-36] A lipid having a well hydrated head group will have a larger head group area and favor an L_α phase.[27,37] The environment also plays a role in manipulating a lipid's phase behavior. For some lipids, altering the temperature may be used to transition between L_β and L_α, denoted by T_M and from L_α to H_{II}, denoted by T_H (Figure 1.3). Applying heat to a lipid increases the energy in the acyl chain bonds.[38,39] This results in an increased chain motion, less hydrogen bonding between adjacent acyl chains, and a larger volume of the overall non-polar region.

The factors mentioned above have a combinatory effect on the phase of a lipid. To explain these effects, a comparison is made between PC and PE lipids. PC lipids contain three methyl groups bound to the amine of the polar head group, and it typically favors a lamellar phase (Figure 1.2). Their headgroups are much larger than PE lipids which in turn have three hydrogens bound to the amine.[40] The geometrical arrangement of a lipid favors either "cylindrical" or "conical" packing arrangement, resulting in a lamellar or hexagonal phase (Figure 1.4).[40,41] This packing parameter (*P*) is the head-to-tail volume ratio and is mathematically modeled as the total volume of the lipid (*v*) divided by the product of the area of the polar region (*a*) and the length of the non-polar region (*l*).[40] The lipid favors the cylinder packing arrangement of a bilayer when the head-to-tail ratio is even ($P = 1$) and the cone packing arrangement of an inverted hexagonal phase when the head group is smaller than its non-polar region ($P > 1$).

Equation 1.1 $$P = \frac{v}{al}$$

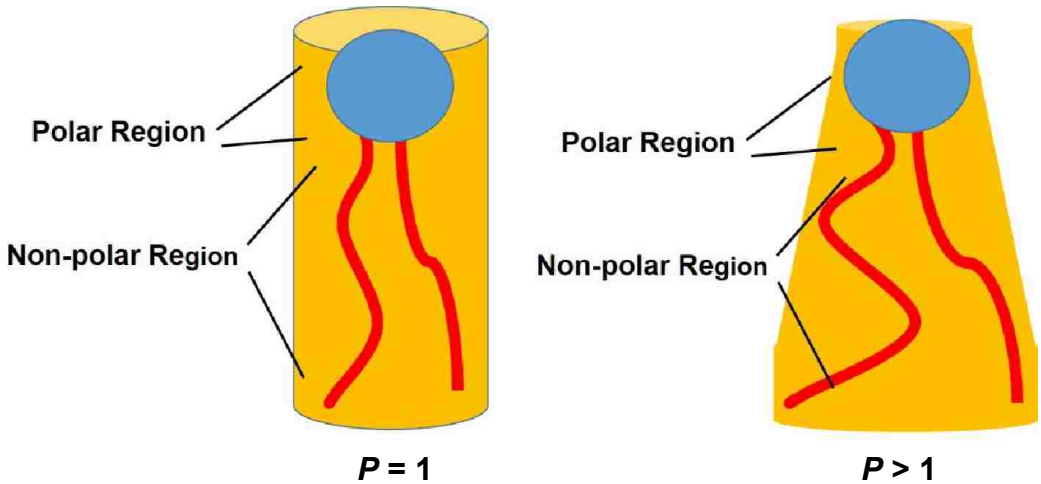

Figure 1.4. The head-to-tail ratio (*P*) of a lipid is a property of lipid packing parameter. When *P* = 1, the lipid favors the cylindrical geometry of a lamellar bilayer. When *P* > 1, the lipid favors the conical geometry of an inverted hexagonal phase.

Because PC lipids have a bulky head group and are more hydrated, which intrinsically increases the area of the non-polar region, the geometry of PC lipids is more resilient to changes to PC aqueous environment.[27] PE lipids, on the other hand, are more susceptible to changes to their environment (e.g., temperature, pH, ions) and exhibit a wider array of polymorphic phase behavior.[38,39,42,43] For example, elevating the temperature increases the energy in the acyl chain. This weakens the hydrogen bonding between adjacent chains and increases their area of motion, ultimately resulting in a larger non-polar region volume (*P* > 1). Dehydration at the water-lipid interface by lowering pH or ionic interactions, decreases the area of the polar region (*P* > 1).[27,37] Lipids intrinsically having bulky head groups (e.g., PG, PS, and PC) or functionalized headgroups (e.g., *N*-acyl-PE and Q_{PA}-DOPE) have larger polar areas (*P* = 1).[1,44] For an $L_{\alpha} \rightarrow H_{II}$ phase transition, the area of the head group decreases, and the packing parameter (*P*) increases.[34,36]

1.2.3 Curvature of Apposed Bilayers

The free energy of two opposing lipid bilayers is dependent on the contributions of three forces: repulsive hydration force, electrostatic charge-charge repulsion, and a

van der Waals attractive force.[45-47] The balance between the attractive and repulsive forces is responsible for stable lamellar structures.[46] The repulsive force of two opposed bilayers arises from the electrostatics of the charged-polar head groups and hydration of all polar groups, which requires a work potential for water removal.[45]

A bilayer can be modeled as an electrostatic double layer.[48,49] Strong electrostatic forces generated by the polar head groups can prevent membrane contact.[46,50] Boström et al. found that SCN^- is more attracted to a bilayer than Cl^-, and when SCN^- is bound to the bilayer, the surface has larger net charge, resulting in an increase in the bilayer's repulsive force.[51] An ion near a bilayer surface can shield the charge of the membrane's surface, effectively decreasing the slipping plane of the vesicle.[52, 53] Afzal et al. measured the dependence of monovalent salts on these forces for a neutral lipid surface and observed that an increased concentration of a monovalent salt resulted in a decrease in both the net repulsive hydration force and van der Waals attractive force.[54]

LeNeveu has done an extensive amount of work in measuring the repulsive hydration force in bilayers.[45,46] He found that the force vs distance curve of two opposed bilayers varies with the hydration force.[46] When a larger number of water molecules are bound to a lipid, the thickness of a lipid bilayer increases, which causes repulsion of opposed bilayers.[45] Lafrance et al. investigated the hydration effect of various *N*-acyl functionalized PE lipids and found that more water molecules were bound to the polar headgroup with stretching the acyl chains.[55] The repulsive hydration force extends 2–3 nm from the surface and increases exponentially closer to the surface.[56]

An attractive van der Waals force comes from interaction of the bilayers between two opposed vesicles.[46] PE lipids are more sensitive to van der Waals interactions than

PC lipids, because PE lipid bilayers form both intra– and intermolecular hydrogen bonds.[57] When this force becomes the dominant force, opposing bilayers come into contact causing transitions into the inverted hexagonal phase.[58]

As a bilayer membrane begins to destabilize into the inverted hexagonal phase, the radius of curvature (*R*) decreases, and its membrane curvature increases (Figure 1.6).[59] Rand et al. investigated the bilayer effects with various ratios of DOPC:DOPE lipid and found that at higher DOPC/DOPE ratios, the radius of curvature increased.[60] The cause of the change in *R* was due to increased hydration of the DOPE bilayer with DOPC. The bilayer membrane curvature effects associated with dehydration arise from compression of the polar region and expansion of the non-polar region, which has a flattening effect (Figure 1.5).[61] This creates a large flat surface so that opposed bilayers can approach each other and gain enough attractive force to come into contact.[58, 62] It is from these contact sites that the inverted hexagonal phase forms.[63]

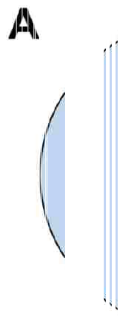

Figure 1.5. (A) The spontaneous radius of curvature for a bilayer membrane is denoted R_o. (B) As the membrane is dehydrated the membrane begins to flatten, which results in a more curved membrane (arcTan (θ) > arcTan (Φ), where θ = Φ, and $R_o > R$. The flattening of the bilayer is due to a decrease in polar area and an increase in non-polar area. Once $R << R_o$, the inverted hexagonal phase is the more favorable phase.

1.3 Liposome Drug Delivery Systems

With 1.6 million new diagnoses and over 580,000 deaths projected in 2015, cancer is the second leading cause of death in the United States.[64] Cancers having a 5–year survival rate below than 50% are: liver (16.6%), ovarian (44.6%), pancreatic (6.7%) and lung and bronchial (16.8%) cancers.[64] These low survival rates are due to late detection and few treatment options; therefore, new cancer therapies that target these deadly types of cancer is an area of need. Conventional chemotherapeutic tumor treatments of cancerous tissues are non-discriminating and come with an unwanted side effect of healthy tissue damage. Liposomes have been shown to minimize this effect, as they exploit abnormalities in both the vascular structure and inefficient lymphatic drainage of solid tumors.[65,66] Tumors have hyperpermeable vasculatures that allows the passive diffusion of ~70–500 nm particles into the interstitial area.[67-71] Additionally, solid tumors suffer from poor lymphatic drainage, causing bio-accumulation of such sized particles at the tumor site.[72-76] This phenomenon is known as the enhanced permeability and retention (EPR) effect and has been shown to elevate drug concentrations 7–10x higher relative to healthy tissue (Figure 1.6).[2]

As early as the 1970s, unmodified phospholipid liposomes were being used as drug carriers to tumor sites.[77-83] This was the 1st–generation of liposomal DDSs. These liposomes relied solely on the EPR effect for bioaccumulation at the tumor site and released their contents by passive diffusion. By the mid-1970s, researchers had learned that modification of the bilayer and complexing the drug with macromolecules decreased the diffusion of the entrapped contents, but also led to more of the carried drugs reaching the tumor site.[84,85] It was not until much later that researchers discovered that lipoproteins recognized unmodified phospholipid bilayers as foreign

bodies and removed the liposomes from circulation, while modified bilayers have longer circulation times.[86,87] Lipoproteins are components of the mononuclear phagocyte system (MPS) also referred to as the reticuloendothelial system.[88] The proteins bind to the surface of phospholipid vesicles, and the complex is recognized by the MPS, where it is then taken to the liver and lymph nodes for removal. The circulation time of the 1st–generation liposomal DDS before recognition and removal by the MPS is less than 6 hours.[89, 90] While this immune response has been harnessed as an effective treatment method for parasitic and bacterial infections of the MPS, it renders the liposomes ineffective in delivering their cargo beyond MPS recognition.[91-93]

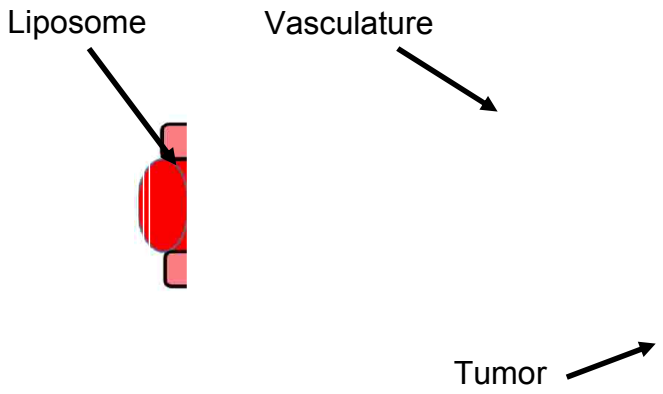

Figure 1.6. The enhanced permeability and retention (EPR) effect is phenomena where ~70–500 nm particles (blue) enter into tumor sites (grey) via leaky vasculatures and bio-accumulate due to poor lymphatic drainage of the tumor's interstitial fluid.

Allen et al. reported the first surface modification of liposomes with gangliosides and sphingomyelin to improve circulation times by hindering recognition from the macrophages.[94] Their discovery brought about the idea of including of poly–ethylene glycol, PEG) in the bilayer, which resulted in a prolonged blood circulation time (>48 hours).[95-98] Modification of the lipid to have a hydrophilic polymer, such as PEG attached to its head group, shields the bilayer surface from protein binding.[99]

These 2nd–generation liposomes are commonly referred to as “stealth” liposomes, because they circulate in the blood and go unrecognized by the MPS.[100] PEGylated or other surface–coated liposomes have a decreased rate of drug diffusion from inside the liposome; however, in most cases this drawback is outweighed by longer circulation times.[3] Several reviews have been written on surface modifications of liposomes to inhibit MPS recognition and applications of “stealth” liposomes.[101-103]

The number of liposomal DDS peer reviewed publications has increased exponentially since the discovery of “stealth” liposomes, Figure 1.7. Since 1990, the United States Patent and Trade Office has issued over 75 patents for liposome applications and formulations: 23+ for liposomal DDS, 18+ for cancer therapy, and 12+ classified as “stealth” liposomes.[104] A list of current liposomal DDS currently on the market or at various stages of clinical development are shown in Table 1.1. In 2012, the liposomal DDS market accounted for 22.5 billion USD in global sales, 9.3 billion USD in the United States alone. This market is project to grow to 43.3 billion USD on global sales by 2017 (14% CAGR).[105] It is expected that 49% of all injectable nano-DDS will be lipid based formulations by 2021. Currently, the United States accounts for 41% of liposomal DDS intellectual property with Taiwan (19%), South Korea (14%), and China (10%) being the closest competitors.[105, 106]

While liposomes offer a more site-specific delivery of chemotherapeutic agents to the tumor sites, the passive release mechanism of liposomal DDS make it difficult to determine the quantity of the drug that remains encapsulated and the amount released into the tumor site.[129,130] Additionally, high concentrations of liposomes yield unwanted side effects (e.g., skin reactions, asthenia, hand-foot syndrome, nausea, and neutropenia) limiting dosage amounts.[131-134] Liposomal DDS currently marketed for

cancer therapy depend on passive diffusion or carrier degradation for contents release.[135] In order to increase the bioavailability of the anti-tumor agents being delivered and lower the concentration of liposomes, there is a need for a 3rd–generation of liposomes capable of releasing their payload from the triggering of an endogenous stimulus present at the tumor site.

Table 1.1 Listed are the liposomal drug delivery formulations currently on the market or at various phases of development. In the adjacent column of the liposomal system's name is its corresponding treatment application.

Compound	Name	Status	Indication
Cytarabine Liposomal[103, 109]	DepoCyt	Market	Lymphomatous meningitis
Liposomal daunorubicin[103, 110, 111]	DaunoXome	Market	Kaposi's sarcoma
PEG- asparaginase[112]	Oncaspar	Market	Acute lymphoblastic leukemia
PEG-immunoliposome-doxorubicin[113]	MCC-465	Phase I	Various cancers, particularly stomach cancer
PEG-interferon-α-2a[114]	PEGASYS	Market	Hepatitis C
PEG-human growth factor antagonist[115]	Somavert	Market	Acromegaly
PEG-anti-TNF-α[116]	CDP 870	Phase III	Crohn's disease; rheumatoid arthritis
PG-TXL or polyglutamate paclitaxel[103, 117]	Xyotax	Phase III	Non-small lung cancer
Stealth liposomal doxorubicin[118-120]	Doxil/Caelyx	Market	Kaposi's sarcoma; refractory ovarian cancer, refractory breast cancer
Amphotericin B complex[103]	Abelcet	Market	Aspergillosis; invasive fungal infections
Liposomal all-trans-retinoic acid[103]	ATRA-IV	Phase II	T cell non-Hodgkin's lymphoma
Liposomal doxorubicin[103, 121]	Myocet	Market (Europe)	Metastatic breast cancer combination with cyclophosphamide
Liposomal cisplatin[103]	SPI-077	Phase III	Various cancers
Liposomal prostaglandin E-1[122]	Liprostin	Phase II	Peripheral artery disease and erectile dysfunction
Liposomal paclitaxel[103, 123]	LEP ETU	Phase I/II	Advanced solid tumors
Liposomal irinotecan[103]	LE-SN38	Phase I/II	Advanced solid tumors

Table 1.1 Continued

Compound	Name	Status	Indication
Liposomal vincristine[103, 124]	Onco-TCS	Market	Relapsed non-Hodgkin's lymphoma
Liposomal lurtotecan[103]	OSI-211	Phase II	Recurrent ovarian cancer; recurrent small cell-lung cancer
Liposomal oxaliplatin[103]	Aroplatin	Phase II	Advanced colorectal cancer
Liposomal irinotecan HCL/floxuridine[125]	CPX-1	Phase III	Advanced colorectal cancer
Mitoxantrone liposomal[126]	2010LO4017	Phase I	Lymphoma and solid tumors
HMPA-linked doxorubicin[127]	HPMA-PK1	Phase II (UK)	Advanced breast, colon and non-small cell lung cancer
HPMA-linked doxorubicin - galactosamine[128]	HPMA-PK2	Phase I/II	Primary and secondary liver cancer
Topotecan Liposomal[103]	Brakiva	Phase I	Ovarian cancer and small cell lung cancer
Vinorelbin Liposomal [103]	Alocrest	Phase I	Breast cancer and lung cancer

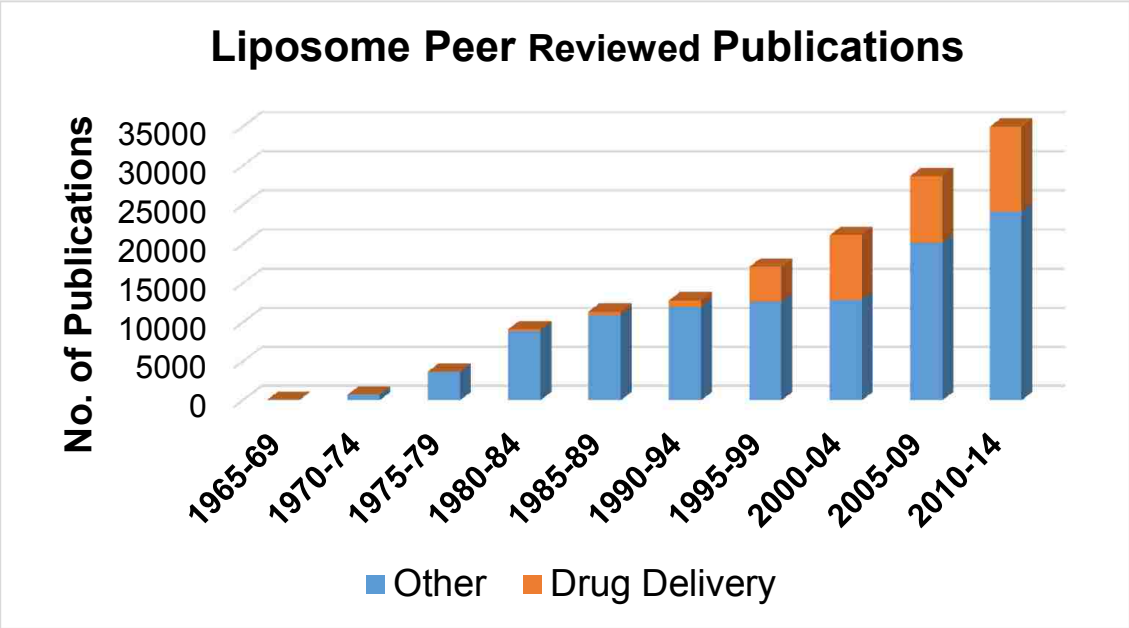

Figure 1.7. The number of peer-reviewed publications involving liposomal-based research has grown exponentially since its genesis in the late 1960s. Applications of the systems reported included drug encapsulation, cosmetics, contrast agents for detection, food additives, coatings, and other miscellaneous applications.[107, 108] The surge in publications relating to liposomal drug delivery systems surged in the mid-1990s due to the emergence of PEGylated "stealth" liposomes.

1.4 Stimuli-responsive Liposomes

There are four key requirements for a successful drug delivery system: "Retain, Evade, Target, and Release."[136] As discussed earlier, liposomal DDSs passively "Target" tumor sites by making use of their leaky vasculatures where they are "Retained" by the EPR effect. Moreover, liposomes can be engineered with PEG to "Evade" the MPS. This section will address how liposomes can be stimulated to "Release" their contents. Drug delivery systems that control or have a triggered function tuned to a specific stimulus are termed "intelligent" and are further defined as "open–circuit" or "closed–circuit" systems.[137-139] Closed–circuit DDSs respond to changes in biological variables (e.g., temperature, pH, enzymes, or any other endogenous species) and are switched from "off" to "on" in its response. Open–circuit DDSs respond to an external stimuli independent of its biological surroundings (e.g., irradiation, heat, electricity, magnetism, and ultrasound).[135,140-142]

1.4.1 Open-circuit Stimuli

Temperature. The simplest method to stimulate the release of contents from a liposome is elevating the temperature above its T_H to induce an $L_\alpha \rightarrow H_{II}$ phase transition.[143-145] Yatvin et al. was the first to suggest using the T_H phase transition of liposomes as a delivery system in 1978.[146] The goal is to have engineered a liposome that has a T_H just above physiological temperature and apply localized heating to that area in the body.[147] Lipid-polymer mixtures with pore forming amphiphiles can be tuned to be thermally sensitive and have been termed "thermally gated liposomes."[148] The liposomes develop pores in the bilayer at or above lipid T_M and are stable below this temperature. Needham et al. reported a highly successful thermal gated liposomal formulation using a DPPC:MPPC:DSPE-PEG-2000 (90:10:4) liposome that released

their contents in vivo at 39–40 °C.[149] A significant drawback using a temperature as a liposomal DDS is placing a patient first in a hyperthermic state during administration of the therapy, and localized heating of the tumor site may be necessary.[150]

Photochemical. Liposomes have been used as carriers of photo-activated pro-drugs but with little success.[151-154] Recent focus in the area of radiation–triggered liposomes has been on photo-sensitive lipids.[155,156] The mode of photo-triggered or light sensitive liposomes can be either photopolymerization or photochemical triggering.[155,157] The principle in photopolymerization is to incorporate a non-polar compound that can be polymerized when in a lipid bilayer. Upon exposure to light, the compounds polymerize into local domains in the bilayer, resulting in extensive leakage.[158] Bonduran et al. incorporated a photoreactive lipid, 1,2-bis[10-(29,49-hexadienoyloxy)de-canoyl]-*sn*-glycero-3-phosphocholine (bis-SorbPC), into a 1,2-dioleoylphosphatidylethanol-3-methoxy-poly(ethyleneoxide)amide, DOPE-PEG-2000, and found that this mixture formed stable liposomes. Under irradiation of UV light, a cross-linked polymer network cause lateral phase separation resulting in trans-membrane pores.[159]

Photochemical triggering uses light to destabilize a bilayer to cause rupturing of the vesicle or its lysis. Thompson et al. have had much success with photo-oxidative liposomes.[160,161] Their strategy is built on lipids having a plasmalogen vinyl ether–linked hydrocarbon chain. In the presence of light, the vinyl ether bond is broken, thereby generating a hydrocarbon chain and a lysolipid, which induces $L_\alpha \rightarrow H_{II}$ phase change.[162] In photo-deprotected systems, a lipid that does not favor a L_α phase is functionalized with a photo-cleavable head group to form liposomes. Upon exposure to UV light, the head group cleaves, which induces an $L_\alpha \rightarrow H_{II}$ phase change.[163,164] Despite these

achievements, these systems are limited by the depth light penetrates the body. Radiation of light having a wavelength below < 700 nm is limited to a penetration depth << 1.0 cm.[165,166] For liposomal DDS, adequate radiation only reaches a depth of 0.05 mm.[167]

pH. Tumors tend to have a pH lower than normal tissue.[168-174] The most success in pH–triggered liposomal DDSs to date utilize PEGylated liposomes that have pH–sensitive linkers which degrade under acidic conditions. These linkers include: double esters,[175] vinyl esters,[176,177] cleavable lipopolymers,[178] and hydrazones.[179] In principle, stable "stealth" liposomes will bioaccumulate at tumor sites where the acid-labile bonds connecting PEG to the lipid degrade, facilitating destabilization of the bilayer and contents release.[100,180,181] The limiting factor in developing pH sensitive liposomal DDS is their sensitivity to changes in pH is low, wherein the in situ pH which can vary from 0.2 to 0.8 units based on the tumor and location.[182]

1.4.2 Closed-circuit Stimuli

Enzymes. Utilizing enzyme expression unique to tumor sites to activate anti-cancer prodrugs is an explosive area of research.[183] The principle with enzymatic triggering is to introduce an inactive molecule into the body and have the inactive molecule reach a targeted site where the enzyme chemically activates the molecule into its anti-cancer form. This same principle has been used to enzymatically trigger the release of liposomal contents.[135,184,185] While alkaline phosphatase and phospholipase C have been studied, the most success with enzymatically triggered liposomal DDS has been achieved using phospholipase A2, matrix metalloproteases (MMPs), and elastase.[135,183,184,186-189]

Phospholipase A2 is a lipolytic enzyme that specifically hydrolyzes the 2-acyl position of glycerolphospholipids, forming fatty acids and lysolipids that induce a micellar or inverted hexagonal phase.[6,190] This enzyme is overexpressed in stomach, breast, prostate, pancreas, colon, lung, liver, esophageal, and uterus cancerous tissue.[191-195] It has been found that this enzyme is more successful at stimulating anionic charged liposomes (PS) as opposed to neutral (PC & PE).[196]

Matrix metalloproteases (MMPs) have been used for prodrug activation, as they are overexpressed in brain, breast, cervical, colon, stomach, lung, skin, and ovarian cancers.[197] Using MMP enzymes for liposomal DDS activation requires a specialized lipopeptide to be included in the bilayer to serve as substrates for MMP activation.[198,199] This has been demonstrated with PEGylated liposomes.[200,201] Once bound to the membrane substrate, the MMP hydrolyzes the peptide-lipid bond, thereby inducing an $L_{\alpha} \rightarrow H_{II}$ phase change.[202]

Elastase has also been targeted for liposomal DDS triggering. It is upregulated in cancerous breast and skin tissue, as well as other types of diseased tissues.[203-210] Similar to proteases, a peptide must be anchored onto the bilayer surface to act as a substrate for elastase to bind. Different anchors have been used to bind the peptide but success has been achieved using an *N*-acyl bound peptide to DOPE to induce a lamellar to inverted hexagonal phase change, which results in liposomal contents release.[211]

Other Liposomal DDS Stimuli. There has been recent success in using ultrasound–sensitive liposomes to control liposomal contents release.[212] The mechanism relies on encapsulating air or gas inside the vesicle and using ultrasound to release the contents.[213] Liposomal DDS with encapsulated doxorubicin–containing

microbubbles have been successfully released using this method.[214] Another stimulus method being used is that based on sequential triggers. Sawant et al. bound antibody 2G4 to PEG–modified bilayers. The PEG prevented antibody recognition and internalization by the targeted cells; however, when the pH was lowered between 5.0–6.0 the PEG groups were removed by acidic hydrolysis of hydrozone bound PEG-hz-PE.[215]

The McCarley group is interested in a reduction–activated liposomal DDS. A 100–1000x redox potential difference exists between the intra- and extra-cellular space.[216] Most redox-sensitive DDS are for various gene therapies and rely on endocytosis.[217,218] Saji et al. reported a redox–stimulated surfactant that utilized a ferrocene moiety.[219] This system showed reversible micelle formation and disruption having a one electron oxidation step at +0.428 V vs SCE and a one electron reduction step at +0.440 V vs SCE.[219] Both Fe^{2+} and Ni^{2+} transition metals have been complexed with hydrocarbon tails to make an amphiphile capable of intercalating into a bilayer. These complexes trigger vesical lysis upon reduction and cleavage from their hydrocarbon chains.[220,221]

1.5 NAD(P)H:Quinone Oxidoreductase Type 1

It has been known that certain cancer cells have different enzymatic expression relative to healthy cells. Human NAD(P)H:quinone oxidoreductase isozyme 1 (hNQO1) is one such enzyme. hNQO1 is overexpressed 2–to–50–fold in breast, colon, pancreatic, lung, stomach, kidney, head and neck, and ovarian cancers.[9,183,222-228] hNQO1 is a homodimeric flavin enzyme of the DT-diaphorase class of enzymes and catalyzes the two–electron reduction of quinones to the corresponding hydroquinones.[229,230] The enzyme accepts electrons from either NADH or NADPH and

transfers a hydride to its 1,5-dihydro-flavin adenine dinucleotide ($FADH_2$).[231-233] There are three distinct binding regions in hNQO1: FAD, NAD(P), and a third for either NADH or NAD(P)H.[232] The enzymatic hNQO1–catalyzed reduction follows a ping-pong bi–bi mechanism, where NADH or NAD(P)H binds and donates two electron to hNQO1 and a hydride to FAD, reducing it to $FADH_2$. The NAD or NADP cofactor leaves its binding site with hNQO1 and is replaced by a quinone, which is promptly reduced to a hydroquinone (Scheme 1.2).[234,235]

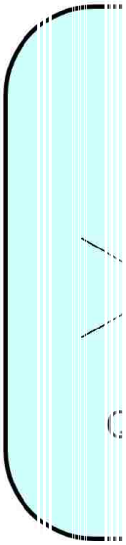

Scheme 1.2. The ping-pong, bi-bi scheme of NQO1 catalysis of a quinone to hydroquinone. The quinone, NADH, and FAD bind to NQO1 at three different sites. 1e- from NADH is used to reduce the quinone to a semi-quinone and a hydride transferred to FAD. A second e^- from NADH completes the reduction process and its hydride is transferred to the NQO1 bound FADH.

Naturally occurring prodrugs have been investigated for DT-diaphorase (NQO1) activation: streptonigrin, mitomycin C, CB 1954, and diaziquone.[183] Streptonigrin is an aminoquinone with anti-tumor activity when activated by DT-diaphorase.[236] While the active drug molecule is not known, the result of the redox activation of streptonigrin is inhibition of DNA and RNA synthesis as well as ATP depletion.[237] Mitomycin C is a natural prodrug activated by DT-diaphorase.[238] Like streptonigrin, mitomycin C disrupts DNA production when activated; however, hNQO1 was less effective when compared

to other DT-diaphorases for mitomycin C activation.[239,240] 5-(Aziridin-1-yl)-2,4-dinitrobenzamide or CB 1954 is activated by DT-diaphorase but is kinetically slow with hNQO1.[241-243] Diaziquone is an antitumor prodrug that increases cytotoxicity and breaks DNA strands upon reduction.[244, 245] Faig et al. studied the hNQO1 activation of three synthetic chemotherapeutic quinone based prodrugs with success: one benzoquinone derivative and two indolequinone derivatives.[246] Other groups have also reported synthetic quinone prodrugs that are triggered by hNQO1.[247,248]

Wang et al. first reported the use of a redox-triggered quinone based protective group for amines.[11] After reduction from a quinone to a hydroquinone, the protecting group lactonizes and is released from the amine (Figure 1.8). $Na_2S_2O_4$ is a mild reducing agent capable of stimulating the quinone reduction process and has a redox potential of -0.66 V vs SHE at pH 7.[249] Silvers et al. showed the ability of hNQO1 to reduce a trimethyl-quinone propionic acid (Q_{PA}) protecting group in the presence of NADH and reported its reduction potential to be -0.28 V vs SHE.[250] Recent work in the McCarley lab has shown the ability of hNQO1 to activate fluorescent quinone based dyes in cell lines with overexpressed levels of hNQO1.[250-252] To date, no other lab has investigated a liposomal DDS capable of enzymatic redox destabilization by hNQO1.

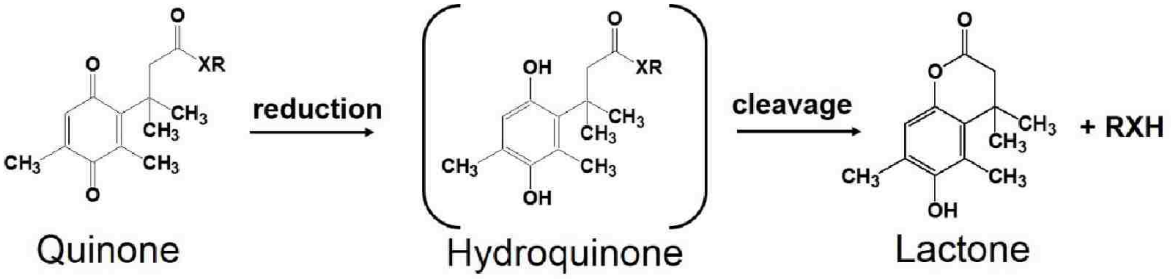

Scheme 1.3. Shown is the scheme of activation for a quinone protected amine reported by Wang et al.[11] The terminal RX group on the carboxylic acid can be either OH, OR', or NR'R'". Reduction and subsequent cyclization frees the protected group bound at "RX" from the quinone.

1.6 Redox-triggered Q_{PA}-DOPE

The McCarley group first reported a 3rd–generation, quinone–based liposomal DDS capable of encapsulating a dye and chemically triggering release of its contents by stimulating a $2e^-$ reduction of the quinone marker.[1] This liposomal system is composed of a trimethyl quinone propionic acid (Q_{PA}) bound to the amine group of 1,2-dioleolyl-sn-glycero-3-phosphatidylethanolamine, DOPE. This system is chemically unique in that no other liposomal DDS is defined by having one component bilayer, a system triggered by a chemical redox stimulus, a change from an anionic to zwitterionic lipid after reduction, and a contact–mediated release between two opposing bilayers, all in the same system.

The McCarley group has investigated the effect of the aqueous environment properties (i.e., salt concentration, ion identity, and pH), as well as bilayer mixtures (DOPE and PEG) on Q_{PA}-DOPE liposomes.[42,43] The $L_\alpha \rightarrow H_{II}$ phase transition of PE lipids typically starts with aggregation of opposed bilayers.[89] To facilitate the close proximity of the bilayers, the lipid-water interface of the outer leaflet of the bilayer must dehydrate to overcome the long range repulsive hydration force.[45,46] Various salts can interact with the surface of the bilayer to destabilize/dehydrate (kosmotropic salt) or support (chaotropic salt) the lipid-water interface. McCarley et al. found the effect of salt identity on Q_{PA}-DOPE to align with the Hofmeister effect where the presence of a more polarizable and less hydrated chaotropic salts resulted in a significantly slower release, 50% contents release (t_{50}) at 44 min vs 34 min for SCN^- and Cl^-, respectively.[42, 253] Additionally, a decrease in overall salt concentration resulted in the longer t_{50} values.

(Kosmotrope) $SO_4^{2-} > Cl^- > NO_3^- > ClO_4^- > SCN^-$ (Chaotropes)

Q_{PA}-DOPE mixtures containing DOPE and PEG have also been investigated at LSU.[43] Q_{PA}-DOPE mixtures containing 3.0% PEG in the bilayer resulted in complete hindrance of redox-triggered contents release. This is due to the well hydrated PEG sterically hindering bilayer contact. Incorporating non-functionalized DOPE into the Q_{PA}-DOPE lipid bilayer resulted in a dramatic decrease in the system's t_{50} value, and deformation was no longer observed with 10% DOPE. Q_{PA}-DOPE also shows dependence on environmental pH. At pH 9.5, DOPE favors the lamellar phase and can be made to form bilayers.[143] Cleavage of the Q_{PA} head group on the outer leaflet of Q_{PA}-DOPE vesicles does not result in a phase change, thus no contents release is observed.[43]

Because of the unique chemical nature of Q_{PA}-DOPE, conventional methods used to study the phase behavior of lipids cannot be employed for this system. While the observed contents release of Q_{PA}-DOPE liposomes after reduction is suspected to cause a triggered $L_\alpha \rightarrow H_{II}$ phase transition, no one has attempted to measure the polymorphic behavior of this dynamic system. It is pivotal that the phase behavior is known to confirm the contents release of this system is active release and not passive diffusion from a stabilized vesicle. Additionally, temporal observation of the phase behavior before and after reduction would yield key insights into the mechanism of this event. Also, harnessing a mechanistic understanding of the L_α to H_{II} phase transition process is key to understanding how biological cells fuse.[254-257]

1.7 References

(1) Ong, W.; Yang, Y.; Cruciano, A. C.; McCarley, R. L., Redox-triggered Contents Release from Liposomes. *Journal of the American Chemical Society* **2008,** *130* (44), 14739-14744.

(2) Greish, K.; Sawa, T.; Fang, J.; Akaike, T.; Maeda, H., SMA–doxorubicin, a New Polymeric Micellar Drug for Effective Targeting to Solid Tumours. *Journal of Controlled Release* **2004,** *97* (2), 219-230.

(3) Gabizon, A. A., Liposome Circulation Time and Tumor Targeting: Implications For Cancer Chemotherapy. *Advanced Drug Delivery Reviews* **1995,** *16* (2–3), 285-294.

(4) Duncan, R.; Gac-Breton, S.; Keane, R.; Musila, R.; Sat, Y. N.; Satchi, R.; Searle, F., Polymer–drug Conjugates, PDEPT and PELT: Basic Principles for Design and Transfer from the Laboratory to Clinic. *Journal of Controlled Release* **2001,** *74* (1–3), 135-146.

(5) Andresen, T. L.; Jensen, S. S.; Thomas Kaasgaard and Kent Jorgensen, Triggered Activation and Release of Liposomal Prodrugs and Drugs in Cancer Tissue by Secretory Phospholipase A2. *Current Drug Delivery* **2005,** *2* (4), 353-362.

(6) Andresen, T. L.; Thompson, D. H.; Kaasgaard, T.; Jørgensen, K., Enzyme-Triggered Nanomedicine: Drug Release Strategies in Cancer Therapy. *Molecular Membrane Biology* **2010,** *27* (7), 353-363.

(7) Siegel, D.; Franklin, W. A.; Ross, D., Immunohistochemical Detection of NAD(P)H:Quinone Oxidoreductase in Human Lung and Lung Tumors. *Clinical Cancer Research* **1998,** *4* (9), 2065-2070.

(8) Buranrat, B.; Chau-in, S.; Prawan, A.; Puapairoj, A.; Zeekpudsa, P.; Kukongviriyapan, V., NQO1 Expression Correlates with Cholangiocarcinoma Prognosis. *Asian Pacific Journal of Cancer Prevention* **2012,** *13* (Suppl), 131-136.

(9) Awadallah, N. S.; Dehn, D.; Shah, R. J.; Russell Nash, S.; Chen, Y. K.; Ross, D.; Bentz, J. S.; Shroyer, K. R., NQO1 Expression in Pancreatic Cancer and its Potential Use as a Biomarker. *Applied Immunohistochemistry & Molecular Morphology* **2008,** *16* (1), 24-31.

(10) Garate, M.; Wani, A. A.; Li, G., The NAD(P)H:Quinone Oxidoreductase 1 Induces Cell Cycle Progression and Proliferation of Melanoma Cells. *Free Radical Biology & Medicine* **2010,** *48* (12), 1601-1609.

(11) Wang, B.; Liu, S.; Borchardt, R. T., Development of a Novel Redox-Sensitive Protecting Group for Amines Which Utilizes a Facilitated Lactonization Reaction. *The Journal of Organic Chemistry* **1995,** *60* (3), 539-543.

(12) Bangham, A. D.; Standish, M. M.; Watkins, J. C., Diffusion of Univalent Ions Across the Lamellae of Swollen Phospholipids. *Journal of Molecular Biology* **1965,** *13* (1), 238-252.

(13) Bangham, A. D.; Horne, R. W., Negative Staining of Phospholipids and Their Structural Modification by Surface-active Agents as Observed in the Electron Microscope. *Journal of Molecular Biology* **1964,** *8* (5), 660-668.

(14) Deamer, D. W., From “Banghasomes” to Liposomes: A Memoir of Alec Bangham, 1921–2010. *The FASEB Journal* **2010,** *24* (5), 1308-1310.

(15) Sessa, G.; Weissmann, G., Phospholipid Spherules (Liposomes) as a Model for Biological Membranes. *Journal of Lipid Research* **1968,** *9* (3), 310-318.

(16) Gruner, S. M., Non-lamellar Lipid Phases. In *The Structure of Biological Membranes; Yeagle, P.L. Ed.;* CRC Press: Boca Raton, Florida, 2005, pp 173-199.

(17) De Kruijff, B.; Van Den Besselaar, A. M. H. P.; Cullis, P. R.; Van Den Bosch, H.; Van Deenen, L. L. M., Evidence for Isotropic Motion of Phospholipids in Liver Microsomal Membranes. A ^{31}P NMR study. *Biochimica et Biophysica Acta* **1978,** *514* (1), 1-8.

(18) Mariani, P.; Luzzati, V.; Delacroix, H., Cubic Phases of Lipid-containing Systems. Structure Analysis and Biological Implications. *Journal of Molecular Biology* **1988,** *204* (1), 165-189.

(19) Gustafsson, J.; Ljusberg-Wahren, H.; Almgren, M.; Larsson, K., Cubic Lipid−Water Phase Dispersed into Submicron Particles. *Langmuir* **1996,** *12* (20), 4611-4613.

(20) Nieva, J. L.; Alonso, A.; Basanez, G.; Goni, F. M.; Gulik, A.; Vargas, R.; Luzzati, V., Topological Properties of Two Cubic Phases of a Phospholipid:cholesterol:diacylglycerol Aqueous System and Their Possible Implications in the Phospholipase C-induced Liposome Fusion. *FEBS Letters* **1995,** *368* (1), 143-147.

(21) Funari, S. S.; Rebbin, V.; Marzorati, L.; di Vitta, C., Membrane Morphology Modifications Induced by Hydroquinones. *Langmuir* **2011,** *27* (13), 8257-8262.

(22) Siegel, D. P., Fourth-Order Curvature Energy Model for the Stability of Bicontinuous Inverted Cubic Phases in Amphiphile−Water Systems. *Langmuir* **2010,** *26* (11), 8673-8683.

(23) Ellens, H.; Siegel, D. P.; Alford, D.; Yeagle, P. L.; Boni, L.; Lis, L. J.; Quinn, P. J.; Bentz, J., Membrane Fusion and Inverted Phases. *Biochemistry* **1989,** *28* (9), 3692-3703.

(24) Yang, L.; Ding, L.; Huang, H. W., New Phases of Phospholipids and Implications to the Membrane Fusion Problem. *Biochemistry* **2003,** *42* (22), 6631-6635.

(25) Frohlich, M.; Brecht, V.; Peschka-Suss, R., Parameters Influencing the Determination of Liposome Lamellarity by ^{31}P-NMR. *Chemistry and Physics of Lipids* **2001,** *109* (1), 103-112.

(26) F. Bordi, C. C., and S. Sennato, Electrical Properties in Planar Lipid Bilayers and Liposomes. In *Advances in Planar Lipid Bilayers and Liposomes*: Lui, A. L., Ed.; Academic Press:New York, 2006; Vol. 4, pp 281-320.

(27) Rand, R. P., and Parsegian, V. A., Hydration, Curvature, and Bending Elasticity of Phospholipid Monolayers. In *Current Topics in Mebranes*, Epand, R. M., Ed.; Academic Press: New York, 1997; Vol. 44, pp 167-189.

(28) Rawicz, W.; Olbrich, K. C.; McIntosh, T.; Needham, D.; Evans, E., Effect of Chain Length and Unsaturation on Elasticity of Lipid Bilayers. *Biophysical Journal* **2000,** *79* (1), 328-339.

(29) Koynova, R.; Caffrey, M., Phases and Phase Transitions of the Phosphatidylcholines. *Biochimica et Biophysica Acta* **1998,** *1376* (1), 91-145.

(30) Lewis, B. A.; Engelman, D. M., Lipid Bilayer Thickness Varies Linearly with Acyl Chain Length in Fluid Phosphatidylcholine Vesicles. *Journal of Molecular Biology* **1983,** *166* (2), 211-217.

(31) Smaby, J. M.; Momsen, M. M.; Brockman, H. L.; Brown, R. E., Phosphatidylcholine Acyl Unsaturation Modulates the Decrease in Interfacial Elasticity Induced by Cholesterol. *Biophysical Journal* **1997,** *73* (3), 1492-1505.

(32) Subczynski, W. K.; Wisniewska, A.; Yin, J. J.; Hyde, J. S.; Kusumi, A., Hydrophobic Barriers of Lipid Bilayer Membranes Formed by Reduction of Water Penetration by Alkyl Chain Unsaturation and Cholesterol. *Biochemistry* **1994,** *33* (24), 7670-7681.

(33) Koenig, B. W.; Strey, H. H.; Gawrisch, K., Membrane Lateral Compressibility Determined by NMR and X-ray Diffraction: Effect of Acyl Chain Polyunsaturation. *Biophysical Journal* **1997,** *73* (4), 1954-1966.

(34) Rand, R. P.; Fuller, N. L.; Gruner, S. M.; Parsegian, V. A., Membrane Curvature, Lipid Segregation, and Structural Transitions for Phospholipids Under Dual-Solvent Stress. *Biochemistry* **1990,** *29* (1), 76-87.

(35) Gruner, S. M., Intrinsic Curvature Hypothesis for Biomembrane Lipid Composition: A Role for Nonbilayer Lipids. *Proceedings of the National Academy of Sciences of the United States of America* **1985,** *82* (11), 3665-3669.

(36) Lagi, M.; Nostro, P. L.; Fratini, E.; Ninham, B. W.; Baglioni, P., Insights into Hofmeister Mechanisms: Anion and Degassing Effects on the Cloud Point of Dioctanoylphosphatidylcholine/Water Systems. *The Journal of Physical Chemistry B* **2007,** *111* (3), 589-597.

(37) Rand, R. P., and Parsegian, V.A., Hydration forces between phospholipid bilayers. *Biochima et Biophysica Acta.* **1989,** *988*, 351-376.

(38) Mouritsen, O. G.; Boothroyd, A.; Harris, R.; Jan, N.; Lookman, T.; MacDonald, L.; Pink, D. A.; Zuckermann, M. J., Computer Simulation of the Main Gel–Fluid Phase Transition of Lipid Bilayers. *The Journal of Chemical Physics* **1983,** *79* (4), 2027-2041.

(39) Lewis, R. N., and McElhaney, R. N., Calorimetric and Spectroscopic Studies of the Thermotropic Phase Behavior of Lipid Bilayer Model Membranes Composed of a Homologous Series of Linear Saturated Phosphatidylserines. *Biophysical Journal* **2000,** *79* (4), 2043-2055.

(40) Wolf, J., and Steponkus, P. L., The Membrane Geometry of the Prolamellar Body. *Protoplasma* **1980,** *102* (3-4), 315-321.

(41) Marsh, D., Intrinsic Curvature in Normal and Inverted Lipid Structures and in Membranes. *Biophysical Journal* **1996,** *70* (5), 2248-2255.

(42) McCarley, R. L.; Forsythe, J. C.; Loew, M.; Mendoza, M. F.; Hollabaugh, N. M.; Winter, J. E., Release Rates of Liposomal Contents are Controlled by Kosmotropes and Chaotropes. *Langmuir* **2013,** *29* (46), 13991-13995.

(43) Loew, M.; Forsythe, J. C.; McCarley, R. L., Lipid Nature and Their Influence on Opening of Redox-Active Liposomes. *Langmuir* **2013,** *29* (22), 6615-6623.

(44) Akoka, S.; Tellier, C.; Leroux, C.; Marion, D., A Phosphorus Magnetic-Resonance Spectroscopy and a Differential Scanning Calorimetry Study of the Physical-Properties of N-Acylphosphatidylethanolamines in Aqueous Dispersions. *Chemistry and Physics of Lipids* **1988,** *46* (1), 43-50.

(45) LeNeveu, D. M.; Rand, R. P.; Parsegian, V. A., Measurement of Forces Between Lecithin Bilayers. *Nature* **1976,** *259* (5544), 601-603.

(46) LeNeveu, D. M.; Rand, R. P., Measurement and Modification of Forces Between Lecithin Bilayers. *Biophysical Journal* **1977,** *18* (2), 209-230.

(47) Marra, J.; Israelachvili, J., Direct Measurements of Forces Between Phosphatidylcholine and Phosphatidylethanolamine Bilayers in Aqueous Electrolyte Solutions. *Biochemistry* **1985,** *24* (17), 4608-4618.

(48) Ninham, B. W.; Yaminsky, V., Ion Binding and Ion Specificity: The Hofmeister Effect and Onsager and Lifshitz Theories. *Langmuir* **1997,** *13* (7), 2097-2108.

(49) McLaughlin, S., The Electrostatic Properties of Membranes. *Annual Review of Biophysics and Biophysical Chemistry* **1989,** *18*, 113-136.

(50) Gingell, D.; Fornes, J. A., Demonstration of Intermolecular Forces in Cell Adhesion Using a New Electrochemical Technique. *Nature* **1975,** *256* (5514), 210-211.

(51) Bostrom, M.; Williams, D. R.; Ninham, B. W., Specific Ion Effects: Why the Properties of Lysozyme in Salt Solutions Follow a Hofmeister Series. *Biophysical Journal* **2003,** *85* (2), 686-694.

(52) McLaughlin, S.; Mulrine, N.; Gresalfi, T.; Vaio, G.; McLaughlin, A., Adsorption of Divalent Cations to Bilayer Membranes Containing Phosphatidylserine. *The Journal of General Physiology* **1981,** *77* (4), 445-473.

(53) Parsons, D. F.; Bostrom, M.; Nostro, P. L.; Ninham, B. W., Hofmeister effects: Interplay of Hydration, Nonelectrostatic Potentials, and Ion Size. *Physical Chemistry Chemical Physics* **2011,** *13* (27), 12352-12367.

(54) Afzal, S.; Tesler, W. J.; Blessing, S. K.; Collins, J. M.; Lis, L. J., Hydration Force between Phosphatidylcholine Surfaces in Aqueous-Electrolyte Solutions. *Journal of Colloid and Interface Science* **1984,** *97* (2), 303-307.

(55) Lafrance, D.; Marion, D.; Pezolet, M., Study of the Structure of *N*-acyldipalmitoylphosphatidylethanolamines in Aqueous Dispersion by Infrared and Raman Spectroscopies. *Biochemistry* **1990,** *29* (19), 4592-4959.

(56) Israelachvili, J. N., Solvation, Entropic, Structural, and Hydration Forces. In *Intermolecular and Surface Forces*, 3rd ed., Israelachvili, J. N., Ed.; Academic Press: Boston, 2011, pp 341-380.

(57) Gurtovenko, A. A.; Vattulainen, I., Effect of NaCl and KCl on Phosphatidylcholine and Phosphatidylethanolamine Lipid Membranes: Insight from Atomic-Scale Simulations for Understanding Salt-Induced Effects in the Plasma Membrane. *The Journal of Physical Chemistry. B* **2008,** *112* (7), 1953-1962.

(58) Israelachvili, J. N., Van der Waals Forces between Particles and Surfaces. In *Intermolecular and Surface Forces*, 3rd ed., Israelachvili, J. N., Ed.; Academic Press: Boston, 2011, pp 253-289.

(59) Jung, H. T.; Coldren, B.; Zasadzinski, J. A.; Iampietro, D. J.; Kaler, E. W., The Origins of Stability of Spontaneous Vesicles. *Proceedings of the National Academy of Sciences of the United States of America* **2001,** *98* (4), 1353-1357.

(60) Rand, R. P.; Fuller, N.; Parsegian, V. A.; Rau, D. C., Variation in Hydration Forces between Neutral Phospholipid Bilayers: Evidence for Hydration Attraction. *Biochemistry* **1988,** *27* (20), 7711-7722.

(61) Kirk, G. L.; Gruner, S. M., Lyotropic Effects of Alkanes and Headgroup Composition on the L_{α}–H_{II} Lipid Liquid Crystal Phase Transition: Hydrocarbon Packing Versus Intrinsic Curvature. *Journal de Physique (France)* **1985,** *46* (5), 761-769.

(62) Israelachvili, J. N., Interactions of Biological Membranes and Structures. In *Intermolecular and Surface Forces* 3rd ed., Israelachvili, J. N., Ed.; Academic Press: Boston, 2011, pp 577-616.

(63) Ellens, H.; Bentz, J.; Szoka, F. C., Fusion of Phosphatidylethanolamine-Containing Liposomes and Mechanism of L_{α}–H_{II} Phase Transition. *Biochemistry* **1986,** *25* (14), 4141-4147.

(64) Cancer.gov. Statistics at a Glance: The Burden of Cancer in the United States. http://www.cancer.gov/about-cancer/what-is-cancer/statistics. (accessed January 2015)

(65) Antonini, A.; Mancini, F.; Canesi, M.; Zangaglia, R.; Isaias, I. U.; Manfredi, L.; Pacchetti, C.; Zibetti, M.; Natuzzi, F.; Lopiano, L.; Nappi, G.; Pezzoli, G., Duodenal Levodopa Infusion Improves Quality of Life in Advanced Parkinson's Disease. *Neuro-Degenerative Diseases* **2008,** *5* (3-4), 244-246.

(66) Greish, K., Enhanced Permeability and Retention (EPR) Effect for Anticancer Nanomedicine Drug Targeting. *Methods in Molecular Biology*, 2010; 24, pp 25-37.

(67) Maeda, H.; Wu, J.; Sawa, T.; Matsumura, Y.; Hori, K., Tumor Vascular Permeability and the EPR Effect in Macromolecular Therapeutics: A Review. *Journal of Controlled Release* **2000,** *65* (1–2), 271-284.

(68) Wu, J.; Akaike, T.; Maeda, H., Modulation of Enhanced Vascular Permeability in Tumors by a Bradykinin Antagonist, a Cyclooxygenase Inhibitor, and a Nitric Oxide Scavenger. *Cancer Research* **1998,** *58* (1), 159-165.

(69) Maeda, H.; Akaike, T.; Wu, J.; Noguchi, Y.; Sakata, Y., Bradykinin and Nitric Oxide in Infectious Disease and Cancer. *Immunopharmacology* **1996,** *33* (1–3), 222-230.

(70) Maeda, H.; Matsumura, Y.; Kato, H., Purification and Identification of [hydroxyprolyl3]bradykinin in Ascitic Fluid from a Patient with Gastric Cancer. *Journal of Biological Chemistry* **1988,** *263* (31), 16051-16054.

(71) Doi, K.; Akaike, T.; Horie, H.; Noguchi, Y.; Fujii, S.; Beppu, T.; Ogawa, M.; Maeda, H., Excessive Production of Nitric Oxide in Rat Solid Tumor and its Implication in Rapid Tumor Growth. *Cancer* **1996,** *77* (8), 1598-1604.

(72) Folkman, J., Tumor Angiogenesis: Therapeutic Implications. *The New England Journal of Medicine* **1971,** *285* (21), 1182-1186.

(73) Skinner, S. A.; Tutton, P. J. M.; O'Brien, P. E., Microvascular Architecture of Experimental Colon Tumors in the Rat. *Cancer Research* **1990,** *50* (8), 2411-2417.

(74) Yuan, F.; Salehi, H. A.; Boucher, Y.; Vasthare, U. S.; Tuma, R. F.; Jain, R. K., Vascular Permeability and Microcirculation of Gliomas and Mammary Carcinomas Transplanted in Rat and Mouse Cranial Windows. *Cancer Research* **1994,** *54* (17), 4564-4568.

(75) Folkman, J., Angiogenesis in Cancer, Vascular, Rheumatoid and Other Disease. *Nature Medicine* **1995,** *1* (1), 27-31.

(76) Hashizume, H.; Baluk, P.; Morikawa, S.; McLean, J. W.; Thurston, G.; Roberge, S.; Jain, R. K.; McDonald, D. M., Openings between Defective Endothelial Cells Explain Tumor Vessel Leakiness. *The American Journal of Pathology* **2000,** *156* (4), 1363-80.

(77) Colley, C. M., and Ryman, B. E., Liposomes as Carriers in vivo for Methotrexate. *Biochemical Society Transactions* **1975**, 3 (1), 157-159.

(78) G Gregoriadis, G., Drug Entrapment in Liposomes: Possibilities for Chemotherapy. *Biochemical Society Transactions* **1974**, 2 (1), 117-119

(79) Gregoriadis, G., Drug entrapment in liposomes. *FEBS letters* **1973,** *36* (3), 292-296.

(80) Gregoriadis, G.; Neerunjun, D. E., Control of the Rate of Hepatic Uptake and Catabolism of Liposome-Entrapped Proteins Injected into Rats. Possible therapeutic applications. *European Journal of Biochemistry* **1974,** *47* (1), 179-185.

(81) Kosloski, M. J.; Rosen, F.; Milholland, R. J.; Papahadjopoulos, D., Effect of Lipid Vesicle (Liposome) Encapsulation of Methotrexate on its Chemotherapeutic Efficacy in Solid Rodent Tumors. *Cancer Research* **1978,** *38* (9), 2848-2853.

(82) Papahadjopoulos, D.; Poste, G.; Vail, W. J.; Biedler, J. L., Use of Lipid Vesicles as Carriers to Introduce Actinomycin D into Resistant Tumor Cells. *Cancer Research* **1976,** *36 (9 part 1)*, 2988-2994.

(83) Poste, G.; Papahadjopoulos, D., Drug-Containing Lipid Vesicles Render Drug-Resistant Cell Sensitive to Actinomycin D. *Nature* **1976,** *261* (5562), 699-701.

(84) Gregoriadis, G.; Davisson, P. J.; Scott, S., Binding of Drugs to Liposome-Entrapped Macromolecules Prevents Diffusion of Drugs from Liposomes in vitro and in vivo. *Biochemical Society Transactions* **1977,** *5* (5), 1323-1326.

(85) Tsujii, K.; Sunamoto, J.; Fendler, J. H., Improved Entrapment of Drugs in Modified Liposomes. *Life Sciences* **1976,** *19* (11), 1743-4179.

(86) Scherphof, G.; Roerdink, F.; Waite, M.; Parks, J., Disintegration of Phosphatidylcholine Liposomes in Plasma as a Result of Interaction with High-Density Lipoproteins. *Biochimica et Biophysica acta* **1978,** *542* (2), 296-307.

(87) Tall, A. R.; Small, D. M., Solubilisation of Phospholipid Membranes by Human Plasma High Density Lipoproteins. *Nature* **1977,** *265* (5590), 163-164.

(88) van Furth, R.; Cohn, Z. A.; Hirsch, J. G.; Humphrey, J. H.; Spector, W. G.; Langevoort, H. L., The Mononuclear Phagocyte System: A New Classification of Macrophages, Monocytes, and Their Precursor Cells. *Bulletin of the World Health Organization* **1972,** *46* (6), 845-852.

(89) Torchilin, V. P., Recent Advances with Liposomes as Pharmaceutical Carriers. *Nature Reviews Drug discovery* **2005,** *4* (2), 145-160.

(90) Scherphof, G. L.; Dijkstra, J.; Spanjer, H. H.; Derksen, J. T.; Roerdink, F. H., Uptake and Intracellular Processing of Targeted and Nontargeted Liposomes by Rat Kupffer Cells in vivo and in vitro. *Annals of the New York Academy of Sciences* **1985,** *446*, 368-384.

(91) Alving, C. R.; Steck, E. A.; Chapman, W. L., Jr.; Waits, V. B.; Hendricks, L. D.; Swartz, G. M., Jr.; Hanson, W. L., Therapy of Leishmaniasis: Superior Efficacies of Liposome-Encapsulated Drugs. *Proceedings of the National Academy of Sciences of the United States of America* **1978,** *75* (6), 2959-2963.

(92) Agrawal, A. K.; Gupta, C. M., Tuftsin-Bearing Liposomes in Treatment of Macrophage-Based Infections. *Advanced Drug Delivery Reviews* **2000,** *41* (2), 135-146.

(93) Basu, M. K.; Lala, S., Macrophage Specific Drug Delivery in Experimental Leishmaniasis. *Current Molecular Medicine* **2004,** *4* (6), 681-689.

(94) Allen, T. M.; Chonn, A., Large Unilamellar Liposomes with Low Uptake into the Reticuloendothelial System. *FEBS letters* **1987,** *223* (1), 42-46.

(95) Allen, T. M.; Hansen, C., Pharmacokinetics of Stealth Versus Conventional Liposomes: Effect of Dose. *Biochimica et Biophysica acta* **1991,** *1068* (2), 133-141.

(96) Allen, T. M.; Hansen, C.; Martin, F.; Redemann, C.; Yau-Young, A., Liposomes Containing Synthetic Lipid Derivatives of Poly(ethylene glycol) Show Prolonged Circulation Half-Lives in vivo. *Biochimica et Biophysica acta* **1991,** *1066* (1), 29-36.

(97) Hofmann, A. M.; Wurm, F.; Huhn, E.; Nawroth, T.; Langguth, P.; Frey, H., Hyperbranched Polyglycerol-Based Lipids via Oxyanionic Polymerization: Toward Multifunctional Stealth Liposomes. *Biomacromolecules* **2010,** *11* (3), 568-574.

(98) Blume, G.; Cevc, G., Liposomes for the Sustained Drug Release in vivo. *Biochimica et Biophysica acta* **1990,** *1029* (1), 91-97.

(99) Romberg, B.; Hennink, W. E.; Storm, G., Sheddable Coatings for Long-Circulating Nanoparticles. *Pharmaceutical Research* **2008,** *25* (1), 55-71.

(100) Woodle, M. C.; Lasic, D. D., Sterically Stabilized Liposomes. *Biochimica et Biophysica acta* **1992,** *1113* (2), 171-99.

(101) Storm, G.; Belliot, S. O.; Daemen, T.; Lasic, D. D., Surface Modification of Nanoparticles to Oppose Uptake by the Mononuclear Phagocyte System. *Advanced Drug Delivery Reviews* **1995,** *17* (1), 31-48.

(102) Vonarbourg, A.; Passirani, C.; Saulnier, P.; Benoit, J. P., Parameters Influencing the Stealthiness of Colloidal Drug Delivery Systems. *Biomaterials* **2006,** *27* (24), 4356-4373.

(103) Immordino, M. L.; Dosio, F.; Cattel, L., Stealth Liposomes: Review of the Basic Science, Rationale, and Clinical Applications, Existing and Potential. *International Journal of Nanomedicine* **2006,** *1* (3), 297-315.

(104) United States Patent and Trade Office, Indepent Database Search. *http://www.uspto.gov/*. (accessed January 2015)

(105) MarketandMarkets (Dallas, Texas), Marketandmarkets.com. Injectable Drug Delivery Market by Formulations [Liposomes, Microspheres, & Nanoparticles], Devices [Disposables & Reusable, Fillable & Prefilled, Pen, Needle Free & Auto Injectors] & Therapeutics [Diabetes & Oncology] - Global Forecasts to 2017; http://www.marketsandmarkets.com/Market-Reports/injectable-drug-delivery-market-150.html. (accessed January 2015)

(106) BeforeItsNews.com. Global Injectable Drug Delivery Market to Grow at a CAGR of 14% to 2017. http://beforeitsnews.com/science-and-technology/2014/09/global-injectable-drug-delivery-market-to-grow-at-a-cagr-of-14-to-2017-2723352.html (accessed January 21, 2015).

(107) Lasic, D. D., Novel Applications of Liposomes. *Trends in Biotechnology* **1998,** *16* (7), 307-321.

(108) Andrade, B.; Song, Z.; Li, J.; Zimmerman, S. C.; Cheng, J.; Moore, J. S.; Harris, K.; Katz, J. S., New Frontiers for Encapsulation in the Chemical Industry. *Applied Materials & Interfaces* **2015,** *7* (12), 6359-6368.

(109) Glantz, M. J.; LaFollette, S.; Jaeckle, K. A.; Shapiro, W.; Swinnen, L.; Rozental, J. R.; Phuphanich, S.; Rogers, L. R.; Gutheil, J. C.; Batchelor, T.; Lyter, D.; Chamberlain, M.; Maria, B. L.; Schiffer, C.; Bashir, R.; Thomas, D.; Cowens, W.; Howell, S. B., Randomized Trial of a Slow-Release Versus a Standard Formulation of Cytarabine for the Intrathecal Treatment of Lymphomatous Meningitis. *Journal of Clinical Oncology* **1999,** *17* (10), 3110-3116.

(110) Gill, P. S.; Wernz, J.; Scadden, D. T.; Cohen, P.; Mukwaya, G. M.; von Roenn, J. H.; Jacobs, M.; Kempin, S.; Silverberg, I.; Gonzales, G.; Rarick, M. U.; Myers, A. M.; Shepherd, F.; Sawka, C.; Pike, M. C.; Ross, M. E., Randomized Phase III Trial of Liposomal Daunorubicin Versus Doxorubicin, Bleomycin, and Vincristine in AIDS-Related Kaposi's Sarcoma. *Journal of Clinical Oncology* **1996,** *14* (8), 2353-2364.

(111) Latagliata, R.; Breccia, M.; Fazi, P.; Iacobelli, S.; Martinelli, G.; Di Raimondo, F.; Sborgia, M.; Fabbiano, F.; Pirrotta, M. T.; Zaccaria, A.; Amadori, S.; Caramatti, C.; Falzetti, F.; Candoni, A.; Mattei, D.; Morselli, M.; Alimena, G.; Vignetti, M.; Baccarani, M.; Mandelli, F., Liposomal Daunorubicin Versus Standard Daunorubicin: Long Term Follow-up of the GIMEMA GSI 103 AMLE Randomized Trial in Patients Older than 60 years with Acute Myelogenous Leukaemia. *British Journal of Haematology* **2008,** *143* (5), 681-689.

(112) Dinndorf, P. A.; Gootenberg, J.; Cohen, M. H.; Keegan, P.; Pazdur, R., FDA drug Approval Summary: Pegaspargase (Oncaspar) for the First-Line Treatment of Children with Acute Lymphoblastic Leukemia (ALL). *The Oncologist* **2007,** *12* (8), 991-998.

(113) Matsumura, Y.; Gotoh, M.; Muro, K.; Yamada, Y.; Shirao, K.; Shimada, Y.; Okuwa, M.; Matsumoto, S.; Miyata, Y.; Ohkura, H.; Chin, K.; Baba, S.; Yamao, T.; Kannami, A.; Takamatsu, Y.; Ito, K.; Takahashi, K., Phase I and Pharmacokinetic Study of MCC-465, a Doxorubicin (DXR) Encapsulated in PEG Immunoliposome, in Patients with Metastatic Stomach Cancer. *Annals of Oncology* **2004,** *15* (3), 517-525.

(114) Botnaru, V.; Munteanu, O.; Rusu, D., Interstitial Pneumonitis After Treatment for Hepatitis C Virus Infection. *Pneumologia* **2015,** *64* (1), 46-50.

(115) Khameneh, B.; Jaafari, M. R.; Hassanzadeh-Khayyat, M.; Varasteh, A.; Chamani, J.; Iranshahi, M.; Mohammadpanah, H.; Abnous, K.; Saberi, M. R., Preparation, Characterization and Molecular Modeling of PEGylated Human Growth Hormone with Agonist Activity. *International Journal of Biological Macromolecules* **2015**. (ahead of print)

(116) George, L. A.; Gadani, A.; Cross, R. K.; Jambaulikar, G.; Ghazi, L. J., Psoriasiform Skin Lesions Are Caused by Anti-TNF Agents Used for the Treatment of Inflammatory Bowel Disease. *Digestive Diseases and Sciences* **2015**. (ahead of print)

(117) Gradishar, W. J.; Tjulandin, S.; Davidson, N.; Shaw, H.; Desai, N.; Bhar, P.; Hawkins, M.; O'Shaughnessy, J., Phase III Trial of Nanoparticle Albumin-Bound Paclitaxel Compared with Polyethylated Castor Oil-Based Paclitaxel in Women with Breast Cancer. *Journal of Clinical Oncology* **2005,** *23* (31), 7794-7803.

(118) Stewart, S.; Jablonowski, H.; Goebel, F. D.; Arasteh, K.; Spittle, M.; Rios, A.; Aboulafia, D.; Galleshaw, J.; Dezube, B. J., Randomized Comparative Trial of Pegylated Liposomal Doxorubicin Versus Bleomycin and Vincristine in the Treatment of AIDS-Related Kaposi's Sarcoma. International Pegylated Liposomal Doxorubicin Study Group. *Journal of Clinical Oncology* **1998,** *16* (2), 683-691.

(119) Cianfrocca, M.; Lee, S.; Von Roenn, J.; Tulpule, A.; Dezube, B. J.; Aboulafia, D. M.; Ambinder, R. F.; Lee, J. Y.; Krown, S. E.; Sparano, J. A., Randomized Trial of Paclitaxel Versus Pegylated Liposomal Doxorubicin for Advanced Human Immunodeficiency Virus-Associated Kaposi Sarcoma: Evidence of Symptom Palliation from Chemotherapy. *Cancer* **2010,** *116* (16), 3969-3977.

(120) Orlowski, R. Z.; Nagler, A.; Sonneveld, P.; Blade, J.; Hajek, R.; Spencer, A.; San Miguel, J.; Robak, T.; Dmoszynska, A.; Horvath, N.; Spicka, I.; Sutherland, H. J.; Suvorov, A. N.; Zhuang, S. H.; Parekh, T.; Xiu, L.; Yuan, Z.; Rackoff, W.; Harousseau, J. L., Randomized Phase III Study of Pegylated Liposomal Doxorubicin Plus Bortezomib Compared with Bortezomib Alone in Relapsed or Refractory Multiple Myeloma: Combination Therapy Improves Time to progression. *Journal of Clinical Oncology* **2007,** *25* (25), 3892-3901.

(121) O'Shaughnessy, J. A., Pegylated Liposomal Doxorubicin in the Treatment of Breast Cancer. *Clinical Breast Cancer* **2003,** *4* (5), 318-328.

(122) Foldvari, M.; Oguejiofor, C.; Afridi, S.; Kudel, T.; Wilson, T., Liposome Encapsulated Prostaglandin E1 in Erectile Dysfunction: Correlation between in vitro Delivery through Foreskin and Efficacy in Patients. *Urology* **1998,** *52* (5), 838-843.

(123) Yamamoto, Y.; Kawano, I.; Iwase, H., Nab-Paclitaxel for the Treatment of Breast Cancer: Efficacy, Safety, and Approval. *Journal of OncoTargets and Therapy* **2011,** *4*, 123-136.

(124) Rodriguez, M. A.; Pytlik, R.; Kozak, T.; Chhanabhai, M.; Gascoyne, R.; Lu, B.; Deitcher, S. R.; Winter, J. N., Vincristine Sulfate Liposomes Injection (Marqibo) in Heavily Pretreated Patients with Refractory Aggressive non-Hodgkin Lymphoma: Report of the Pivotal Phase 2 Study. *Cancer* **2009,** *115* (15), 3475-3482.

(125) Neijzen, R.; Wong, M. Q.; Gill, N.; Wang, H.; Karim, T.; Anantha, M.; Strutt, D.; Waterhouse, D.; Bally, M. B.; Tai, I. T.; Ng, S. S.; Yapp, D. T., Irinophore C, a Lipid Nanoparticulate Formulation of Irinotecan, Improves Vascular Function, Increases the Delivery of Sequentially Administered 5-FU in HT-29 Tumors, and Controls Tumor Growth in Patient Derived Xenografts of Colon Cancer. *Journal of Controlled Release* **2015,** *199*, 72-83.

(126) Li, C.; Zhao, X.; Deng, C.; Wang, C.; Wei, N.; Cui, J., Pegylated Liposomal Mitoxantrone is more Therapeutically Active than Mitoxantrone in L1210 Ascitic Tumor and Exhibits Dose-Dependent Activity Saturation Effect. *International Journal of Pharmaceutics* **2014,** *460* (1-2), 165-172.

(127) Seymour, L. W.; Ferry, D. R.; Kerr, D. J.; Rea, D.; Whitlock, M.; Poyner, R.; Boivin, C.; Hesslewood, S.; Twelves, C.; Blackie, R.; Schatzlein, A.; Jodrell, D.; Bissett, D.; Calvert, H.; Lind, M.; Robbins, A.; Burtles, S.; Duncan, R.; Cassidy, J., Phase II Studies of Polymer-Doxorubicin (PK1, FCE28068) in the Treatment of Breast, Lung and Colorectal Cancer. *International Journal of Oncology* **2009,** *34* (6), 1629-1636.

(128) Hopewel, J. W.; Duncan, R.; Wilding, D.; Chakrabarti, K., Preclinical Evaluation of the Cardiotoxicity of PK2: a Novel HPMA Copolymer-Doxorubicin-Galactosamine Conjugate Antitumour Agent. *Human and Experimental Toxicology* **2001,** *20* (9), 461-470.

(129) Pastorino, F.; Brignole, C.; Di Paolo, D.; Nico, B.; Pezzolo, A.; Marimpietri, D.; Pagnan, G.; Piccardi, F.; Cilli, M.; Longhi, R.; Ribatti, D.; Corti, A.; Allen, T. M.; Ponzoni, M., Targeting Liposomal Chemotherapy via both Tumor Cell-Specific and Tumor Vasculature-Specific Ligands Potentiates Therapeutic Efficacy. *Cancer Research* **2006,** *66* (20), 10073-10082.

(130) Zamboni, W. C.; Gervais, A. C.; Egorin, M. J.; Schellens, J. H.; Zuhowski, E. G.; Pluim, D.; Joseph, E.; Hamburger, D. R.; Working, P. K.; Colbern, G.; Tonda, M. E.; Potter, D. M.; Eiseman, J. L., Systemic and Tumor Disposition of Platinum After Administration of Cisplatin or STEALTH Liposomal-Cisplatin Formulations (SPI-077 and SPI-077 B103) in a Preclinical Tumor Model of Melanoma. *Cancer Chemotherapy and Pharmacology* **2004,** *53* (4), 329-336.

(131) Gordon, A. N.; Fleagle, J. T.; Guthrie, D.; Parkin, D. E.; Gore, M. E.; Lacave, A. J., Recurrent Epithelial Ovarian Carcinoma: A Randomized Phase III Study of Pegylated Liposomal Doxorubicin Versus Topotecan. *Journal of Clinical Oncology* **2001,** *19* (14), 3312-3322.

(132) Katsumata, N.; Fujiwara, Y.; Kamura, T.; Nakanishi, T.; Hatae, M.; Aoki, D.; Tanaka, K.; Tsuda, H.; Kamiura, S.; Takehara, K.; Sugiyama, T.; Kigawa, J.; Fujiwara, K.; Ochiai, K.; Ishida, R.; Inagaki, M.; Noda, K., Phase II Clinical Trial of Pegylated Liposomal Doxorubicin (JNS002) in Japanese Patients with Mullerian Carcinoma (Epithelial Ovarian Carcinoma, Primary Carcinoma of Fallopian Tube, Peritoneal Carcinoma) having a Therapeutic History of Platinum-Based Chemotherapy: A Phase II Study of the Japanese Gynecologic Oncology Group. *Japanese Journal of Clinical Oncology* **2008,** *38* (11), 777-785.

(133) Chan, A.; Shih, V.; Tham Chee, K., Liposomal Doxorubicin-Associated Acute Hypersensitivity Despite Appropriate Preventive Measures. *Journal of Oncology Pharmacy Practice* **2007,** *13* (2), 105-107.

(134) Ibrahim, N. K.; Desai, N.; Legha, S.; Soon-Shiong, P.; Theriault, R. L.; Rivera, E.; Esmaeli, B.; Ring, S. E.; Bedikian, A.; Hortobagyi, G. N.; Ellerhorst, J. A., Phase I and Pharmacokinetic Study of ABI-007, a Cremophor-Free, Protein-Stabilized, Nanoparticle Formulation of Paclitaxel. *Clinical Cancer Research* **2002,** *8* (5), 1038-1044.

(135) Andresen, T. L.; Jensen, S. S.; Jorgensen, K., Advanced Strategies in Liposomal Cancer Therapy: Problems and Prospects of Active and Tumor Specific Drug Release. *Progress in Lipid Research* **2005,** *44* (1), 68-97.

(136) Needham, D., Materials Engineering of Lipid Bilayers for Drug Carrier Performance. *MRS Bulletin* **1999,** *24* (10), 32-41.

(137) Kost, J.; Langer, R., Responsive Polymeric Delivery Systems. *Advanced Drug Delivery Reviews* **2001,** *46* (1-3), 125-148.

(138) Sershen, S.; West, J., Implantable, Polymeric Systems for Modulated Drug Delivery. *Advanced Drug Delivery Reviews* **2002,** *54* (9), 1225-1235.

(139) Qiu, Y.; Park, K., Environment-Sensitive Hydrogels for Drug Delivery. *Advanced Drug Delivery Reviews* **2001,** *53* (3), 321-339.

(140) Murdan, S., Electro-Responsive Drug Delivery from Hydrogels. *Journal of Controlled Release* **2003,** *92* (1-2), 1-17.

(141) Agnihotri, S. A.; Kulkarni, R. V.; Mallikarjuna, N. N.; Kulkarni, P. V.; Aminabhavi, T. M., Electrically Modulated Transport of Diclofenac Salts Through Hydrogels of Sodium Alginate, Carbopol, and their Blend Polymers. *Journal of Applied Polymer Science* **2005,** *96* (2), 301-311.

(142) Rapoport, N., Physical Stimuli-Responsive Polymeric Micelles for Anti-Cancer Drug Delivery. *Progress in Polymer Science* **2007,** *32* (8–9), 962-990.

(143) Ellens, H.; Bentz, J.; Szoka, F. C., Destabilization of Phosphatidylethanolamine Liposomes at the Hexagonal Phase Transition Temperature. *Biochemistry* **1986,** *25* (2), 285-294.

(144) Gaber, M. H.; Hong, K.; Huang, S. K.; Papahadjopoulos, D., Thermosensitive Sterically Stabilized Liposomes: Formulation and in vitro Studies on Mechanism of Doxorubicin Release by Bovine Serum and Human Plasma. *Pharmaceutical Research* **1995,** *12* (10), 1407-1416.

(145) Gaber, M. H.; Wu, N. Z.; Hong, K.; Huang, S. K.; Dewhirst, M. W.; Papahadjopoulos, D., Thermosensitive Liposomes: Extravasation and Release of Contents in Tumor Microvascular Networks. *International Journal of Radiation Ooncology, Biology, Physics* **1996,** *36* (5), 1177-1187.

(146) Yatvin, M. B.; Weinstein, J. N.; Dennis, W. H.; Blumenthal, R., Design of Liposomes for Enhanced Local Release of Drugs by Hyperthermia. *Science* **1978,** *202* (4374), 1290-1293.

(147) Needham, D.; Dewhirst, M. W., The Development and Testing of a New Temperature-Sensitive Drug Delivery System for the Treatment of Solid Tumors. *Advanced Drug Delivery Reviews* **2001,** *53* (3), 285-305.

(148) Chen, W. H.; Regen, S. L., Thermally Gated Liposomes. *Journal of the American Chemical Society* **2005,** *127* (18), 6538-6539.

(149) Needham, D.; Anyarambhatla, G.; Kong, G.; Dewhirst, M. W., A New Temperature-Sensitive Liposome for use with Mild Hyperthermia: Characterization and Testing in a Human Tumor Xenograft Model. *Cancer Research* **2000,** *60* (5), 1197-1201.

(150) Kong, G.; Anyarambhatla, G.; Petros, W. P.; Braun, R. D.; Colvin, O. M.; Needham, D.; Dewhirst, M. W., Efficacy of Liposomes and Hyperthermia in a Human Tumor Xenograft Model: Importance of Triggered Drug Release. *Cancer Research* **2000,** *60* (24), 6950-6957.

(151) Derycke, A. S.; de Witte, P. A., Liposomes for Photodynamic Therapy. *Advanced Drug Delivery Reviews* **2004,** *56* (1), 17-30.

(152) Yavlovich, A.; Singh, A.; Tarasov, S.; Capala, J.; Blumenthal, R.; Puri, A., Design of Liposomes Containing Photopolymerizable Phospholipids for Triggered Release of Contents. *Journal of Thermal Analysis and Calorimetry* **2009,** *98* (1), 97-104.

(153) Bisby, R. H.; Mead, C.; Morgan, C. G., Active Uptake of Drugs into Photosensitive Liposomes and Rapid Release on UV Photolysis. *Photochemistry and Photobiology* **2000,** *72* (1), 57-61.

(154) Lamparski, H.; Liman, U.; Barry, J. A.; Frankel, D. A.; Ramaswami, V.; Brown, M. F.; O'Brien, D. F., Photoinduced Destabilization of Liposomes. *Biochemistry* **1992,** *31* (3), 685-694.

(155) Shum, P.; Kim, J. M.; Thompson, D. H., Phototriggering of Lposomal Drug Delivery Systems. *Advanced Drug Delivery Reviews* **2001,** *53* (3), 273-284.

(156) Gerasimov, O. V.; Boomer, J. A.; Qualls, M. M.; Thompson, D. H., Cytosolic Drug Delivery using pH- and Light-Sensitive Liposomes. *Advanced Drug Delivery Reviews* **1999,** *38* (3), 317-338.

(157) Alvarez-Lorenzo, C.; Bromberg, L.; Concheiro, A., Light-Sensitive Intelligent Drug Delivery Systems. *Photochemistry and Photobiology* **2009,** *85* (4), 848-860.

(158) Gerasimov, O. V.; Rui, Y.; Thompson, D. H, Triggered Release from Liposomes Mediated by Physically- and Chemically Induced Phase Transitions. In *Vesicels*, Rosof, M. (Ed.); Marcel Dekker: New York, 1996. pp 679-746.

(159) Bondurant, B.; Mueller, A.; O'Brien, D. F., Photoinitiated Destabilization of Sterically Stabilized Liposomes. *Biochimica et Biophysica Acta* **2001,** *1511* (1), 113-122.

(160) Wymer, N. J.; Gerasimov, O. V.; Thompson, D. H., Cascade Liposomal Triggering: Light-Induced Ca^{2+} Release from Diplasmenylcholine Liposomes Triggers PLA_2-Catalyzed Hydrolysis and Contents Leakage from DPPC Liposomes. *Bioconjugate Chemistry* **1998,** *9* (3), 305-308.

(161) Qualls, M. M.; Thompson, D. H., Chloroaluminum Phthalocyanine Tetrasulfonate Delivered via Acid-Labile Diplasmenylcholine-Folate Liposomes: Intracellular Localization and Synergistic Phototoxicity. *International Journal of Cancer.* **2001,** *93* (3), 384-392.

(162) Thompson, D. H.; Gerasimov, O. V.; Wheeler, J. J.; Rui, Y.; Anderson, V. C., Triggerable Plasmalogen Liposomes: Improvement of System Efficiency. *Biochimica et Bbiophysica Acta* **1996,** *1279* (1), 25-34.

(163) Zhang, Z.-Y.; Smith, B. D., Synthesis and Characterization of NVOC-DOPE, a Caged Photoactivatable Derivative of Dioleoylphosphatidylethanolamine. *Bioconjugate Chemistry* **1999,** *10* (6), 1150-1152.

(164) Chandra, B.; Subramaniam, R.; Mallik, S.; Srivastava, D. K., Formulation of Photocleavable Liposomes and the Mechanism of their Content Release. *Organic and Biomolecular Chemistry* **2006,** *4* (9), 1730-1740.

(165) Juzenas, P.; Juzeniene, A.; Kaalhus, O.; Iani, V.; Moan, J., Noninvasive Fluorescence Excitation Spectroscopy During Application of 5-aminolevulinic Acid in vivo. *Photochemical and Photobiological Sciences* **2002,** *1* (10), 745-748.

(166) Klohs, J.; Wunder, A.; Licha, K., Near-Infrared Fluorescent Probes for Imaging Vascular Pathophysiology. *Basic Research in Cardiology* **2008,** *103* (2), 144-151.

(167) Spratt, T.; Bondurant, B.; O'Brien, D. F., Rapid Release of Liposomal Contents upon Photoinitiated Destabilization with UV Exposure. *Biochimica et Biophysica Acta* **2003,** *1611* (1-2), 35-43.

(168) Roux, E.; Francis, M.; Winnik, F. M.; Leroux, J. C., Polymer Based pH-Sensitive Carriers as a Means to Improve the Cytoplasmic Delivery of Drugs. *International Journal of Pharmaceutics* **2002,** *242* (1-2), 25-36.

(169) Simoes, S.; Moreira, J. N.; Fonseca, C.; Duzgunes, N.; de Lima, M. C., On the Formulation of pH-Sensitive Liposomes with Long Circulation Times. *Advanced Drug Delivery Reviews* **2004,** *56* (7), 947-965.

(170) Collins, D.; Litzinger, D. C.; Huang, L., Structural and Functional Comparisons of pH-Sensitive Liposomes Composed of Phosphatidylethanolamine and Three Different Diacylsuccinylglycerols. *Biochimica et Biophysica Acta* **1990,** *1025* (2), 234-242.

(171) Ellens, H.; Bentz, J.; Szoka, F. C., pH-Induced Destabilization of Phosphatidylethanolamine-Containing Liposomes: Role of Bilayer Contact. *Biochemistry* **1984,** *23* (7), 1532-1538.

(172) Ishida, T.; Kirchmeier, M. J.; Moase, E. H.; Zalipsky, S.; Allen, T. M., Targeted Delivery and Triggered Release of Liposomal Doxorubicin Enhances Cytotoxicity Against Human B Lymphoma Cells. *Biochimica et Biophysica Acta* **2001,** *1515* (2), 144-158.

(173) Venugopalan, P.; Jain, S.; Sankar, S.; Singh, P.; Rawat, A.; Vyas, S. P., pH-Sensitive Liposomes: Mechanism of Triggered Release to Drug and Gene Delivery Prospects. *Die Pharmazie* **2002,** *57* (10), 659-671.

(174) Yatvin, M. B.; Kreutz, W.; Horwitz, B. A.; Shinitzky, M., pH-Sensitive Liposomes: Possible Clinical Implications. *Science* **1980,** *210* (4475), 1253-1255.

(175) Guo, X.; Szoka, F. C., Jr., Steric Stabilization of Fusogenic Liposomes by a Low-pH Sensitive PEG--Diortho Ester--Lipid Conjugate. *Bioconjugate Chemistry* **2001,** *12* (2), 291-300.

(176) Boomer, J. A.; Thompson, D. H., Synthesis of Acid-Labile Diplasmenyl Lipids for Drug and Gene Delivery Applications. *Chemistry and Physics of Lipids* **1999,** *99* (2), 145-153.

(177) Shin, J.; Shum, P.; Grey, J.; Fujiwara, S.; Malhotra, G. S.; Gonzalez-Bonet, A.; Hyun, S. H.; Moase, E.; Allen, T. M.; Thompson, D. H., Acid-labile mPEG-Vinyl Ether-1,2-Dioleylglycerol Lipids with Tunable pH Sensitivity: Synthesis and Structural Effects on Hydrolysis Rates, DOPE Liposome Release Performance, and Pharmacokinetics. *Molecular Pharmaceutics* **2012,** *9* (11), 3266-3276.

(178) Zhang, J. X.; Zalipsky, S.; Mullah, N.; Pechar, M.; Allen, T. M., Pharmaco Attributes of Dioleoylphosphatidylethanolamine/cholesterylhemisuccinate Liposomes Containing Different Types of Cleavable Lipopolymers. *Pharmacological Research* **2004,** *49* (2), 185-198.

(179) Sawant, R. M.; Hurley, J. P.; Salmaso, S.; Kale, A.; Tolcheva, E.; Levchenko, T. S.; Torchilin, V. P., "SMART" Drug Delivery Systems: Double-Targeted pH-Responsive Pharmaceutical Nanocarriers. *Bioconjugate Chemistry* **2006,** *17* (4), 943-949.

(180) Leroux, J.; Roux, E.; Le Garrec, D.; Hong, K.; Drummond, D. C., *N*-Isopropylacrylamide Copolymers for the Preparation of pH-Sensitive Liposomes and Polymeric Micelles. *Journal of Controlled Release* **2001,** *72* (1-3), 71-84.

(181) Roux, E.; Stomp, R.; Giasson, S.; Pezolet, M.; Moreau, P.; Leroux, J. C., Steric Stabilization of Liposomes by pH-Responsive *N*-Isopropylacrylamide Copolymer. *Journal of Pharmaceutical Sciences* **2002,** *91* (8), 1795-1802.

(182) Stubbs, M.; McSheehy, P. M.; Griffiths, J. R.; Bashford, C. L., Causes and Consequences of Tumour Acidity and Implications for Treatment. *Molecular Medicine Today* **2000,** *6* (1), 15-19.

(183) Rooseboom, M.; Commandeur, J. N.; Vermeulen, N. P., Enzyme-Catalyzed Activation of Anticancer Prodrugs. *Pharmacological Reviews* **2004,** *56* (1), 53-102.

(184) Andresen, T. L.; Thompson, D. H.; Kaasgaard, T., Enzyme-Triggered Nanomedicine: Drug Release Strategies in Cancer Therapy. *Molecular Membrane Biology* **2010,** *27* (7), 353-363.

(185) Meers, P., Enzyme-Activated Targeting of Liposomes. *Advanced Drug Delivery and Reviews* **2001,** *53* (3), 265-272.

(186) Simopoulos, T. T.; Jencks, W. P., Alkaline Phosphatase is an Almost Perfect Enzyme. *Biochemistry* **1994,** *33* (34), 10375-10380.

(187) Davis, S. C.; Szoka, F. C., Jr., Cholesterol Phosphate Derivatives: Synthesis and Incorporation into a Phosphatase and Calcium-Sensitive Triggered Release Liposome. *Bioconjugate Chemistry* **1998,** *9* (6), 783-792.

(188) Pattinson, N. R., Identification of a Phosphatidylcholine Active Phospholipase C in Human Gallbladder Bile. *Biochemical and Biophysical Research Communications* **1988,** *150* (2), 890-896.

(189) Ramoni, C.; Spadaro, F.; Menegon, M.; Podo, F., Cellular localization and functional role of phosphatidylcholine-specific phospholipase C in NK cells. *Journal of immunology (Baltimore, Md. : 1950)* **2001,** *167* (5), 2642-50.

(190) Vadas, P.; Pruzanski, W., Role of Secretory Phospholipases A2 in the Pathobiology of Disease. *Laboratory Investigation* **1986,** *55* (4), 391-404.

(191) Yamashita, S.; Ogawa, M.; Sakamoto, K.; Abe, T.; Arakawa, H.; Yamashita, J., Elevation of Serum Group II Phospholipase A2 Levels in Patients with Advanced Cancer. *Clinica Chimica Acta* **1994,** *228* (2), 91-99.

(192) Abe, T.; Sakamoto, K.; Kamohara, H.; Hirano, Y.; Kuwahara, N.; Ogawa, M., Group II Phospholipase A2 is Increased in Peritoneal and Pleural Effusions in Patients with Various Types of Cancer. *International Journal of Cancer* **1997,** *74* (3), 245-250.

(193) Yamashita, S.; Yamashita, J.; Sakamoto, K.; Inada, K.; Nakashima, Y.; Murata, K.; Saishoji, T.; Nomura, K.; Ogawa, M., Increased Expression of Membrane-Associated Phospholipase A2 Shows Malignant Potential of Human Breast Cancer Cells. *Cancer* **1993,** *71* (10), 3058-3064.

(194) Jiang, J.; Neubauer, B. L.; Graff, J. R.; Chedid, M.; Thomas, J. E.; Roehm, N. W.; Zhang, S.; Eckert, G. J.; Koch, M. O.; Eble, J. N.; Cheng, L., Expression of Group IIA Secretory Phospholipase A2 is Elevated in Prostatic Intraepithelial Neoplasia and Adenocarcinoma. *The American Journal of Pathology* **2002,** *160* (2), 667-671.

(195) Kashiwagi, M.; Friess, H.; Uhl, W.; Berberat, P.; Abou-Shady, M.; Martignoni, M.; Anghelacopoulos, S. E.; Zimmermann, A.; Buchler, M. W., Group II and IV Phospholipase A(2) are Produced in Human Pancreatic Cancer Cells and Influence Prognosis. *Gut* **1999,** *45* (4), 605-612.

(196) T.L Andresen, O. G. M., M. Begtrup, K. Jorgesen, Phospholipase A2 Activity: Dependence on Liposome Surface Charge and Polymer Coverage *Biophysical Journal* **2002,** *82*, 148A.

(197) Vihinen, P.; Kahari, V. M., Matrix Metalloproteinases in Cancer: Prognostic Markers and Therapeutic Targets. *International Journal of Cancer.* **2002,** *99* (2), 157-166.

(198) Sarkar, N. R.; Rosendahl, T.; Krueger, A. B.; Banerjee, A. L.; Benton, K.; Mallik, S.; Srivastava, D. K., "Uncorking" of Liposomes by Matrix Metalloproteinase-9. *Chemical Communications* **2005,** (8), 999-1001.

(199) Briknarova, K.; Gehrmann, M.; Banyai, L.; Tordai, H.; Patthy, L.; Llinas, M., Gelatin-Binding Region of Human Matrix Metalloproteinase-2: Solution Structure, Dynamics, and Function of the COL-23 Two-Domain Construct. *The Journal of Biological Chemistry* **2001,** *276* (29), 27613-27621.

(200) Terada, T.; Iwai, M.; Kawakami, S.; Yamashita, F.; Hashida, M., Novel PEG-Matrix Metalloproteinase-2 Cleavable Peptide-Lipid Containing Galactosylated Liposomes for Hepatocellular Carcinoma-Selective Targeting. *Journal of Controlled Release* (201) Hatakeyama, H.; Akita, H.; Kogure, K.; Oishi, M.; Nagasaki, Y.; Kihira, Y.; Ueno, M.; Kobayashi, H.; Kikuchi, H.; Harashima, H., Development of a novel systemic gene delivery system for cancer therapy with a tumor-specific cleavable PEG-lipid. *Gene therapy* **2007,** *14* (1), 68-77.

(202) Pinnaduwage, P.; Huang, L., Beta-Galactosidase-Induced Destabilization of Liposome Composed of Phosphatidylethanolamine and Ganglioside GM1. *Biochimica et Biophysica Acta* **1988,** *939* (2), 375-382.

(203) Al-Haik, N.; Lewis, D. A.; Struthers, G., Neutral Protease, Collagenase and Elastase Activities in Synovial Fluids from Arthritic Patients. *Agents and Actions* **1984,** *15* (3-4), 436-442.

(204) Gysen, P.; Malaise, M.; Gaspar, S.; Franchimont, P., Measurement of Proteoglycans, Elastase, Collagenase and Protein in Synovial Fluid in Inflammatory and Degenerative Arthropathies. *Clinical Rheumatology* **1985,** *4* (1), 39-50.

(205) Tate, R. M.; Repine, J. E., Neutrophils and the Adult Respiratory Distress Syndrome. *The American Review of Respiratory Disease* **1983,** *128* (3), 552-559.

(206) Janoff, A., Elastases and emphysema. Current Assessment of the Protease-Antiprotease Hypothesis. *The American Review of Respiratory Disease* **1985,** *132* (2), 417-433.

(207) Suter, S.; Schaad, U. B.; Roux, L.; Nydegger, U. E.; Waldvogel, F. A., Granulocyte Neutral Proteases and Pseudomonas Elastase as Possible Causes of Airway Damage in Patients with Cystic Fibrosis. *The Journal of Infectious Diseases* **1984,** *149* (4), 523-531.

(208) Birrer, P.; McElvaney, N. G.; Rudeberg, A.; Sommer, C. W.; Liechti-Gallati, S.; Kraemer, R.; Hubbard, R.; Crystal, R. G., Protease-Antiprotease Imbalance in the Lungs of Children with Cystic Fibrosis. *American Journal of Respiratory and Critical Care Medicine* **1994,** *150* (1), 207-213.

(209) Yamashita, J. I.; Ogawa, M.; Ikei, S.; Omachi, H.; Yamashita, S. I.; Saishoji, T.; Nomura, K.; Sato, H., Production of Immunoreactive Polymorphonuclear Leucocyte Elastase in Human Breast Cancer Cells: Possible Role of Polymorphonuclear Leucocyte Elastase in the Progression of Human Breast Cancer. *British Journal of Cancer* **1994,** *69* (1), 72-76.

(210) Starcher, B.; O'Neal, P.; Granstein, R. D.; Beissert, S., Inhibition of Neutrophil Elastase Suppresses the Development of Skin Tumors in Hairless Mice. *The Journal of Investigative Dermatology* **1996,** *107* (2), 159-163.

(211) Pak, C. C.; Ali, S.; Janoff, A. S.; Meers, P., Triggerable Liposomal Fusion by Enzyme Cleavage of a Novel Peptide-Lipid Conjugate. *Biochimica et Biophysica Acta* **1998,** *1372* (1), 13-27.

(212) Schroeder, A.; Kost, J.; Barenholz, Y., Ultrasound, Liposomes, and Drug Delivery: Principles for using Ultrasound to Control the Release of Drugs from lLposomes. *Chemistry and Physics of Lipids* **2009,** *162* (1-2), 1-16.

(213) Huang, S. L., Liposomes in Ultrasonic Drug and Gene Delivery. *Advanced Drug Delivvery Reviews* **2008,** *60* (10), 1167-1176.

(214) Lentacker, I.; Geers, B.; Demeester, J.; De Smedt, S. C.; Sanders, N. N., Design and Evaluation of Doxorubicin-Containing Microbubbles for Ultrasound-Triggered Doxorubicin Delivery: Cytotoxicity and Mechanisms Involved. *Molecular Therapy* **2010,** *18* (1), 101-108.

(215) Sawant, R. M.; Hurley, J. P.; Salmaso, S.; Kale, A.; Tolcheva, E.; Levchenko, T. S.; Torchilin, V. P., "SMART" Drug Delivery Systems: Double-Targeted pH-Responsive Pharmaceutical Nanocarriers. *Bioconjugate Chemistry* **2006,** *17* (4), 943-949.

(216) Saito, G.; Swanson, J. A.; Lee, K. D., Drug Delivery Strategy Utilizing Conjugation via Reversible Disulfide Linkages: Role and Site of Cellular Reducing Activities. *Advanced Drug Delivery Reviews* **2003,** *55* (2), 199-215.

(217) Ponce, A. M.; Vujaskovic, Z.; Yuan, F.; Needham, D.; Dewhirst, M. W., Hyperthermia Mediated Liposomal Drug Ddelivery. *International Journal of Hyperthermia* **2006,** *22* (3), 205-213.

(218) Collins, D. S.; Unanue, E. R.; Harding, C. V., Reduction of Disulfide Bonds within Lysosomes is a Key Step in Antigen Processing. *Journal of Immunology* **1991,** *147* (12), 4054-4059.

(219) Saji, T.; Hoshino, K.; Aoyagui, S., Reversible Formation and Disruption of Micelles by Control of the Redox State of the Head Group. *Journal of the American Chemical Society* **1985,** *107* (24), 6865-6868.

(220) Medina, J. C.; Gay, I.; Chen, Z.; Echegoyen, L.; Gokel, G. W., Redox-Switched Molecular Aggregates: the First Example of Vesicle Formation from Hydrophobic Ferrocene Derivatives. *Journal of the American Chemical Society* **1991,** *113* (1), 365-366.

(221) Munoz, S.; Gokel, G. W., Redox-Switched Vesicle Formation from Two Novel, Structurally Distinct Metalloamphiphiles. *Journal of the American Chemical Society* **1993,** *115* (11), 4899-4900.

(222) Pastorino, F.; Brignole, C.; Di Paolo, D.; Nico, B.; Pezzolo, A.; Marimpietri, D.; Pagnan, G.; Piccardi, F.; Cilli, M.; Longhi, R.; Ribatti, D.; Corti, A.; Allen, T. M.; Ponzoni, M., Targeting Liposomal Chemotherapy via Both Tumor Cell–Specific and Tumor Vasculature–Specific Ligands Potentiates Therapeutic Efficacy. *Cancer Research* **2006,** *66* (20), 10073-10082.

(223) Fitzsimmons, S. A.; Workman, P.; Grever, M.; Paull, K.; Camalier, R.; Lewis, A. D., Reductase Enzyme Expression Across the National Cancer Institute Tumor Cell Line Panel: Correlation with Sensitivity to Mitomycin C and EO9. *Journal of the National Cancer Institute* **1996,** *88* (5), 259-269.

(224) Cresteil, T.; Jaiswal, A. K., High Levels of Expression of the NAD(P)H:Quinone Oxidoreductase (NQO1) Gene in Tumor Cells Compared to Normal Cells of the Same Origin. *Biochemical Pharmacology* **1991,** *42* (5), 1021-1027.

(225) Siegel, D.; Franklin, W. A.; Ross, D., Immunohistochemical Detection of NAD(P)H:Quinone Oxidoreductase in Human Lung and Lung Tumors. *Clinical Cancer Research* **1998,** *4* (9), 2065-2070.

(226) Schlager, J. J.; Powis, G., Cytosolic NAD(P)H:(quinone-acceptor)oxidoreductase in Human Normal and Tumor Tissue: Effects of Cigarette Smoking and Alcohol. *International Journal of Cancer* **1990,** *45* (3), 403-409.

(227) Riley, R. J.; Workman, P., DT-Diaphorase and Cancer Chemotherapy. *Biochemical Pharmacology* **1992,** *43* (8), 1657-1669.

(228) Spanswick, V. J.; Cummings, J.; Smyth, J. F., Current Issues in the Enzymology of Mitomycin C Metabolic Activation. *General Pharmacology* **1998,** *31* (4), 539-544.

(229) Ross, D.; Beall, H.; Traver, R. D.; Siegel, D.; Phillips, R. M.; Gibson, N. W., Bioactivation of Quinones by DT-Diaphorase, Molecular, Biochemical, and Chemical Studies. *Oncology Research* **1994,** *6* (10-11), 493-500.

(230) Monks, T. J.; Hanzlik, R. P.; Cohen, G. M.; Ross, D.; Graham, D. G., Quinone Chemistry and Toxicity. *Toxicology and Applied Pharmacology* **1992,** *112* (1), 2-16.

(231) Phillips, R. M.; Naylor, M. A.; Jaffar, M.; Doughty, S. W.; Everett, S. A.; Breen, A. G.; Choudry, G. A.; Stratford, I. J., Bioreductive Activation of a Series of Indolequinones by Human DT-Diaphorase: Structure-Activity Relationships. *Journal of Medicinal Chemistry* **1999,** *42* (20), 4071-4080.

(232) Faig, M.; Bianchet, M. A.; Talalay, P.; Chen, S.; Winski, S.; Ross, D.; Amzel, L. M., Structures of Recombinant Human and Mouse NAD(P)H:Quinone Oxidoreductases: Species Comparison and Structural Changes with Substrate Binding and Release. *Proceedings of the National Academy of Sciences of the United States of America* **2000,** *97* (7), 3177-3182.

(233) Li, R.; Bianchet, M. A.; Talalay, P.; Amzel, L. M., The Three-Dimensional Structure of NAD(P)H:Quinone Reductase, a Flavoprotein Involved in Cancer Chemoprotection and Chemotherapy: Mechanism of the Two-Electron Reduction. *Proceedings of the National Academy of Sciences of the United States of America* **1995,** *92* (19), 8846-8850.

(234) Ernster, L. , DT-diaphorase: A Historical Review. *Chemica Scripta.* **1987,** *27A*, 1-13.

(235) Iyanagi, T.; Yamazaki, I., One-Electron-Transfer Reactions in Biochemical Systems. V. Difference in the Mechanism of Quinone Reduction by the NADH Dehydrogenase and the NAD(P)H Dehydrogenase (DT-Diaphorase). *Biochimica et Biophysica Acta* **1970,** *216* (2), 282-294.

(236) Kremer, W. B.; Laszlo, J., Biochemical Effects of the Methyl Ester of Streptonigrin. *Biochemical Pharmacology* **1966,** *15* (8), 1111-1118.

(237) Beall, H. D.; Liu, Y.; Siegel, D.; Bolton, E. M.; Gibson, N. W.; Ross, D., Role of NAD(P)H:Quinone Oxidoreductase (DT-Diaphorase) in Cytotoxicity and Induction of DNA Damage by Streptonigrin. *Biochemical Pharmacology* **1996,** *51* (5), 645-652.

(238) Keyes, S. R.; Fracasso, P. M.; Heimbrook, D. C.; Rockwell, S.; Sligar, S. G.; Sartorelli, A. C., Role of NADPH:Cytochrome C Reductase and DT-Diaphorase in the Biotransformation of Mitomycin C1. *Cancer Research* **1984,** *44* (12 Pt 1), 5638-5643.

(239) Cummings, J.; Spanswick, V. J.; Smyth, J. F., Re-Evaluation of the Molecular Pharmacology of Mitomycin C. *European Journal of Cancer* **1995,** *31a* (12), 1928-1933.

(240) Chen, S.; Knox, R.; Wu, K.; Deng, P. S.; Zhou, D.; Bianchet, M. A.; Amzel, L. M., Molecular Basis of the Catalytic Differences Among DT-Diaphorase of Human, Rat, and Mouse. *The Journal of Biological Chemistry* **1997,** *272* (3), 1437-1439.

(241) Knox, R. J.; Friedlos, F.; Sherwood, R. F.; Melton, R. G.; Anlezark, G. M., The Bioactivation of 5-(Aziridin-1-yl)-2,4-Dinitrobenzamide (CB1954)--II. A Comparison of an Escherichia Coli Nitroreductase and Walker DT Diaphorase. *Biochemical Pharmacology* **1992,** *44* (12), 2297-2301.

(242) Knox, R. J.; Jenkins, T. C.; Hobbs, S. M.; Chen, S.; Melton, R. G.; Burke, P. J., Bioactivation of 5-(Aziridin-1-yl)-2,4-Dinitrobenzamide (CB 1954) by Human NAD(P)H Quinone Oxidoreductase 2: A Novel Co-Substrate-Mediated Antitumor Prodrug Therapy. *Cancer Research* **2000,** *60* (15), 4179-4186.

(243) Boland, M. P.; Knox, R. J.; Roberts, J. J., The Differences in Kinetics of Rat and Human DT Diaphorase Result in a Differential Sensitivity of Derived Cell Lines to CB 1954 (5-(Aziridin-1-yl)-2,4-Dinitrobenzamide). *Biochemical Pharmacology* **1991,** *41* (6-7), 867-875.

(244) Ross, D.; Siegel, D.; Gibson, N. W.; Pacheco, D.; Thomas, D. J.; Reasor, M.; Wierda, D., Activation and Deactivation of Quinones Catalyzed by DT-Diaphorase. Evidence for Bioreductive Activation of Diaziquone (AZQ) in Human Tumor Cells and Detoxification of Benzene Metabolites in Bone Marrow Stroma. *Free Radical Research Communications* **1990,** *8* (4-6), 373-381.

(245) Siegel, D.; Gibson, N. W.; Preusch, P. C.; Ross, D., Metabolism of Diaziquone by NAD(P)H:(Quinone Acceptor) Oxidoreductase (DT-Diaphorase): Role in Diaziquone-Induced DNA Damage and Cytotoxicity in Human Colon Carcinoma Cells. *Cancer Research* **1990,** *50* (22), 7293-7300.

(246) Faig, M.; Bianchet, M. A.; Winski, S.; Hargreaves, R.; Moody, C. J.; Hudnott, A. R.; Ross, D.; Amzel, L. M., Structure-Based Development of Anticancer Drugs: Complexes of NAD(P)H:Quinone Oxidoreductase 1 with Chemotherapeutic Quinones. *Structure* **2001,** *9* (8), 659-667.

(247) Maskell, L.; Blanche, E. A.; Colucci, M. A.; Whatmore, J. L.; Moody, C. J., Synthesis and Evaluation of Prodrugs for Anti-Angiogenic Pyrrolylmethylidenyl Oxindoles. *Bioorganic and Medicinal Chemistry Letters* **2007,** *17* (6), 1575-1578.

(248) Volpato, M.; Abou-Zeid, N.; Tanner, R. W.; Glassbrook, L. T.; Taylor, J.; Stratford, I.; Loadman, P. M.; Jaffar, M.; Phillips, R. M., Chemical Synthesis and Biological Evaluation of a NAD(P)H:Quinone Oxidoreductase-1 Targeted Tripartite Quinone Drug Delivery System. *Molecular Cancer Therapeutics* **2007,** *6* (12 Pt 1), 3122-3130.

(249) Mayhew, S. G., The Redox Potential of Dithionite and SO^{-2} from Equilibrium Reactions with Flavodoxins, Methyl Viologen and Hydrogen Plus Hydrogenase. *European Journal of Biochemistry* **1978,** *85* (2), 535-547.

(250) Silvers, W. C.; Payne, A. S.; McCarley, R. L., Shedding Light by Cancer Redox-Human NAD(P)H:Quinone Oxidoreductase 1 Activation of a Cloaked Fluorescent Dye. *Chemical Communications* **2011,** *47* (40), 11264-11266.

(251) Hettiarachchi, S. U.; Prasai, B.; McCarley, R. L., Detection and Cellular Imaging of Human Cancer Enzyme using a Turn-On, Wavelength-Shiftable, Self-Immolative Profluorophore. *Journal of the American Chemical Society* **2014,** *136* (21), 7575-7578.

(252) Prasai, B.; Silvers, W. C.; McCarley, R. L., Oxidoreductase-Facilitated Visualization and Detection of Human Cancer Cells. *Analytical Chemistry* **2015,** *87* (12), 6411-6418.

(253) Hofmeister, F., A*bout Regularities in the Protein Precipitating Effects of Salts and the Relation of These Effects with the Physiological Behaviour of Salts. Archiv Fur Experimentelle Pathologie und Pharmakologie* **1888,** *24*, 247-260.

(254) Gruner, S. M., Intrinsic Curvature Hypothesis for Biomembrane Lipid Composition: A Role for Nonbilayer Lipids. *Proceedings of the National Academy of Sciences of the United States of America* **1985,** *82* (11), 3665-3669.

(255) Chernomordik, L. V.; Zimmerberg, J.; Kozlov, M. M., Membranes of the World Unite! *The Journal of Cell Biology* **2006,** *175* (2), 201-207.

(256) Luzzati, V.; Reiss-Husson, F.; Rivas, E.; Gulik-Krzywicki, T., Structure and Polymorphism in Lipid-Water Systems, and Their Possible Biological Implications. *Annals of the New York Academy of Sciences* **1966,** *137* (2), 409-413.

(257) Kuzmin, P. I.; Zimmerberg, J.; Chizmadzhev, Y. A.; Cohen, F. S., A Quantitative Model for Membrane Fusion Based on Low-Energy Intermediates. *Proceedings of the National Academy of Sciences of the United States of America* **2001,** *98* (13), 7235-7240.

CHAPTER 2
EXPERIMENTAL METHODS

2.1 Aqueous Media

When properly hydrated, lipids organize into bilayers to from liposomes, which are defined as colloidal particles that possess both polar and non-polar regions.[1] In Chapter 1, the effects of polarity, salt identity, ionic strength, viscosity, pH, and temperature on lipid phase behavior were discussed. Thus, it is important to not only consider the chemical structures lipids but also the physical environment that interacts with them. A difference in osmotic pressure across a lipid bilayer creates membrane stress that can lead to deformation, swelling, leaking and/or rupturing of the membrane.[2] Moreover, charged salts in the encapsulated media can strongly interact with oppositely charged lipids in the inner leaflet of a bilayer membrane, thus requiring addition of chelating agents to sequester the charged salt components.[3-5] The aqueous environment inside liposomal delivery systems is inherently different; therefore, these media must be properly tuned. Presented here are the methods used to prepare and control the environment of the lipids used in this work. Also addressed are the precautions needed in order to account for analyte differences across a liposome.

2.1.1 Buffer Preparation

Commonly referred to as “Good’s buffers,” Good et al. investigated 20 different buffering agents for use in biological research (pH 6–8).[6-8] Good’s buffers are hydrogen ion buffers that have adequate solubility and pK_a values near physiological pH. While these buffers are still used today, a more recent comprehensive list consisting of 64 buffers was prepared by Goldberg et al. in 2002.[9] This reference should be used as a starting point when selecting an ideal buffer.

All buffers were prepared with components purchased, of Bioultra (> 99%) grade or better. Typically, phosphate-buffered saline (PBS) having a concentration of 50.0 mM phosphate and 100 mM KCl, buffered to pH 7.40 was used in liposome experiments. A concentrated solution of KOH was used to titrate the pH of the buffer media to the desired level. Unless noted otherwise, 0.10 mM ethylenediamine-tetraacetic acid (EDTA) was incorporated into all buffer solutions as a divalent cationic chelating agent; divalent cations (i.e., Ca^{2+} and Mg^{2+}) charge screen opposed anionic bilayers, and as a result can induce aggregation and fusion of liposomal vesicles.[10,11] Additionally, divalent cations can form quenching complexes with anionic fluorophores, such as calcein.[12] In experiments requiring a non-phosphorus-containing buffer system, 2-[2-hydroxy-1,1-bis(hydroxymethyl)ethyl)amino] ethanesulfonic acid (TES; pK_a=7.55) was substituted for phosphate buffer. All buffers were filtered through a sterile 0.22–μm pore size polyethersulfone membrane and stored in a refrigerator until used, to prevent the growth of bacteria. Immediately prior to use, an aliquot of the buffer media was transferred into a sterile transport tube, brought to room temperature, and degassed with nitrogen.

2.1.2 Vapor Pressure Osmometry

In an instance where there is a difference in chemical species between the inside or outside media of a liposome, a difference in osmotic pressure can place unwanted stress on the lipid membrane.[2] While this stress can be negligible and go unnoticed, the osmotic pressures between the inner and outer membrane must be equal for fusion assays or when molecular diffusion is concerned.[13-15] Fusion of opposed vesicles requires a balance of local, packing, hydration, and charge free energies, which sum to a net free energy and dedicates in intrinsic radius of curvature of the membrane and

thereby the phase of the lipid.[16,17] A difference in osmotic pressure across a liposomal bilayer results in a new force that is exerted onto the membrane changing the net free energy and altering the radius of curvature. A vapor pressure osmometer is commonly employed to measure and correct the osmotic pressure of various buffer media to negate this force.

A Vapro Vapor Pressure Osmometer 5520 (Wescor, Logan, UT) was used to measure and tune the vapor pressure of the buffer media examined in this work. For a single measurement, 10 μL of the buffer media being investigated was inoculated into a single-use disposable solute-free paper disk (Wescor, SS-033) positioned on a sample holder atop a tray then locked into place inside the osmometer. After initiating the heating cycle, the vapor pressure value was displayed in mm Hg. For a typical PBS buffer, the measured osmotic pressure was ~170 mm Hg. A solution of 1.0 M KCl was titrated into the buffer media(s) having the lower vapor pressure so as to elevate its osmotic pressure to within 5% of the lighter. Measurements were made in triplicate.

2.2 Liposome Preparation

Numerous liposome preparation methods have been reported in literature.[18-20] In general, each method has four basic steps: (1) the lipids are dispersed in an organic solvent, (2) the solvent is removed, (3) aqueous media is added to the vessel in order to hydrate the lipids, and (4) a sizing procedure is used to produce relatively monodispersed (polydispersion index (PDI) ≤ 0.2). Where these methods vary are in the specifics of these steps. There are two more commonly accepted benchtop methods to prepare large unilamellar vesicles (LUVs): size-extrusion and reverse vaporization.[21-23] The size-extrusion method is the primary mode of LUV preparation used in this work; however, the reverse vaporization method was used in contents

mixing assays to study vesicle fusion. For the purpose of this section, only the size extrusion will be discussed. The reverse vaporization method will be presented in the section addressing vesicle fusion assays (Section 2.5).

2.2.1 Large Unilamellar Vesicles (LUVs)

Typically, approximately 3–5 mg of dry lipid was dispersed in CH_2Cl_2 and transferred into a ground glass joint test tube. The solvent was removed via rotary evaporation, taking care not to bump the organic solvent, so as to leave a thin lipid film on the walls of the test tube that was visually confirmed by formation of sequential rings of a waxy film. Once the solvent was removed, the test tube was placed under high vacuum for no less than 1 h to ensure all solvent had been removed. The lipid was then removed from vacuum, and 1.0 mL of the desired hydrating media was added. For content release studies, a 40 mM calcein 100 mM KCl/0.10 mM EDTA aqueous solution buffered with 50.0 mM phosphate, pH 7.40, was used. The hydrating lipid was then placed in a water bath above the T_M and below the T_H of the lipid. After 30 min, the vessel was agitated by six freeze/thaw cycles. This entails submerging the bottom half of the glass test tube containing the lipid into a dry ice acetone bath for no less than 1 min, then thawing the vessel in a water bath ($T_M < T < T_H$), vortexing in-between. To generate 100-nm diameter vesicles, an Avanti mini-extruder (Avanti Polar Lipids; Birmingham, AL) equipped with a 100-nm pore track-etched polycarbonate membrane was used to size the vesicles. This entails passing the hydrated lipid dispersion through the membrane 19 times. Different sized membranes can be used to size the vesicles, as desired.

2.2.2 Size-Exclusion Chromatography

In this work, size-exclusion chromatography was used to remove the analyte(s) of interest from the buffer media outside the vesicle. Dialysis is another method commonly used to replace the exterior buffer media; however, relative to size-exclusion chromatography dialysis, requires more time, larger volumes of buffer, and dilutes the total lipid concentration. Sephadex G-50 fine purchased from GE Healthcare Lifesciences (Pittsburgh, PA) was used as the stationary phase. The Sephadex used was hydrated in the desired aqueous media for no less than 5 h before use. For calcein content release assays, the aqueous matrix consisted of 100 mM KCl 0.10 mM EDTA buffered with 50.0 mM phosphate, pH 7.4. A homemade spin column was typically used over the traditional gravimetric column to save both Sephadex material and time. (Scheme 2.1)

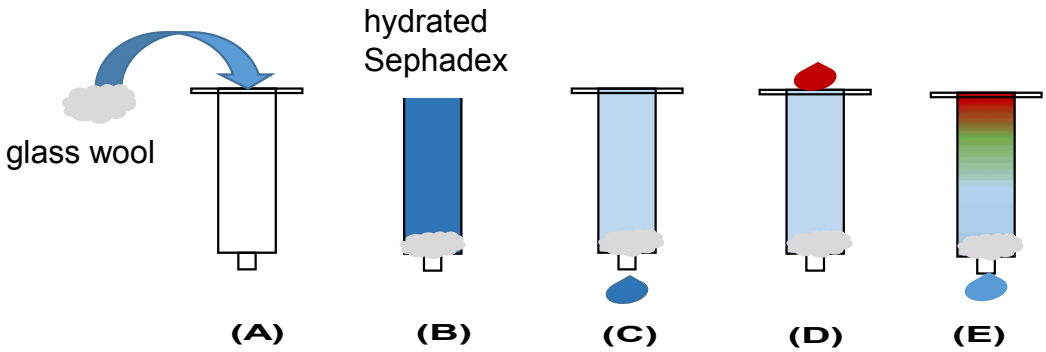

Scheme 2.1. A schematic of a spin column used for size exclusion chromatography. (A) Damp glass wool was placed inside the bottom section of a 3-mL disposable plastic syringe at the outlet nipple to prevent loss of the stationary phase, then (B) hydrated Sephadex was transferred into the vessel atop the glass wool. The spin column was placed in a disposable 10-mL plastic test tube to collect the eluting aqueous media. (C) The column was centrifuged to remove excess buffer media. (D) 250 μL of the lipid vesicle solution was added to the spin column and centrifuged again for 3 min, collecting the lipid into an Eppendorf vial situated between the bottom of the spin column and the disposable plastic tube. (E) The resulting eluant contains vesicles encapsulated with the analyte of interest and a minimal amount of free analyte dispersed in the aqueous media which was used to hydrate the Sephadex.

2.2.3 Determining Lipid Concentration

The characteristics and behavior of bulk vesicles can be dependent on lipid concentration as it relates to the number of particles in solution. To perform comparative studies, experimental methods require the same concentration of lipid be used in every experiment. Because of the loss of lipid in the extrusion step and dilution during size-exclusion chromatography, the concentration of lipid in the eluted vesicle containing solution must be determined prior to any study using this lipid. Multiple methods to measure lipid concentration have been reported in literature, with the most widely employed method being the Bartlett assay.[24-27] Absorption of light by the quinone head group in functionalized PE-lipids, a modified Bartlett-total phosphorus assay, and modified Stewart-total organic phosphorus assay were used in this work. The Bartlett assay is the more accurate and precise of the three methods used in this work; however, it is a total phosphorous assay and cannot be employed when working in a phosphate-buffered system and requires ~3 h to complete. The Stewart assay was utilized in the instances when the lipid being studied did not contain a quinone group and was in a phosphate-buffered system.

Quinone UV-Vis Absorption Assay. The quinone group of Q_{PA}-DOPE strongly absorbs at 265 nm (ε = 5500 M^{-1} cm^{-1}). In a typical Q_{PA}-DOPE quantification experiment, 490 μL of the aqueous media being used is transferred into a 0.5 mL quartz cuvette and blank absorbance spectrum acquired on a Cary-50 UV-Vis spectrometer (Varian-Agilent). 10 μL of the eluted vesicle solution is added to the cuvette containing the 490 μL aqueous media. The absorbance spectrum was measured and the intensity at 265 nm was recorded (Appendix 4).

Bartlett Assay. Use of a modified Bartlett Assay to determine the concentration of phospholipids in vesicle form has been well documented.[10,13,24,28] It is important to note a second time that this assay is a total phosphorus assay and thus cannot be used to determine the concentration of phospholipids that are in aqueous media buffered with phosphate. A set of phosphate standards (0.01–0.10 μmol) were prepared in triplicate from a 1.00 g L^{-1} phosphate standard purchased from Sigma-Aldrich (St. Louis, MO) and placed in 10-mL disposable glass test tubes. 10 μL of the eluted vesicle solution being measured was also aliquoted into a test tube in triplicate. A 0.4-mL aliquot of 5.0 M H_2SO_4 was added to each vial, and the vials were placed in a heating block at 180 °C fo 30 min. The vials were removed from the heat and amiably brought to < 100 °C before 0.100 mL of 30% H_2O_2 was added to remove all color from the solution. The vials were returned to the heating block where they remained at 180 °C until H_2O_2 was no longer present, as determined by H_2O_2 indicator strips. This process can take up to 90 min. Once the H_2O_2 had been removed, the vials were allowed to cool to room temperature before adding 4.6 mL of 0.22% ammonium molybdate in 0.125 M H_2SO_4 and 0.200 mL of a freshly prepared 0.16 g/mL Fiske-SubbaRow reducer solution (Sigma). The vials were vortexed to ensure the contents were well mixed and then placed in a 100 °C water bath for 10 min. The presence of phosphorus is apparent by the formation of an aqua-blue color in the solutions. The absorbance at 830 nm of the phosphorus-molybdate complex was without dilution using a Cary-50 UV-Vis spectrometer (Varian-Agilent; Appendix 5).

Stewart Assay. The use of a Stewart assay to measure the concentration of phospholipids has also been reported.[25,29] This assay measures the concentration of organic-soluble phosphorous, and allows the concentration of phospholipids hydrated

in phosphate-buffered media to be determined accurately. Because this method is a lipid water-organic extraction method, the Stewart assay has a lower precision and accuracy than the Bartlett assay. A standard stock solution of 0.1 mg mL^{-1} POPE lipid in $CHCl_3$ was made using lipids purchased from Avanti Polar Lipid (Birmingham, AL). POPE standards (0.01–0.20 μmol) were made in triplicate from the stock solution and then placed in 10-mL disposable glass test tubes, along with 10 μL aliquots of the vesicle eluant solution being measured. Each standard was brought to a total volume of 2.00 mL using $CHCl_3$, and then 2.00 mL $CHCl_3$ was added to the vesicle solution being measured. The vesicle-$CHCl_3$ mixture was subjected to 3 sonication and vortex cycles to disperse the lipids into the organic phase. 2.00 mL of a 0.1 M $FeCl_3$/0.4 M NH_4SCN solution was added to each vial, then subjected to 3 cycles of sonication and vortexing to ensure adequate mixing of the organic and aqueous phases. The vials underwent centrifugation to separate the organic (bottom) and aqueous (top) phases. A change in color from colorless to faint red indicates the presence of phosphorus in the organic phase. The bottom layer was extracted with a glass pipette and transferred into a new glass test tube. $Na_2S_2O_4$ was added to the vials containing the organic layer to remove any latent water. The absorbance (485 nm) of the extracted organic layers was measured on a Cary-50 UV-Vis spectrometer without any further preparation or dilution (Appendix 6).

2.3 Liposomal Contents Release and Aggregation

To test the ability of a lipid to encapsulate and release its encapsulated cargo upon being stimulated, liposomes were prepared using the procedure outlined in Section 2.2 with 40 mM calcein added as the encapsulated analyte. A stock solution of 100 μM lipid was prepared from the eluted vesical containing solution post

size-exclusion chromatography. A 3.00 mL aliquot of the stock solution was transferred into a quartz cuvette equipped with a rubber septum, and this was degassed with nitrogen for no less than 15 min. The cuvette was placed in an LS-55 Perkin Elmer Fluorescence Spectrometer (Waltham, MA) and the fluorescence of calcein measured with time using the following parameters: 2.5/2.5 nm excitation/emission monochromator slit widths, excitation/emission wavelengths of 491/515 nm, 5 s data acquisition interval, and 1 s signal integration. Both water Peltier and thermoelectric Peltier systems were used to maintain the temperature of the sample. A baseline was taken for no less than 15 min to allow for thermal equilibrium prior to addition of a chemical stimulus. To reduce the quinone functionalized lipid to a hydroquinone, thereby triggering contents release of the Q_{PA}-DOPE system, a freshly prepared solution of sodium dithionite ($Na_2S_2O_4$) degassed with argon was added to the cuvette (5:1, $S_2O_4^{2-}$lipid mol). After there was no significant change in signal upon release, and the fluorescence signal had plateaued, 30 μL of 30% Triton X-100 stock solution was added to lyse the remaining liposomes and free any calcein still encapsulated (total concentration 1.0% vol/vol). The percentage of calcein released with time can be calculated by normalizing the dynamic signal (I) with the average baseline (I_0) and maximum possible signal (I_{100}) which is determined by lysing the vesicle with Triton X-100 detergent (Equation 2.1).

Equation 2.1 $$\%\ Contents\ Release = \frac{I - I_0}{I_{100} - I_0} \times 100$$

To correlate the aggregation of liposomes with contents release, a light scattering study was carried out with the same stock solution used for contents release study. The experimental protocol is identical to the calcein contents release protocol outlined above but with an excitation/emission wavelengths of 600/610 nm and

excitation/emission monochromator slit widths of 5.0/5.0 nm. If the liposomes aggregate post $S_2O_4^{2-}$ addition, the incident light is scattered, and an increase in 610 nm signal is observed. The light scattering data can be normalized in the same manner as calcein. Figure 2.1 depicts the normalized calcein contents release and light scattering data of a 100 μM Q_{PA}-DOPE liposomal system in 100 mM KCl/0.10 mM EDTA, buffered with 50.0 mM phosphate, pH 7.40.

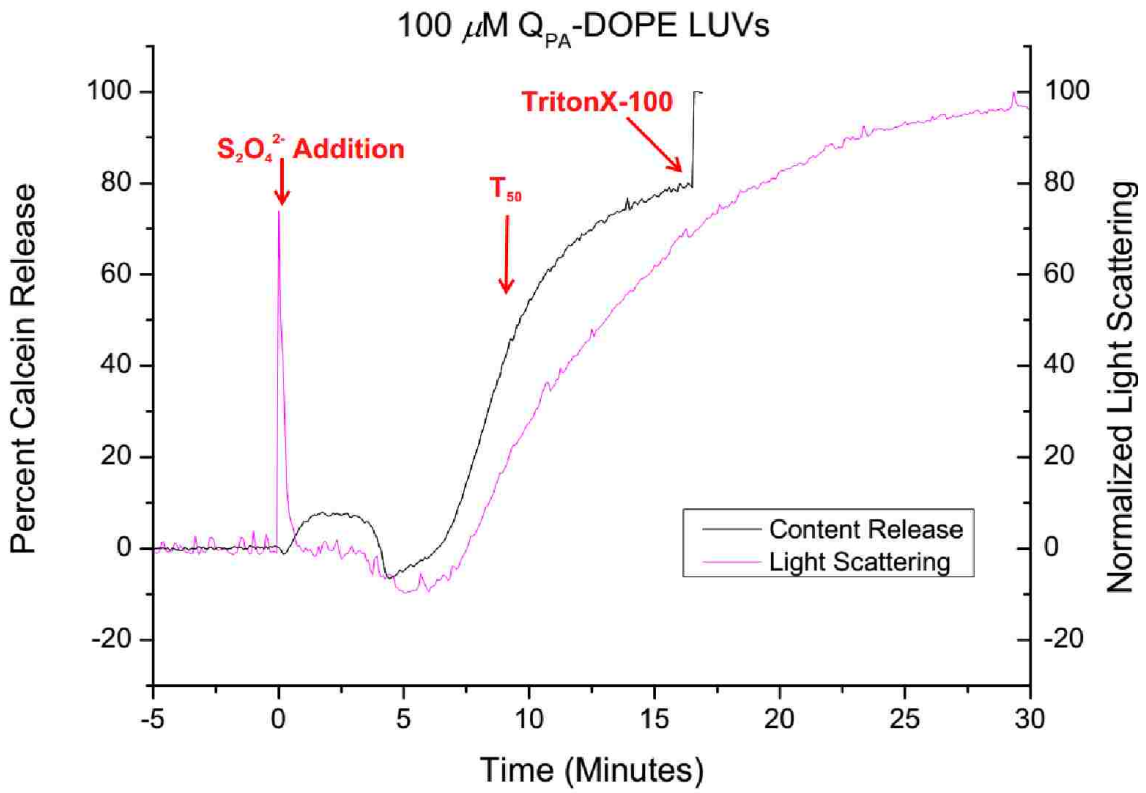

Figure 2.1. The content release curve of Q_{PA}-DOPE LUVs in PBS media (pH 7.40) triggered by $S_2O_4^{2-}$ addition. The time for 50% of the content to be released (T_{50}) is 10.2 min with 75% of the total contents being released. Triton X-100 was the surfactant used to lyse the remaining vesicles to determine 100% release.

2.4 Tb^{3+}/DPA^{2-} Fusion Assay

Wilschut et al. first reported a fluorescence contents mixing assay for fused vesicles that is based on encapsulating Tb^{3+} and dipicolinic acid (DPA^{2-}).[13,30] DPA instantly chelates Tb^{3+} to form a highly fluorescent $Tb(DPA)_3^{3-}$ complex that absorbs at 276 nm and emits at 490 and 545 nm. This assay has been widely used to

study the fusogenic properties of liposomes.[31] ANTS/DPX is another fusion assay commonly used to study liposomal content mixing; however, it has a pH dependence.[32,33]

2.4.1 Encapsulation Media

99.9% $TbCl_3$, 99.0% 2,6-pyridinecarboxylic acid (DPA), and 98.0% potassium citrate ($K_3C_6H_5O_7$) were obtained from Sigma-Aldrich (St. Louis, MO) at the highest purity available. Three different solutions of buffer media are needed for the Tb^{3+}/DPA^{2-} liposome fusion assay: one containing 5.0 mM $TbCl_3$ and 50.0 mM $K_3C_6H_5O_7$ buffered with 10.0 mM TES, pH 7.4 for encapsulation; a second containing 20.0 mM DPA^{2-} and 80 mM KCl buffered with 10.0 mM TES, pH 7.4 for encapsulation; and a third solution as an interstitial medium containing 100 mM KCl and 1.0 mM EDTA buffered with 10.0 mM TES, pH 7.4. To keep Tb^{3+} from binding with the anionic lipid bilayer, citrate is included in its buffer media as a weak chelator. The buffers were tuned to the same osmotic pressure by titrating with a 1.0 M KCl stock solution as to prevent unwanted contents leakage.

2.4.2 Reverse Phase Vaporization

LUVs encapsulated with their respective Tb^{3+} and DPA^{2-} media were prepared using a reverse phase vaporization.[23] 3–4 mg of lipid were dissolved in $CHCl_3$ and transferred to a 25-mL round-bottom flask. The solvent was removed with a rotary evaporator, and then placed on a high-vacuum line (< 2 Torr) for no less than 1 h. The lipid was dissolved in 0.6 mL of diethyl ether and 0.2 mL of the respective media for encapsulation added to the flask. The flask was sonicated for 5 min to ensure emulsification of the two phases. The flask was placed on a rotary evaporator (30 °C, 350 mm Hg, 200 RPM) until a gel was observed to form. The flask was vortexed

for 5 s (no more than 10 s) and then placed back on a rotary evaporator (30 °C, 150 mm Hg, 200 RPM) for 2 min before adding an additional 0.5 mL of the respective buffer medium. The flask was placed back on the rotary evaporator for a third time (30 °C, 10 mm Hg, 200 RPM) for 20–30 min to remove any latent ether. The aqueous solution containing the vesicles was extruded 11 times through a hand held, mini-extruder purchased from Avanti Polar Lipids (Birmingham, AL) and equipped with a 100-nm polycarbonate track-etched membrane.

2.4.3 Size-Exclusion Chromatography: Fusion Assay

A traditional gravimetric size-exclusion chromatography column was used to separate the non-encapsulated analytes from the liposomes. This method was selected over a spin column so as to minimize the force exerted on the liposomes in an attempt to avoid contents leakage. Two columns (20'' x 0.5'') were loaded with hydrated Sephadex G-50 fine; one contained 100 mM KCl/1.0 mM EDTA buffered with 10.0 mM TES, pH 7.4 and a second contained 100 mM KCl buffered with 10.0 mM TES, pH 7.40 (no EDTA). The entire volume of the liposomes after extrusion (~1 mL) was loaded onto their respective columns and the eluents were collected with disposable 10-mL glass test tubes. The liposomes coming off the column were observed by a distinct change in the solution, changing from clear to cloudiness in the eluting media. The concentrations of the eluted liposome solutions were determined by a Bartlett assay and stored on ice until they were used.

2.4.4 Ca^{2+}-induced Fusion

Fusion of anionic liposomes was observed by loading 50 μM of the liposome stock solution containing the DPA^{2-} media and 50 μM of the liposome stock solution containing the Tb^{3+} media, in a 3.0-mL quartz cuvette containing 100 mM KCl/1.0 mM EDTA

buffered with 10.0 mM TES, pH 7.40 as the matrix. The fluorescence was observed with a Perkin Elmer LS-55 Fluorimeter using the following parameters: excitation/emission wavelengths of 276 nm/545 nm, a 550 ± 10 nm bandpass filter equipped in front of the emission monochromator slit entrance, excitation/emission monochromator slit widths 2.5 nm/10 nm, 5 s data interval/1 second integration, 25 °C. A baseline signal was obtained for 5 min prior to injecting 50 μL of a 610 mM Ca^{2+} stock solution (10.0 mM Ca^{2+} final concentration).

2.5 Q_{PA}-DOPE Synthesis

This section begins with a word of caution. It is imperative that steps are taken to avoid any and all hydrocarbon contaminants, especially as they relate the final Q_{PA}-DOPE coupling reaction. Contaminants from silicon oil baths, glass ground-joint grease, and chemical impurities, such as urea, adversity impacts the performance of the liposome systems here. These species can intercalate into the non-polar region of the lipid membrane, which alter the phase behavior of the liposome.[34,35] To this end, all glassware, glass joint-attachments, and equipment used in this synthetic work were cleaned meticulously before each use. All glassware is cleaned with Alconox after use. The glassware used is kept in a base bath (500 g NaOH in 8 L isopropyl alcohol) for no less than 24 h prior to use. In the instances where a grease contamination was observed or suspected, the glassware in question was cleaned with Piranha solution (3:7 vol:vol 30% hydrogen peroxide:concentrated sulfuric acid). Please note: Piranha solution is a strong oxidizer and is extremely exothermic; take all safety precautions when preparing or handling this solution.

Lactone (1c)

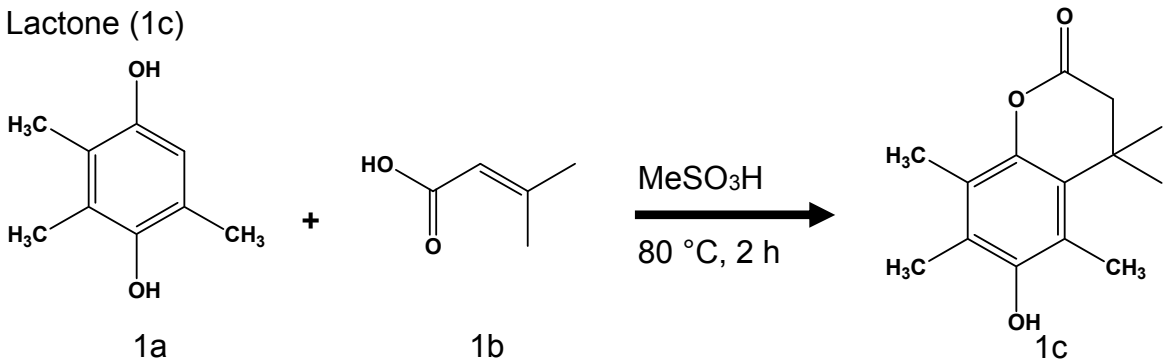

(1c). 2,3,5-trimethylhydroquinone 1a (1.0 g, 6.57 mmol) and 3,3–dimethylacrylic acid (0.724 g, 7.23 mmol) were added to 10 mL of methanesulfonic acid, and then the mixture was heated to 80 °C in a water bath with stirring. It is important to note that a water bath and not an oil bath was used to maintain temperature, so as to avoid hydrocarbon contamination. The mixture was stirred for 2 h, and then the reaction was diluted with 100 mL of H_2O, yielding a red-brown precipitate. The resulting inhomogeneous mixture was extracted with ethyl acetate (3 x 50 mL) or until the ethyl acetate was colorless. The collected ethyl acetate extracts were combined and washed with H_2O (1 x 50 mL) before being washed with a saturated $NaHCO_3$ solution (3 x 50 mL). The organic layer was washed a second time with H_2O and then with brine, before the organic layer was dried with $MgSO_4$. The solvent was removed with the aid of a rotary evaporator, affording a pail-brown solid. Recrystallization of the solid from acetone/hexanes (minimal acetone to dissolve) afforded 1.28 g (83%) of a white powder. ^{1}H NMR (400 MHz, $CDCl_3$) δ 1.46 ppm (s, 6H, geminal CH_3), 2.19 and 2.22 ppm (s, 3H, CH_3), 2.36 ppm (s, 3H, CH_3), 2.55 ppm (s, 2H CH_2). ^{13}C NMR (100.61 MHz, $CDCl_3$) δ 12.34, 12.56, 14.51, 27.72, 35.47, 46.07, 119.11, 122.06, 123.40, 128.19, 143.47, 148.92, and 169.08 ppm. HRMS (ESI) *m/z* $[M+H]^+$, calculated = 234.1256 (calculated for $C_{14}H_{18}O_3$), observed = 234.1258, -1.01 ppm error. (Appendix 7–8)

Quinone Propionic Acid (Q_{PA}, 2b)

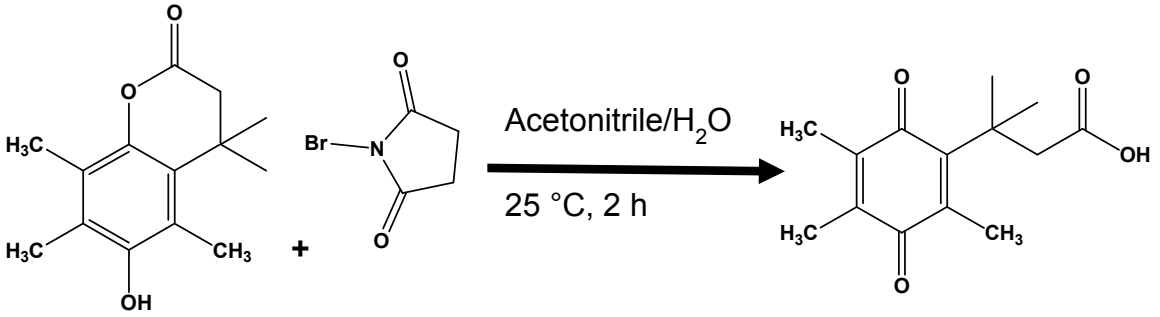

(2b)**.** The lactone product 1c (1.0 g, 4.27 mmol) was dissolved in a 30-mL solution of acetonitrile and water (9/1 vol/vol). *N*-Bromosuccinimide 2a (0.84 g, 4.70 mmol) was dissolved in 5 mL of the acetonitrile/water solution, and it was added dropwise over 1 h. The reaction was stirred for an additional hour after NBS addition, and this was then diluted with 200 mL with H_2O, transferred to a separatory funnel, and the product extracted using CH_2Cl_2 (3 x 50 mL) from the aqueous phase. The combined organic layers were washed with H_2O (1 x 50 mL) and then with brine (1 x 50 mL) before being dried over $MgSO_4$. The solvent was removed with a rotary evaporator to yield a yellow-brown solid. Recrystallization in acetone/hexane (minimal acetone to dissolve product) afforded 0.92 g (86%) of a yellow-brown crystalline solid. ^{1}H NMR (400 MHz, $CDCl_3$) δ 1.43 ppm (s, 6H, geminal CH_3), 1.93 and 1.96 ppm (s, 3H, CH_3), 2.14 (s, 3H, CH_3), 3.02 ppm (s, 2H CH_2). ^{13}C NMR (100.61 MHz, $CDCl_3$) δ 12.09, 12.49, 14.30, 28.79, 37.93, 47.26, 138.38, 139.03, and 142.98, 152.02, 178.74, 187.44, 190.85 ppm. HRMS (ESI) *m/z* [M+H]-, calculated = 250.1205 (calculated for $C_{14}H_{18}O_4$), observed = 250.1205, 0.06 ppm error (Appendix 9–10).

Quinone-NHS (3b)

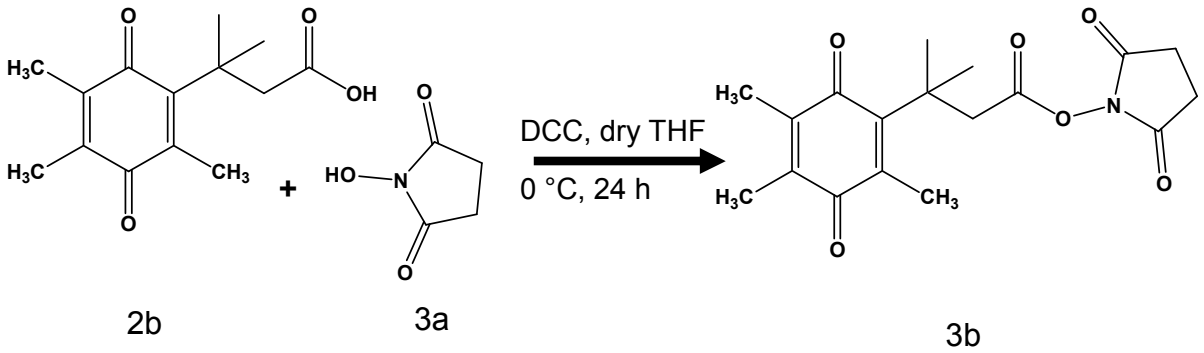

(3b). The quinone propionic acid (Q_{PA}) product 2b (0.5 g, 2.00 mmol) was dissolved in 20 mL of dry THF and then stirred at 0 °C under argon. *N*-Hydroxysuccinimide (NHS) 3a (0.25 g, 2.20 mmol) was dissolved in a minimal amount of dry THF, and this was added to the vessel containing the Q_{PA}/THF solution. Dicyclohexylcarbodiimide (DCC, 0.48 g, 2.20mmol) was dissolved in a minimal amount of dry THF with aid of sonication, and this was added to the reaction. The reaction was left to stir at 0 °C for 24 h under a positive pressure of argon. After completion, the reaction vessel contents (including the white urea precipitate) were dried over $MgSO_4$. Both the white urea precipitate and wet $MgSO_4$ were removed via vacuum filtration and rinsed with cold ethyl acetate. The yellow liquid was collected and the solvent was removed using a rotary evaporator. To remove the remaining urea impurity, the product was loaded onto a 50-g silica column using CH_2Cl_2. A mobile phase gradient of CH_2Cl_2/ethyl acetate (9/1 vol/vol) was used to elute the yellow product off the column, while the urea impurity was retained on the column. Yellow fractions were combined, and the solvent was removed via rotary evaporation, affording 0.69 g (64%) of a bright-yellow solid. ^{1}H NMR (400 MHz, $CDCl_3$) δ 1.55 ppm (s, 6H, geminal CH_3), 1.98 ppm (s, 6H, CH_3), 2.19 ppm (s, 3H, CH_3), 2.80 ppm (s, 4H CH_2), and

3.30 ppm (s, 2H CH_2). ^{13}C NMR (100.61 MHz, $CDCl_3$) δ 12.17, 12.20, 12.56, 25.98, 29.14, 38.84, 44.13, 138.78, 140.35, 142.81, 149.98, 167.87, 168.92, 187.33, and 190.25 ppm. HRMS (ESI) *m/z* [M+H]+, calculated = 347.1369 (calculated for $C_{18}H_{21}O_6N$), observed = 347.1359, 2.93 ppm error. (Appendix 11–12)

Q_{PA}-DOPE (4b)

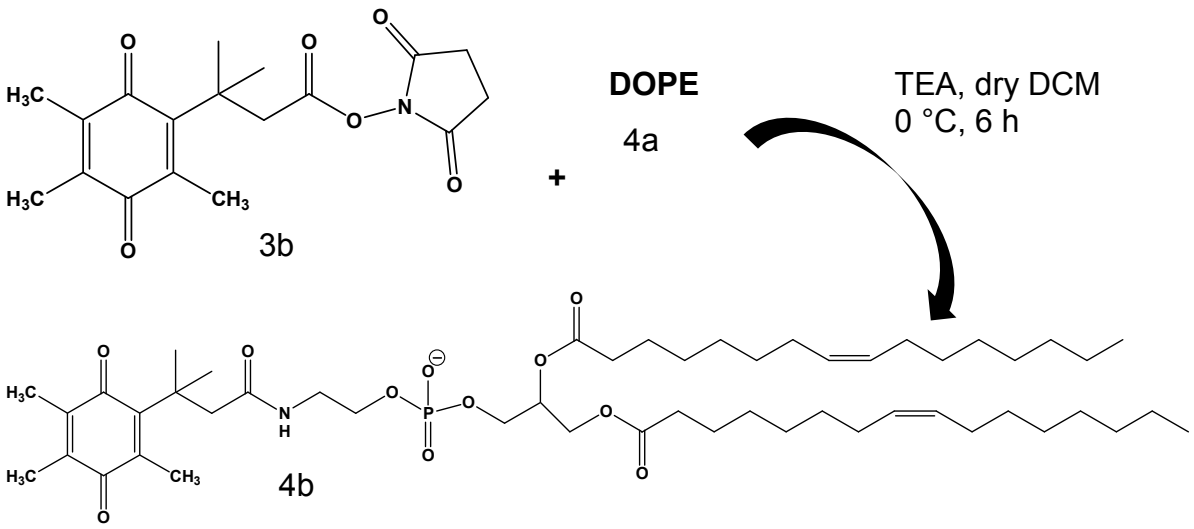

(4b). All lipid used in this work was purchased from Avanti Polar Lipids (Birmingham, AL). DOPE 4a (100 mg, 0.134 mmol) in powder form was dissolved in a minimal amount of dry CH_2Cl_2 and transferred to a three-neck round bottom flask. The exact mass of DOPE used was determined from weight by difference of the vial containing the lipid. The flask was purged with argon and placed in an ice bath (0 °C). The Q_{PA}-NHS head group 3b (51.2 mg, 147 mmol) was dissolved in a minimal amount of dry CH_2Cl_2 and added to the DOPE-containing flask. Triethylamine (TEA, 66 µL, 47.5 mg, 0.469 mmol) was added, and the reaction was stirred at 0 °C under argon for 6 h. The reaction contents were transferred to a separatory funnel, and then washed with 5 % $NaHCO_3$ (3 x 50 mL). The organic layer was washed with H_2O (1 x 50 mL) and brine (1 x 50 mL) before being dried over Na_2SO_4. The solvent was removed with

a rotary evaporator before being loaded onto a 15-g silica column. The column was packed with CH_2Cl_2. Once the product was loaded onto the column, the mobile phase was changed to CH_2Cl_2/ethyl acetate (1:1 vol). Two yellow bands were observed: the eluting band was excess Q_{PA}-NHS, and the retained band was Q_{PA}-DOPE. Once the first band had eluted, an equal column volume of the mobile phase was allowed to pass through the column. A second mobile phase of CH_2Cl_2/MeOH/hexanes (3:1:2 vol/vol) was used to elute the product. This yellow band was collected, and the solvent removed via rotary evaporation to yield 111.47 mg (85%) of a yellow waxy film. ^{1}H NMR (400 MHz, $CDCl_3$) δ 0.90 ppm (t, 6H CH_3), 1.29 ppm (bs, 40H CH_2), 1.40 ppm (s, 6H, geminal CH_3), 1.60 ppm (bs, 4H CH_2), 1.96 ppm (s, 8H CH_2), 2.02 ppm (s, 6H CH_3), 2.13 ppm (s, 3H, CH_3), 2.31 ppm (bs, 4H, CH_2), 2.87 ppm (s, 2H CH_2), 3.39 ppm (s, 2H CH_2), 3.88 ppm (s, 2H CH_2), 3.96 ppm (s, 2H CH_2), 4.42 ppm and 4.44 ppm (split s, 2H CH_2), 5.35 ppm (s, 1H CH), 5.36 ppm (s, 4H CH). HRMS (ESI) *m/z* $[M+H]^+$, calculated = 975.6564 (calculated for $C_{55}H_{95}O_{11}NP$), observed = 975.6556, 0.83 ppm error (Appendix 13–14).

2.6 Q_{Br}-DOPE Synthesis

2,6-dimethyl-hydroquinone lactone (5b)

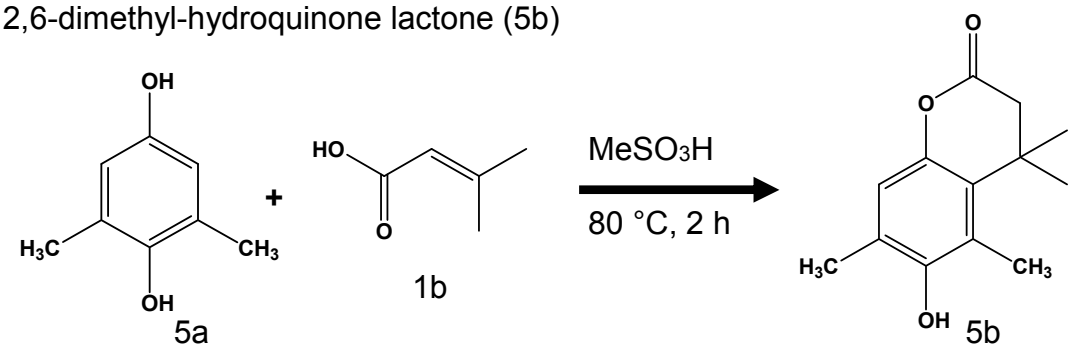

(5b). 2,6-dimethyl-hydroquinone (5a) was purchased from TCI America (Philadelphia, PA). 5a (1.0 g, 7.25 mmol) and 3,3-dimethylacrylic acid (1b, 0.78 g, 7.75 mmol) were dissolved in 20 mL of methanesulfonic acid and then

stirred at 80 °C for 2 h. The reaction mixture was diluted to 200 mL with water, and the product was extracted with ethyl acetate (3 × 50 mL). The combined ethyl acetate extracts were then washed with H_2O (1 x 50 mL), saturated $NaHCO_3$ solution (3 × 50 mL), H_2O (1 x 50 mL), and brine (1 x 50 mL), followed by drying over $MgSO_4$. The solvent was removed by rotary evaporation to yield a light-brown solid. This product was recrystallized in acetone/hexane (minimal acetone to dissolve product) to afford 1.17 g (74%). ^{1}H NMR (400 MHz, $CDCl_3$) δ 1.46 ppm (s, 6H, geminal CH_3), 2.23 and 2.38 ppm (s, 3H, CH_3), 2.57 ppm (s, 2H, CH_2), 4.50 ppm (s, 1H, OH), 6.73 ppm (s, 1H, aryl H). ^{13}C NMR (100.61 MHz, $CDCl_3$) δ 14.42, 15.90, 27.75, 35.39, 46.02, 116.81, 122.10, 122.68, 128.57, 144.80, 149.26, and 168.78 ppm. HRMS (ESI) *m/z* $[M-H]^-$, calculated = 219.1020 (calculated for $C_{13}H_{15}O_3$), observed = 219.1026, −2.9 ppm error (Appendix 15–16).

1-bromo-2,4-dimethyl-quinone propionic acid (Q_{Br}-Acid, 6b)

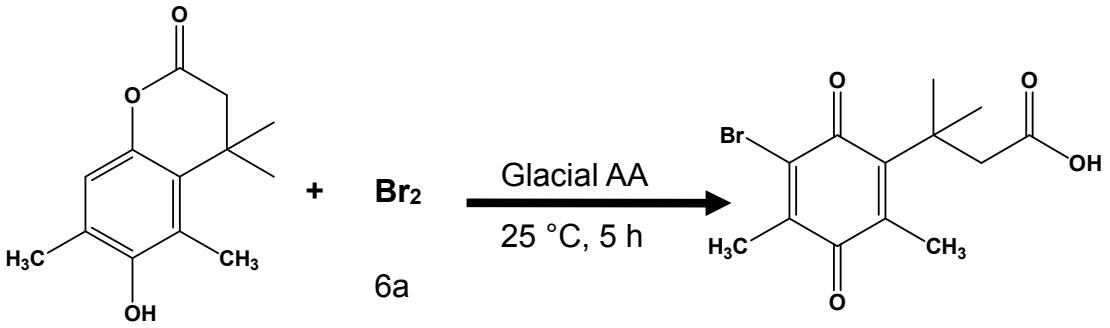

5b 6b

(6b). 2,6-dimethyl-hydroquinone lactone 5b (1.0 g, 7.25 mmol) was dissolved in 20 mL of glacial acetic acid. A ≥ 99.5% bromine solution 6a (1.1 g, 6.88 mmol) in 5.0 mL of acetic acid was added dropwise over 1 h, and the mixture was stirred for an additional 5 h at room temperature. The reaction was diluted with 100 mL H_2O, and the product extracted with CH_2Cl_2 (3 x 50 mL). The combined CH_2Cl_2 extracts were washed

with H_2O (1 x 50 mL), and 6b was extracted by saturated sodium bicarbonate washes (3 x 50 mL). 6b was precipitated from the combined sodium bicarbonate washes by acidifying the solution with 30% HCl. The yellow precipitate (6b) was brought up in $CHCl_3$ (3 x 50 mL). After rinsing with water (1 x 50 mL), a saturated sodium bicarbonate solution was slowly added to neutralize any remaining acid, with subsequent rinsing with H_2O (1 x 50 mL) and with brine (1 x 50 mL). The product was dried over $MgSO_4$, and the solvent was removed by rotary evaporation, affording 0.75 g (52%) of a brown waxy solid (6d). ^{1}H NMR (400 MHz, $CDCl_3$) δ 1.47 ppm (s, 6H, geminal CH_3), 2.19 ppm (s, 3H, CH_3), 2.21 ppm (s, 3H, CH_3), 3.06 ppm (s, 2H CH_2). HRMS (ESI) *m/z* $[M+H]^+$, calculated = 314.0159 (calculated for $C_{13}H_{15}O_4Br$), observed = 314.0115, 0.16 ppm error (Appendix 17).

Q_{Br}-NHS (7a)

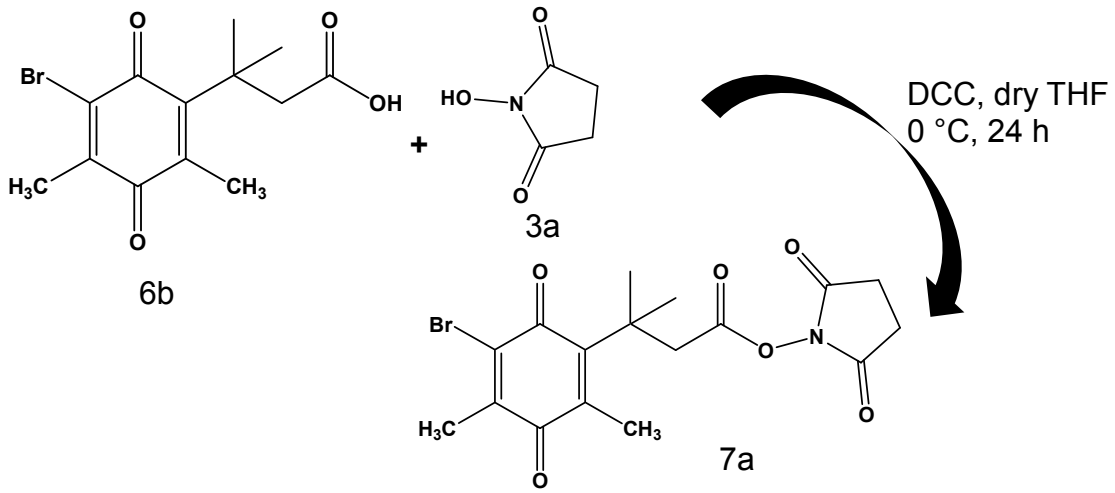

(7a). 1-bromo-2,4-dimethyl-quinone propionic acid 6b (0.5 g, 1.6 mmol), *N*-hydroxysuccinimide 3a (0.21 g, 1.8 mmol), and dicyclohexylcarbodiimide (0.37 g, 1.8 mmol) were dissolved in 50 mL of dry THF at 0 °C under argon. The reaction was stirred for 24 h. The white dicyclohexylurea precipitate was removed via vacuum filtration and the solvent was removed with a rotary evaporator. To remove any latent

urea, 7a was dissolved in a minimal amount of CH_2Cl_2 and added onto a 50-g silica column. The product was eluted off the column with a CH_2Cl_2/ethyl acetate grandient mobile phase (95/5 vol/vol) with collection of the yellow band. The solvent was removed by rotary evaporation to yield 0.37 g (56%) of 7a-a bright yellow solid. ^{1}H NMR (400 MHz, $CDCl_3$) δ 1.56 ppm (s, 6H, geminal CH_3), 2.17 ppm (s, 3H, CH_3), 2.23 ppm (s, 3H, CH_3), 2.78 ppm (s, 4H CH_2), 3.26 ppm (s, 2H CH_2). ^{13}C NMR (100.61 MHz, $CDCl_3$) δ 14.70, 15.87, 25.88, 29.94, 39.72, 44.49, 135.28, 142.07, 142.24, 149.12, 167.87, 169.22, 187.56, and 189.56 ppm. HRMS (ESI) *m/z* $[M+H]^+$, calculated = 412.0396 (calculated for $C_{17}H_{19}O_6NBr$), observed = 412.0398, 0.58 ppm error (Appendix 18–19).

Q_{Br}-DOPE (8a)

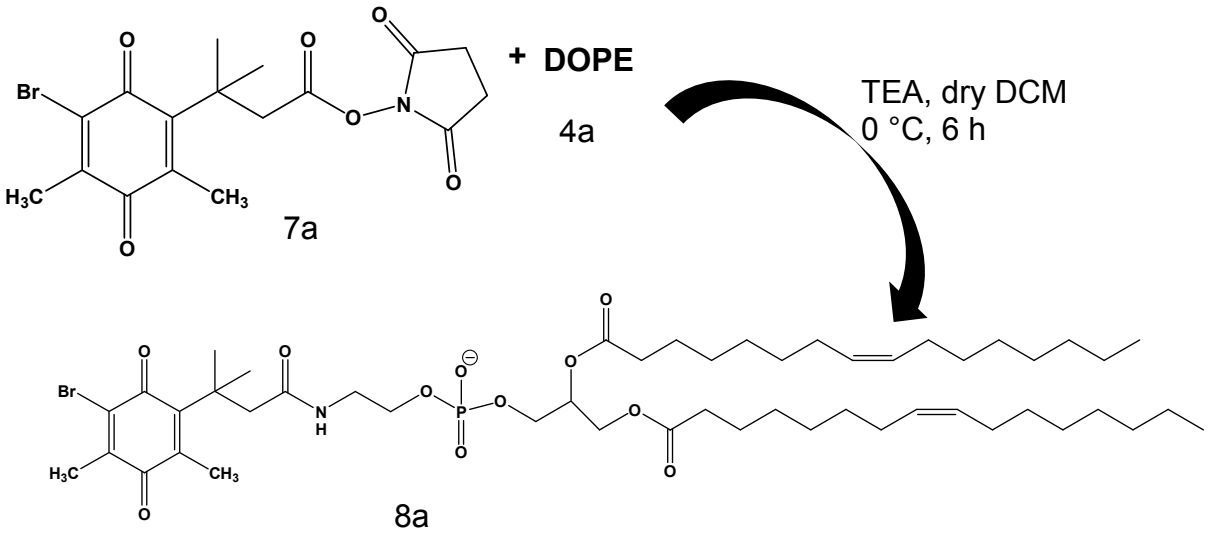

(8a). All lipids used in this work were purchased from Avanti Polar Lipids (Birmingham, AL). DOPE (109 mg, 0.147 mmol) in powder form was dissolved in a minimal amount of dry CH_2Cl_2 and transferred to a three-neck round bottom flask. Its exact mass was determined from weight by difference of the vial. The flask was purged with argon and placed in an ice bath (0 °C). The 1-bromo Q_{PA}-NHS head group

7a (62.2 mg, 0.151 mmol) was dissolved in a minimal amount of dry CH_2Cl_2 and added to the DOPE containing flask. Triethylamine (TEA) (66 μL, 47.5 mg, 0.469 mmol) was added, and the reaction was stirred at 0 °C under argon for 6 h. The reaction contents were transferred to a separatory funnel and washed with 5% $NaHCO_3$ (3 x 50 mL). The organic layer was then washed with H_2O (1 x 50 mL) and brine (1 x 50 mL) before drying over Na_2SO_4. The solvent was removed with a rotary evaporator, brought up in a minimal volume of $CHCl_3$, then the liquid was loaded onto a 15-g silica column. The column was packed with CH_2Cl_2. Once the product was loaded onto the column the mobile phase was changed to CH_2Cl_2/ethyl acetate (1:1 vol/vol). Two bands were observed: the eluting band consisting of excess Q_{Br}-NHS 7a (yellow) and a retained red-brown band containing 8a. Once the first band had eluted, an equal column volume of the mobile phase was allowed to pass through the column. A second mobile phase of CH_2Cl_2/MeOH/hexanes (3:1:2 vol/vol) was used to elute the product. Two bands are observed to elute: a leading red-brown impurity and a second brown-yellow band 8a. This brown-yellow band was collected and the solvent removed via rotary evaporation to yield 152 mg (63%) of 8a as a brown-yellow wax. ^{1}H NMR (400 MHz, $CDCl_3$) δ 0.88 ppm (t, 6H CH_3), 1.27 ppm (bs, 40H CH_2), 1.40 ppm (s, 6H, geminal CH_3), 1.58 ppm (bs, 4H CH_2), 2.00 ppm (s, 8H CH_2), 2.14 ppm (s, 6H CH_3), 2.31 ppm (q, 4H, CH_2), 2.87 ppm (s, 2H CH_2), 3.38 ppm (s, 2H CH_2), 3.87 ppm (s, 2H CH_2), 3.95 ppm (s, 2H CH_2), 4.17 ppm and 4.40 ppm (split s, 2H CH_2), 5.25 ppm (s, 1H CH), 5.34 ppm (s, 4H CH). HRMS (ESI) *m/z* $[M+H]^+$, calculated = 1038.5440 (calculated for $C_{54}H_{90}O_{11}NP$), observed = 1038.5445, 0.54 ppm error (Appendix 20).

2.7 Physical Characterization of Liposomes

Measurements of a lipid system's physical properties (i.e., hydration, transition states T_M/T_H, phase, surface potential, size) are used to qualify and quantify a lipid's response to a stimulus.[36,37] For the scope of this work, three physical properties of liposomes are needed: (1) the quality of dispersion of the liposomal system as a colloid solution, (2) the surface charge profile of the liposome particles in solution, and (3) the transition temperatures of the $L_\beta \rightarrow L_\alpha$ and $L_\alpha \rightarrow H_{II}$ phases, T_M and T_H, respectively. In the work presented herein, dynamic light scattering (DLS), zeta potential, and differential scanning calorimetry (DSC) were used to make these measurements, respectively. This section covers the methodology of these experiments.

2.7.1 Dynamic Light Scattering

Dynamic light scattering (DLS) was used as a quality control support tool to provide liposome size and dispersion measurements. In a typical study, 0.4 mL of a 100 μM liposomal stock solution was added to a 12-mm square plastic DLS cuvette (Malvern, DTS0012) and placed in a Malvern Zetasizer (Worcestershire, UK). The size and dispersion are measured in triplicate and an average with statistical error reported. For a 100-nm size extrusion, the measured diameter will be between 100–120 nm. Well dispersed vesicles will have a PDI of ≤ 2.0, which is indicative of a mono-dispersed colloid solution.[38,39] A PDI >> 2.0 can be an indication of poly-dispersed particles (Appendix 21).

2.7.2 Zeta Potential

Liposomes, and charged particles alike, polarize and interact with nearby water molecules at their surface-water interface.[40-43] A commonly reported physical value of this property is a particle's zeta potential (ζ).[44-46] This is the potential energy (mV)

measured at the slipping plane or near the outer edge of the double layer and is an indicator of colloidal stability.[47,48] For liposomes, this value is an indirect measurement of their surface potential and is a reflection of their stability not to aggregate because of charge repulsion from opposed bilayers.[37] A typical liposome made up of anionic lipids that are stable will have a zeta potential ~ –50 mV.[48] As opposed liposomes come into contact, this value should decrease (less negative) due to a decrease in the charge repulsion forces on the membranes' surfaces

A Malvern Zetasizer (Worcestershire, UK) was used to measure the zeta potential of liposomes. A 1.0-mL aliquot of a 100 μM liposomal stock solution was added to a Folded Capillary Zeta Cell (Malvern, DTS1070) via a 1.0-mL disposable syringe, taking care to avoid air bubbles. The cell was placed in the Zetasizer, and the potential was measured no less than 3 times for statistical purposes (Appendix 22).

2.7.3 Differential Scanning Calorimetry

Differential scanning calorimetry (DSC) is an analytical method used to measure the thermodynamics between phases.[49] DSC functions by applying heat to a lipid system and referencing the change in temperature to the same buffer media absent lipids. Two lipid thermal phase transitions may be observed between $L_\beta \rightarrow L_\alpha$ and $L_\alpha \rightarrow H_{II}$ phases corresponding to T_M and T_H respectively.[1, 50]

In a typical procedure, 9.4 μmol of lipid were dissolved in $CHCl_3$, transferred into a 10.0-mL ground-glass joint test tube, and the solvent removed via rotary evaporation. The sample was placed on high vacuum (< 2 Torr) for ≥ 1 h before being hydrated with 0.5 mL (18.8 mM total lipid concentration) of either 200 mM sucrose or DI-Nanopure water. The sample was kept at a temperature above its T_M and below it T_H during the hydration process. After ≥ 30 min of initial hydration, the sample was subject to

6 freeze/thaw cycles, using a dry ice/acetone bath to freeze the sample. The sample was stored below its T_M before use.

A Microcal Differential Scanning Calorimeter (GE Heath Sciences, Piscataway, NJ) was used for DSC analysis. Prior to lipid analysis, 0.52 mL of the hydrating media were given to both the sample and reference pans and no less than 12 background spectra were acquired. For each scan, the cells were set to start and hold at 10 °C for 15 min, then the temperature was raised to 85 °C at a rate of 60 °C h^{-1}, holding for 5 min before cycling back to 10 °C at a rate of 60 °C h^{-1}. Once overlap between the background scans were observed, the sample chamber was emptied and the prepared lipid sample added to the one chamber. One upward scan was acquired for each lipid.

2.8 ^{31}P NMR Anisotropy

Understanding the phase behavior of a liposomal DDS before and after application of a stimulus gives insight into the system's pathway for contents release. X-ray diffraction, DSC, Cryo-TEM, and ^{31}P NMR can be used to measure the phase of a lipid.[50-57] X-ray diffraction is the ideal method for determining structure, phase, and hydration of a lipid system; however, this method requires specialized instrumentation with both temperature and humidly chambers.[58-61] Moreover, the dynamics and time frame of Q_{PA}-DOPE reduction and release might prove too challenging for this method, and it has yet to be explored for this system.[62,63] DSC measurements are sensitive to changes in salt concentration, so the addition of $Na_2S_2O_4$ to reduce the lipid makes this method a dubious challenge.[64] Cryo-TEM has been used to study the phase identity of liposomes; however, resolution can be a challenge and time-dependent sample preparation to meet the needs of the required experimental time for Q_{PA}-DOPE analysis

does not make this method easily used. ^{31}P NMR has widely been used as a method to detect the phase of a lipid in a large array of aqueous environments for MLVs.[51,65-68] ^{31}P NMR has the most potential to obtain information on the phase transition of Q_{PA}-DOPE; however, due to the chemical nature of Q_{PA}-DOPE and anisotropy constraints of the method, unilamellar vesicles > 1-μm diameter must be used.[69] Methods to prepare GUVs have been published in literature, but none at a large enough scale and concentration to generate adequate ^{31}P NMR signal.

2.8.1 Hot Buffer Hydration

The challenge is to prepare a large quantity of GUVs at a relatively high concentration. To prepare Q_{PA}-DOPE GUVs, a modification of the procedure first described by Hub et al. was used.[70] 50 mg of Q_{PA}-DOPE was dissolved in 30 mL CH_2Cl_2 and transferred into a 500 mL round bottom flask. The solvent was removed with a rotary evaporator leaving a lipid film on the inner wall of the round bottom flask, characterized by sequential circle layers encompassing the widest part of the flask and 25% down the surface of the flask. The flask containing the film was placed on high vacuum (< 2 Torr) for no less than 1 h to ensure total evaporation of the solvent. The sample was hydrated at 80 °C in 500 mL of a 2.00 x 10^{-2} mM sucrose solution buffered with 10.0 mM TES, pH 7.40. The hydration typically takes, 12 h but can take as long as 5 days, depending on the lipid and temperature. However, the various stages towards completion can be observed as follows: (1) strings of liposomes form in the center around the walls, (2) a circular cloud of liposomes form at the center, and (3) massive aggregation of the circular cloud into a dense sphere. Once the sphere has formed, the GUVs were harvested.

2.8.2 Giant Unilamellar Vesicle Harvesting

The GUV aggregate was collected with a disposable glass Pasteur pipette and transferred into a 2-mL plastic Eppendorf centrifuge vial. The solution was centrifuged at 10,000 x *g* for 3 min: The GUVs settled to the bottom as a colloidal suspension, and the excess aqueous media (1.00 x 10^{-2} mM sucrose buffered with 10.0 mM TES, pH 7.40) was decanted: the GUVs were suspended in 100 mM KCl buffered with 10.0 mM TES, pH 7.40 and centrifuged at 10,000 x *g* for an additional 3 min. With care, the vesicles were collected with a 14'' disposable glass Pasteur pipette and transferred into a specialized NMR tube. 75 μL of D_2O having the same osmotic pressure as the buffered media was added to the NMR tube with gentle mixing.

2.8.3 NMR Experimental: Shigemi NMR Tube & {^{1}H} ^{31}P Spin-echo

A 5-mm Shigemi NMR tube (Shigemi, Allison Park, PA) having the same magnetic susceptibility as D_2O was used for all ^{31}P NMR anisotropy experiments. All NMR experiments were performed on either a Bruker DPX-400 or Bruker AV-400, both operating at a frequency of 161.9 MHz. A ^{1}H-decoupled ^{31}P spin-echo pulse sequence was used to acquire the T_2 relaxation profile of the lipid structures (Figure 2.2). Typically, 2,048 transient scans were acquired, but in instances of weak signal due to dilute sample; as many as 40,960 transients were acquired.

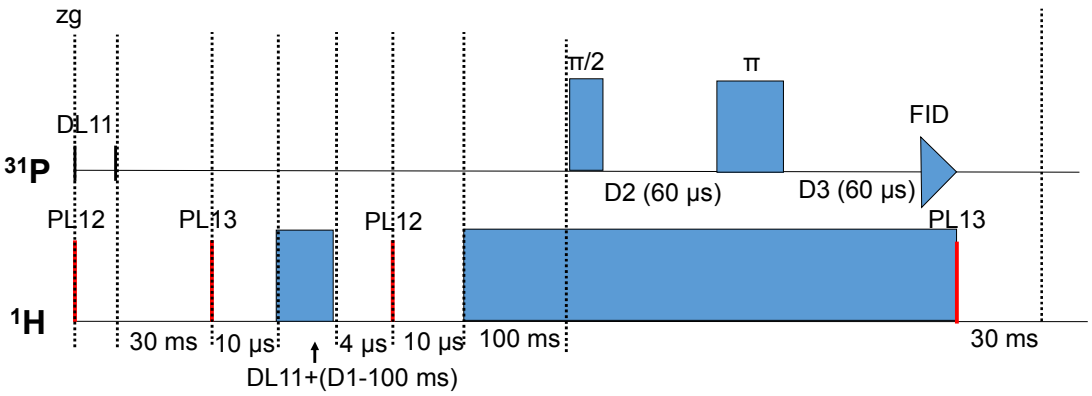

Figure 2.2 The schematic of the {^{1}H} ^{31}P NMR spin-echo pulse sequence used to study the anisotropy behavior of lipid structures. PL12 and PL13 represent the power level for ^{1}H decoupling preset by the NMR, DL11 is a 30 ms disk delay to account for the instrument hardware response, D1 is a relaxation delay for the ^{1}H steady-state pulse, D2 and D3 are the relaxation delays after the 90° and 180° pulses to obtain T_2 phase coherency and delayed relaxation, and the free induction decay (FID) represents the period of time data is acquired.

2.9 References

(1) Gruner, S. M., Non-lamellar Lipid Phases. In *The Structure of Biological Membranes; Yeagle, P.L. Ed.;* CRC Press: Boca Raton, Florida, 2005, pp 173-199.

(2) Levin, Y.; Idiart, M. A., Pore Dynamics of Osmotically Stressed Vesicles. *Physica A: Statistical Mechanics and its Applications* **2004,** *331* (3–4), 571-578.

(3) Casal, H. L.; Mantsch, H. H.; Hauser, H., Infrared Studies of Fully Hydrated Saturated Phosphatidylserine Bilayers. Effect of Li^{+} and Ca^{2+}. *Biochemistry* **1987,** *26* (14), 4408-4416.

(4) Petersheim, M.; Halladay, H. N.; Blodnieks, J., Tb^{3+} and Ca^{2+} Binding to Phosphatidylcholine. A study Comparing Data from Optical, NMR, and Infrared Spectroscopies. *Biophysical Journal* **1989,** *56* (3), 551-557.

(5) Koter, M.; de Kruijff, B.; van Deenen, L. L., Calcium-Induced Aggregation and Fusion of Mixed Phosphatidylcholine-Phosphatidic Acid Vesicles as Studied by ^{31}P NMR. *Biochimica et Biophysica Acta* **1978,** *514* (2), 255-263.

(6) Good, N. E.; Winget, G. D.; Winter, W.; Connolly, T. N.; Izawa, S.; Singh, R. M. M., Hydrogen Ion Buffers for Biological Research. *Biochemistry* **1966,** *5* (2), 467-477.

(7) Good, N. E.; Izawa, S.,Hydrogen Ion Buffers. In *Methods in Enzymology*, Anthony San, P., Ed. Academic Press: 1972; Vol. Volume 24, pp 53-68.

(8) Ferguson, W. J.; Braunschweiger, K. I.; Braunschweiger, W. R.; Smith, J. R.; McCormick, J. J.; Wasmann, C. C.; Jarvis, N. P.; Bell, D. H.; Good, N. E., Hydrogen Ion Buffers for Biological Research. *Analytical Biochemistry* **1980,** *104* (2), 300-310.

(9) Goldberg, R. N.; Kishore, N.; Lennen, R. M., Thermodynamic Quantities for the Ionization Reactions of Buffers. *Journal of Physical and Chemical Reference Data* **2002,** *31* (2), 231-370.

(10) Duzgunes, N.; Allen, T. M.; Fedor, J.; Papahadjopoulos, D., Lipid Mixing During Membrane Aggregation and Fusion: Why Fusion Assays Disagree. *Biochemistry* **1987,** *26* (25), 8435-8442.

(11) McLaughlin, S.; Mulrine, N.; Gresalfi, T.; Vaio, G.; McLaughlin, A., Adsorption of Divalent Cations to Bilayer Membranes Containing Phosphatidylserine. *Journal of General Physiology* **1981,** *77* (4), 445-473.

(12) Kendall, D. A.; MacDonald, R. C., A Fluorescence Assay to Monitor Vesicle Fusion and Lysis. *Journal of Biological Chemistry* **1982,** *257* (23), 13892-13895.

(13) Wilschut, J.; Duzgunes, N.; Fraley, R.; Papahadjopoulos, D., Studies on the Mechanism of Membrane Fusion: Kinetics of Calcium Ion Induced Fusion of Phosphatidylserine Vesicles Followed by a New Assay for Mixing of Aqueous Vesicle Contents. *Biochemistry* **1980,** *19* (26), 6011-6021.

(14) Shang, X.; Liu, Y.; Yan, E.; Eisenthal, K. B., Effects of Counterions on Molecular Transport Across Liposome Bilayer: Probed by Second Harmonic Generation. *The Journal of Physical Chemistry B* **2001,** *105* (51), 12816-12822.

(15) Liu, Y.; Yan, E. C.; Eisenthal, K. B., Effects of Bilayer Surface Charge Density on Molecular Adsorption and Transport Across Liposome Bilayers. *Biophysical Journal* **2001,** *80* (2), 1004-1012.

(16) Kirk, G. L.; Gruner, S. M.; Stein, D. L., A Thermodynamic Model of the Lamellar to Inverse Hexagonal Phase Transition of Lipid Membrane-Water Systems. *Biochemistry* **1984,** *23* (6), 1093-1102.

(17) Anderson, D. M.; Gruner, S. M.; Leibler, S., Geometrical Aspects of the Frustration in the Cubic Phases of Lyotropic Liquid Crystals. *Proceedings of the National Academy of Sciences of the United States of America* **1988,** *85* (15), 5364-5368.

(18) Szoka, F., Jr.; Papahadjopoulos, D., Comparative Properties and Methods of Preparation of Liipid Vesicles (Liposomes). *Annual Review of Biophysics and Bioengineering* **1980,** *9*, 467-508.

(19) Lasic, D. D., The Mechanism of Vesicle Formation. *The Biochemical Journal* **1988,** *256* (1), 1-11.

(20) Vemuri, S.; Rhodes, C. T., Preparation and Characterization of Liposomes as Therapeutic Delivery Systems: A Review. *Pharmaceutica acta Helvetiae* **1995,** *70* (2), 95-111.

(21) Mayer, L. D.; Hope, M. J.; Cullis, P. R., Vesicles of Variable Sizes Produced by a Rapid Extrusion Procedure. *Biochimica et Biophysica Acta* **1986,** *858* (1), 161-168.

(22) Hope, M. J.; Bally, M. B.; Webb, G.; Cullis, P. R., Production of Large Unilamellar Vesicles by a Rapid Extrusion Procedure: Characterization of Size Distribution, Trapped Volume and Ability to Maintain a Membrane Potential. *Biochimica et Biophysica Acta* **1985,** *812* (1), 55-65.

(23) Szoka, F., Jr.; Papahadjopoulos, D., Procedure for Preparation of Liposomes with Large Internal Aqueous Space and High Capture by Reverse-Phase Evaporation. *Proceedings of the National Academy of Sciences of the United States of America* **1978,** *75* (9), 4194-4198.

(24) Bartlett, G. R., Phosphorus Assay in Column Chromatography. *The Journal of Biological Chemistry* **1959,** *234* (3), 466-468.

(25) Stewart, J. C. M., Colorimetric Determination of Phospholipids with Ammonium Ferrothiocyanate. *Analytical Biochemistry* **1980,** *104* (1), 10-14.

(26) Tejera-Garcia, R.; Connell, L.; Shaw, W. A.; Kinnunen, P. K. J., Gravimetric Determination of Phospholipid Concentration. *Chemistry and Physics of Lipids* **2012,** *165* (6), 689-695.

(27) Beaugrand, M.; Arnold, A. A.; Hénin, J.; Warschawski, D. E.; Williamson, P. T. F.; Marcotte, I., Lipid Concentration and Molar Ratio Boundaries for the Use of Isotropic Bicelles. *Langmuir* **2014,** *30* (21), 6162-6170.

(28) Duzgunes, N.; Hoekstra, D.; Hong, K.; Papahadjopoulos, D., Lectins Facilitate Calcium-Induced Fusion of Phospholipid Vesicles Containing Glycosphingolipids. *FEBS Letters* **1984,** *173* (1), 80-84.

(29) Zuidam, N. N.; Van Winden, E.; de Vruch, R.; Crommelin, D. J. A., Stability, Storage and Sterilization of Liposomes. In: *Liposomes*. 2nd ed.; Torchilin, V. P., and Wessig, V. (Eds.); Oxford University Press: **2003**; p 149.

(30) Wilschut, J.; Papahadjopoulos, D., Ca^{2+}-Induced Fusion of Phospholipid Vesicles Monitored by Mixing of Aqueous Contents. *Nature* **1979,** *281* (5733), 690-692.

(31) Glaser, P. E.; Gross, R. W., Plasmenylethanolamine Facilitates Rapid Membrane Fusion: A Stopped-Flow Kinetic Investigation Correlating the Propensity of a Major Plasma Membrane Constituent to Adopt an H_{II} Phase with its Ability to Promote Membrane Fusion. *Biochemistry* **1994,** *33* (19), 5805-5812.

(32) Duzgunes, N., Fluorescence Assays for Liposome Fusion. *Methods in Enzymology* **2003,** *372*, 260-274.

(33) Duzgunes, N.; Wilschut, J., Fusion Assays Monitoring Intermixing of Aqueous Contents. *Methods in Enzymology* **1993,** *220*, 3-14.

(34) Blein, J. P.; Ducruet, J. M.; Gauvrit, C., Identification and Biological Activity of an Impurity of Technical Diuron. *Weed Research* **1979,** *19* (2), 117-121.

(35) Siegel, D. P.; Banschbach, J.; Yeagle, P. L., Stabilization of H_{II} Phases by Low Levels of Diglycerides and Alkanes: an NMR, Calorimetric, and X-ray Diffraction Study. *Biochemistry* **1989,** *28* (12), 5010-5019.

(36) Hirsch-Lerner, D.; Barenholz, Y., Hydration of Lipoplexes Commonly Used in Gene Delivery: Follow-up by Laurdan Fluorescence Changes and Quantification by Differential Scanning Calorimetry. *Biochimica et Biophysica Acta* **1999,** *1461* (1), 47-57.

(37) Carrión, F. J.; De La Maza, A.; Parra, J. L., The Influence of Ionic Strength and Lipid Bilayer Charge on the Stability of Liposomes. *Journal of Colloid and Interface Science* **1994,** *164* (1), 78-87.

(38) E. C. M. Cabral, R. L. Z., and M. H. A. Santana, Preparation and Charcaterization of Liposomes Entratpping Allergenic Proteins. *Brazilian Journal of Chemical Engineering* **2004,** *21* (2), 137-146.

(39) Ruozi, B.; Tosi, G.; Forni, F.; Fresta, M.; Vandelli, M. A., Atomic Force Microscopy and Photon Correlation Spectroscopy: Two techniques for Rapid Characterization of Liposomes. *European Journal of Pharmaceutical Sciences* **2005,** *25* (1), 81-89.

(40) Ninham, B. W.; Yaminsky, V., Ion Binding and Ion Specificity: The Hofmeister Effect and Onsager and Lifshitz Theories. *Langmuir* **1997,** *13* (7), 2097-2108.

(41) McLaughlin, S., The Electrostatic Properties of Membranes. *Annual Review of Biophysics and Bophysical Chemistry* **1989,** *18*, 113-136.

(42) McLaughlin, S.; Mulrine, N.; Gresalfi, T.; Vaio, G.; McLaughlin, A., Adsorption of Divalent Cations to Bilayer Membranes Containing Phosphatidylserine. *The Journal of General Physiology* **1981,** *77* (4), 445-473.

(43) Parsons, D. F.; Bostrom, M.; Nostro, P. L.; Ninham, B. W., Hofmeister Effects: Interplay of Hydration, Nonelectrostatic Potentials, and Ion Size. *Physical Chemistry Chemical Physics* **2011,** *13* (27), 12352-12367.

(44) Egorova, E. M.; Dukhin, A. S.; Svetlova, I. E., Some Problems of Zeta Potential Determination in Electrophoretic Measurements on Llipid Membranes. *Biochimica et Biophysica Bcta* **1992,** *1104* (1), 102-110.

(45) Gonzalez-Rodriguez, M. L.; Rabasco, A. M., Charged Liposomes as Carriers to Enhance the Permeation Through the Skin. *Expert Opinion on Drug Delivery* **2011,** *8* (7), 857-871.

(46) Laouini, A.; Jaafar-Maalej, C.; Limayem-Blouza, I.; Sfar, S.; Charcosset, C.; Fessi, H., Preparation, Characterization and Applications of Liposomes: State of the Art. *Journal of Colloid Science and Biotechnology* **2012,** *1* (2), 147-168.

(47) Hanaor, D.; Michelazzi, M.; Leonelli, C.; Sorrell, C. C., The Effects of Carboxylic Acids on the Aqueous Dispersion and Electrophoretic Deposition of ZrO2. *Journal of the European Ceramic Society* **2012,** *32* (1), 235-244.

(48) O'Brien, R. W.; Midmore, B. R.; Lamb, A.; Hunter, R. J., Electroacoustic Studies of Moderately Concentrated Colloidal Suspensions. *Faraday Discussions of the Chemical Society* **1990,** *90* (0), 301-312.

(49) Chiu, M. H.; Prenner, E. J., Differential Scanning Calorimetry: An Invaluable Tool for a Detailed Thermodynamic Characterization of Macromolecules and Their Interactions. *Journal of Pharmacy and Bioallied Sciences* **2011,** *3* (1), 39-59.

(50) McElhaney, R. N., The Use of Differential Scanning Calorimetry and Differential Thermal Analysis in Studies of Model and Biological Membranes. *Chemistry and Physics of Lipids* **1982,** *30* (2-3), 229-259.

(51) Barry, J. A.; Lamparski, H.; Shyamsunder, E.; Osterberg, F.; Cerne, J.; Brown, M. F.; O'Brien, D. F., ^{31}P NMR and X-ray Diffraction Study of the Effect of Photopolymerization on Lpid Polymorphism. *Biochemistry* **1992,** *31* (41), 10114-10120.

(52) Veiro, J. A.; Khalifah, R. G.; Rowe, E. S., P-31 nuclear magnetic resonance studies of the appearance of an isotropic component in dielaidoylphosphatidylethanolamine. *Biophysical Journal* **1990,** *57* (3), 637-41.

(53) Tilcock, C. P. S.; Cullis, P. R.; Hope, M. J.; Gruner, S. M., Polymorphic Phase Behavior of Unsaturated Lysophosphatidylethanolamines: A Phosphorus-31 NMR and X-ray Diffraction Study. *Biochemistry* **1986,** *25* (4), 816-822.

(54) Powell, G. L.; Marsh, D., Polymorphic Phase Behavior of Cardiolipin Derivatives Studied by Phosphorus-31 NMR and X-ray Diffraction. *Biochemistry* **1985,** *24* (12), 2902-2908.

(55) Siegel, D. P.; Banschbach, J. L., Lamellar/Inverted Cubic (L_α/Q_{II}) Phase Transition in *N*-Methylated-dioleoylphosphatidylethanolamine. *Biochemistry* **1990,** *29* (25), 5975-5981.

(56) Basanez, G.; Ruiz-Arguello, M. B.; Alonso, A.; Goni, F. M.; Karlsson, G.; Edwards, K., Morphological Changes Induced by Phospholipase C and by Sphingomyelinase on Large Unilamellar Vesicles: a Cryo-Transmission Electron Microscopy Study of Liposome Fusion. *Biophysical Journal* **1997,** *72* (6), 2630-2637.

(57) Mariani, P.; Luzzati, V.; Delacroix, H., Cubic Phases of Lipid-Containing Systems. Structure Analysis and Biological Implications. *Journal of Molecular Biology* **1988,** *204* (1), 165-189.

(58) Wiener, M. C.; White, S. H., Structure of a Fluid Dioleoylphosphatidylcholine Bilayer Determined by Joint Refinement of X-ray and Neutron Diffraction Data. II. Distribution and Packing of Terminal Methyl Groups. *Biophysical Journal* **1992,** *61* (2), 428-433.

(59) Rawicz, W.; Olbrich, K. C.; McIntosh, T.; Needham, D.; Evans, E., Effect of Chain Length and Unsaturation on Elasticity of Lipid Bilayers. *Biophysical Journal* **2000,** *79* (1), 328-339.

(60) Katsaras, J., Adsorbed to a Rigid Substrate, Dimyristoylphosphatidylcholine Multibilayers Attain Full Hydration in All Mesophases. *Biophysical Journal* **1998,** *75* (5), 2157-2162.

(61) Katsaras, J., Highly Aligned Lipid Membrane Systems in the Physiologically Relevant "Excess Water" Condition. *Biophysical Journal* **1997,** *73* (6), 2924-2929.

(62) McIntosh, T. J.; Magid, A. D.; Simon, S. A., Steric Repulsion between Phosphatidylcholine Bilayers. *Biochemistry* **1987,** *26* (23), 7325-7332.

(63) Nagle, J. F.; Tristram-Nagle, S., Structure of Lipid Bilayers. *Biochimica et Biophysica Acta* **2000,** *1469* (3), 159-195.

(64) Gill, P.; Moghadam, T. T.; Ranjbar, B., Differential Scanning Calorimetry Techniques: Applications in Biology and Nanoscience. *Journal of Biomolecular Techniques* **2010,** *21* (4), 167-193.

(65) Burnell, E. E.; Cullis, P. R.; de Kruijff, B., Effects of Tumbling and Lateral Diffusion on Phosphatidylcholine Model Membrane ^{31}P-NMR Lineshapes. *Biochimica et Biophysica acta* **1980,** *603* (1), 63-69.

(66) Cullis, P. R.; de Kruijff, B., Lipid Polymorphism and the Functional Roles of Lipids in Biological Membranes. *Biochimica et Biophysica acta* **1979,** *559* (4), 399-420.

(67) De Kruijff, B.; Van Den Besselaar, A. M. H. P.; Cullis, P. R.; Van Den Bosch, H.; Van Deenen, L. L. M., Evidence for Isotropic Motion of Phospholipids in Liver Microsomal Membranes. A ^{31}P NMR study. *Biochimica et Biophysica Acta* **1978,** *514* (1), 1-8.

(68) Frohlich, M.; Brecht, V.; Peschka-Suss, R., Parameters Influencing the Determination of Liposome Lamellarity by ^{31}P-NMR. *Chemistry and Physics of Lipids* **2001,** *109* (1), 103-112.

(69) Thayer, A. M.; Kohler, S. J., Phosphorus-31 Nuclear Magnetic Resonance Spectra Characteristic of Hexagonal and Isotropic Phospholipid Phases Generated from Phosphatidylethanolamine in the Bilayer Phase. *Biochemistry* **1981,** *20* (24), 6831-6834.

(70) Hub, H. H.; Zimmermann, U.; Ringsdorf, H., Preparation of Large Unilamellar Vesicles. *FEBS letters* **1982,** *140* (2), 254-256.

CHAPTER 3
POLYMORPHIC PHASE STUDIES OF Q_{PA}-DOPE USING ^{31}P NMR ANISOTROPY

Fully hydrated, unsaturated PE lipids form either an L_α or H_{II} phase depending on their physical environment (e.g., pH, temperature, salt).[1-3] Currently, the only analytical methods capable of identifying and quantifying lipid phases are: ^{31}P NMR, differential scanning calorimetry (DSC), freeze-fracture microscopies, X-ray diffraction, and IR spectroscopy.[1,4-7] DSC measures the enthalpy of a phase change event with temperature, but is not suitable for non-thermally triggered phase changes.[4,8] Freeze-fracture methods require a significant amount of sample preparation, making temporal phase measurements of triggerable lipids, like Q_{PA}-DOPE, challenging.[9-11] X-ray diffraction can probe a variety of lipid phases, including the cubic phase; however, this method requires a strong radiation source for adequate resolution, typically from a synchrotron.[12-14] ^{31}P NMR is a commonly used analytical method to determine the phase identity of lipid, because of the distinctive lineshapes these phases produce.[1,2,12] Moreover, the ^{31}P NMR method can be carried out in an aqueous environment, thus the physical environment used for other experimental methods is amiable to this method. Because ^{31}P NMR spectroscopy is a widely accepted and utilized analytical method, permits studies in an aqueous environment, and the ease of instrumental access, ^{31}P NMR was use to investigate the phase behavior of Q_{PA}-DOPE before and after reduction.

3.1 Origins of Phospholipid ^{31}P NMR Lineshapes

^{31}P NMR lineshapes contain information regarding the phase of a phospholipid system, as each phase yields a unique spectrum. The lineshape of an L_α phase phospholipid is characterized by a broad linewidth ($\Delta\sigma$) with an intense peak ($\sigma_\perp$) on the right and a less intense shoulder (σ_{II}) on the left (Figure 3.1A).[15,16]

H_{II} phase phospholipids are characterized by a mirror image of the L_α lineshape, but possess one-half the $\Delta\sigma$ value of the L_α phase counterpart (Figure 3.1B).[16] The ^{31}P NMR lineshapes of micelles, small unilamellar vesicles (SUVs), small lipidic particles, and lipid cubic phases produce a single isotropic Lorentzian peak (Figure 3.1C).[1,2,17] The size of a liposome also factors into the measured signal. Because of vesicle tumbling and lateral diffusion in the bilayer, vesicles must have a diameter > 1 μm to have the required anisotropic motion, which yields lineshapes similar to Figure 3A.[15] The dynamic motion of LUVs and SUVs results in an averaging of the signal from the phospholipids, which results in an isotropic peak (Figure 3C).

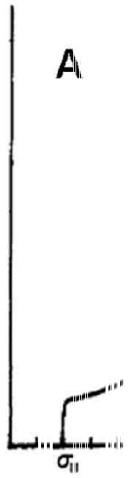

Figure 3.1A-C. ^{31}P NMR lineshapes for phospholipids in various phases: (A) L_α, (B) H_{II} and (C) isotropic phases. Reprint (adapted) with permission from Thayer, Ann M., and Kohler, Susan J., Phosphorus-31 nuclear magnetic resonance spectra characteristic of hexagonal and isotropic phospholipid phases generated from phosphatidylethanolamine in the bilayer phase. *Biochemistry*. 1981, 20 (24), 6831-34. Copyright (1981) American Chemical Society.

^{31}P NMR spectroscopy has also been used as a method to determine the lamellar nature of liposomes (SUVs, LUVs, MLVs, and GUVs).[18] To determine the lamellar nature of a system, Mn^{2+} is added to an NMR tube containing the liposomes, and the isotropic phosphorus signal is measured before and after Mn^{2+} addition.

The ratio of signal before/after is proportional to the number of bilayers, as only the signal form phospholipids in the outer most leaflet phospholipids are quenched by ionic interaction with Mn^{2+}.

3.2 Principles of ^{31}P NMR Anisotropy

^{31}P NMR line shapes observed for both the L_α and H_{II} phases arise from chemical shift anisotropy (CSA) of the phosphorous nuclei in a phospholipid.[19,20] In actuality, three chemical shift tensors (σ_{11}, σ_{22}, σ_{33}) create a principle axis with the phosphorous nucleus as its origin (Figure 3.2).[21] The motion of the chemical shift tensors must be referenced relative to the molecular frame (x, y, z) where the z-axis is the magnetic field (B).[20] The rotation of the chemical shift tensors from their principal axis into the molecular frame is defined by the Euler angles (Φ and θ).[20] When this frame is established, the chemical shift tensors parallel (σ_{II} and perpendicular ($\sigma_{\perp}$) to B can be calculated from Equations 3.1 and 3.2, respectively.[16,19,20] If the assumption is made that the chemical shift tensor components of the principle axis coincide with the molecular frame, both Φ and θ are equal to 0.[20] With this assumption, it is possible to theoretically predict the spectral linewidth ($\Delta\sigma$) without using the Euler angles; as a result, the difference of Equations 3.1 and 3.2 yields Equation 3.3.

The magnitude of the chemical shift tensors can be measured using solid state ^{31}P NMR of lyophilized phospholipids and frequency dependent ^{31}P NMR.[22-24] Because single crystals of lipids are difficult to generate and are thermally unstable, lipid powders are typically used.[24] Without single crystals, the Euler angles cannot be measured. Solid-state ^{31}P NMR spectra of dry lyophilized lipid powders display an axially asymmetric spectrum having two broad shoulders and an isotropic peak in the middle.[24,25]

In this state, the lipids fully exhibit all possible orientations in the magnetic field, and all possible chemical shifts are observed. The three extremity regions correspond to the chemical shift tensors σ_{11}, σ_{22}, and σ_{33} (unitless) and have a magnitude of their spectral chemical shift values (x-axis, ppm).[23, 26]

Equation 3.1

$$\sigma_{\perp} = \frac{\sigma_{11}}{2}\left(\cos^2\theta\cos^2\Phi + \sin^2\Phi\right) + \frac{\sigma_{22}}{2}\left(\cos^2\theta\sin^2\Phi + \cos^2\Phi\right) + \sigma_{33}\sin^2\theta$$

Equation 3.2

$$\sigma_{II} = \sigma_{11}\sin^2\theta\cos^2\Phi + \sigma_{22}\sin^2\theta\sin^2\Phi + \sigma_{33}\cos^2\theta$$

Equation 3.3

$$\Delta\sigma = \sigma_{33} - \frac{\left(\sigma_{22} - \sigma_{11}\right)}{2}$$

3.3 Goals, Aims, and Objectives

Prior to this work, our hypothesis was that the observed contents release of Q_{PA}-DOPE vesicles after reduction was due to an induced $L_{\alpha} \rightarrow H_{II}$ phase change and not from vesicles with leaky bilayers. To confirm that Q_{PA}-DOPE has polymorphic phase behavior using ^{31}P NMR spectroscopy, three objectives were proposed and then accomplished. First, a new buffer system lacking phosphorus was validated for Q_{PA}-DOPE LUVs, and it was found to have a similar contents release profile for Q_{PA}-DOPE LUVs in phosphate buffer, the main buffer used prior to this work.[27,28] Second, a new method was developed to prepare Q_{PA}-DOPE GUVs at a sufficiently high concentration so as to allow ^{31}P NMR analysis. Lastly, Q_{PA}-DOPE ^{31}P NMR lineshapes before and after reduction were successfully acquired.

Figure 3.2. The chemical shift tensors (σ_{11}, σ_{22}, and σ_{33}) of a phosphorus atom in a phospholipid are depicted in the field of the magnet (B_o) where B_o lies in the z-axis of a three dimensional Cartesian coordinate system (B_o, x, y). σ_{11} lies between the two esterified oxygens O(1)-O(2) and is perpendicular to both σ_{22} and σ_{33}. σ_{22} bisects the two non-esterified oxygens O(3)-P-O(4), and σ_{33} lies in the plane of O(3)-P-O(4) bond angle perpendicular to both σ_{11} and σ_{22}. Φ is the angle of rotation of σ_{33} placing σ_{11} in the x-y plane, and θ is the angle of rotation that brings σ_{33} to coincide with the z-axis (B).

3.4 Buffer Media

In previous Q_{PA}-DOPE studies conducted in the McCarley group, a phosphate buffer system was used to characterize contents release.[27,28] For the ^{31}P NMR studies in this dissertation, a different buffer had to be used to avoid additional isotropic phosphate signals that would interfere with the spectra. Both *N*-tris(hydroxymethyl)methyl-2-aminoethanesulfonate (TES) and *N*-2-hydroxy-ethylpiperazine- *N'*-2-ethanesulfonate (HEPES) were tested for Q_{PA}-DOPE, contents release as they have been shown to have a good buffer capacity between pH 6–8 (Figure 3.3).[29] The phosphate buffer system yielded a total contents release of 98%, TES buffer gave 96% release, and HEPES led to 86% release; The t_{50} values were

29 min, 56 min, and 60 min, respectively. The difference in time is either to the Hofmeister nature of phosphate, TES, and HEPES or the known general acid/base catalysis of lactonization.[30-32] Q_{PA}-DOPE LUVs exhibited a deformation feature in their calcein release curves in both TES and HEPES media, suggesting these buffer systems undergo the same mechanism for release. This data supports TES and HEPES are suitable as an alternative buffer for ^{31}P NMR studies. For this work, TES buffer was used.

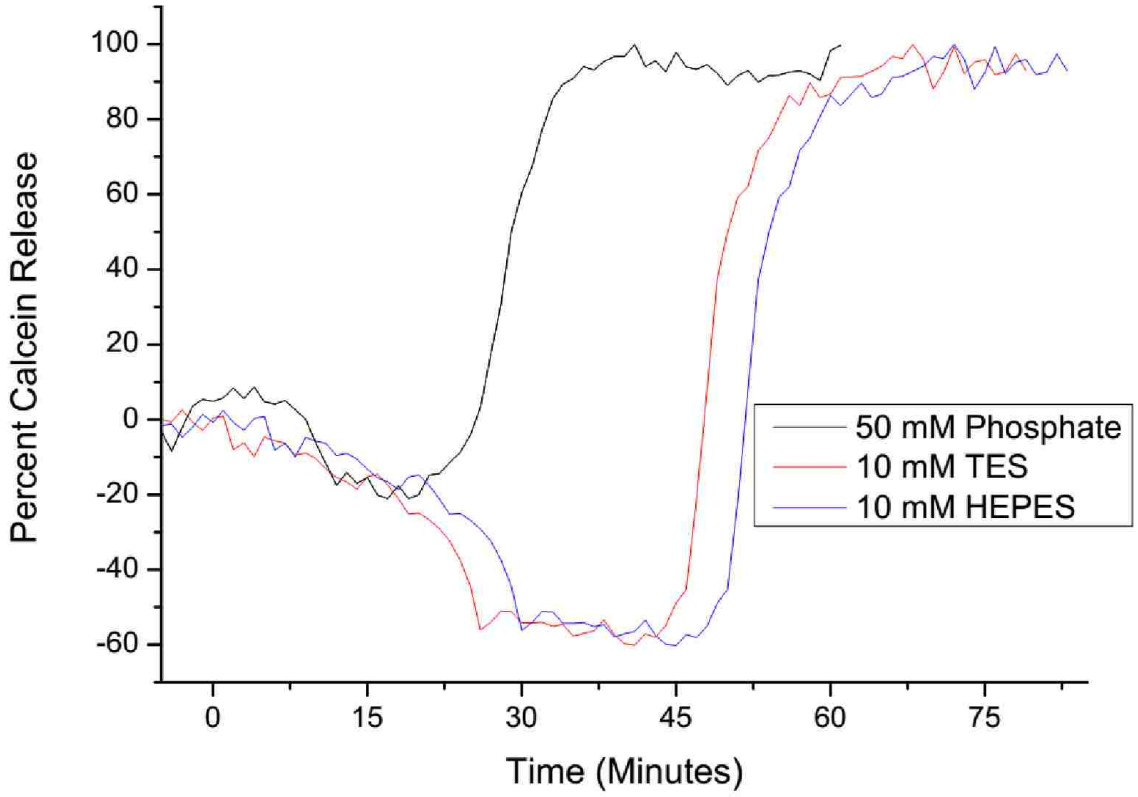

Figure 3.3. The calcein release curves of 100 μM Q_{PA}-DOPE LUVs in 75 mM KCl and 1.0 mM EDTA, pH 7.4 buffered with 50 mM phosphate (Black), 10.0 mM TES (Red), and 10.0 mM HEPES (Blue) at 25 °C. All three buffer systems exhibit the deformation then release; however, TES and HEPES are delayed relative to phosphate.

3.5 Method to Prepare Q_{PA}-DOPE GUVs

Liposomes are categorized on their size as either 0.1–15 μm diameter multilamellar vesicles (MLVs), 25–50 nm diameter small unilamellar vesicles (SUVs),

0.1–1.0 μm diameter large unilamellar vesicles (LUVs), and >1.0 μm diameter giant unilamellar vesicles (GUVs).[33] The type of vesicle(s) present in a liposome solution depends on the preparation method used. In order to obtain the ^{31}P NMR CSA lineshape of liposomes, the vesicle diameter must be > 1 μm in order to minimize the dynamics affecting isotropic averaging of their chemical shift tensor components.[1,15,34] MLVs are commonly used to obtain ^{31}P NMR CSA lineshapes for phospholipids being studied for their lipid phase characteristics, because the thermal trigger used to induce a phase change can affect internal layers of the vesicle.[16,19,35-39] However, only the Q_{PA} head groups in the outer leaflets of Q_{PA}-DOPE vesicles exposed to the reducing agent are cleaved. If Q_{PA}-DOPE MLVs were used, the internal Q_{PA}-DOPE liposomes would stabilize the MLV structure, thereby preventing aggregation and contact from opposed vesicles. This would inhibit contents release and any phase transition. For this reason, unilamellar vesicles that have a diameter > 1 μm are needed to prevent isotropic averaging of its CSA and offer the ability to observe the Q_{PA}-DOPE phase transition with ^{31}P NMR.

There are several reported methods for the preparation of GUVs.[40-43] For ^{31}P NMR studies of Q_{PA}-DOPE, a modified procedure of the one reported by Hub et al. was used.[40] The authors found when a lipid film was hydrated in low ionic strength buffer media at high temperatures, GUVs with 1–50 μm diameters were generated, leading to formation of a large aggregate in the center of the liquid in the vessel. The authors then agitated the vessel to generate a solution of well dispersed LUVs. In this work, the scale was increased 10-fold (~30 mg of lipid in 500 mL of buffer), the GUVs were harvested rather than agitated, and a centrifugation step (5 min at 10,000 x *g*) was added in order to concentrate the GUVs for NMR analysis, as well as to

exchange the non-ionic buffer media used for vesicle growth with the TES/KCl buffer media validated earlier in this work. The centrifugation of LUVs and MLVs has been reported in literature, and it has been shown to not damage the vesicles at forces up to 100,000 x *g* (Figure 3.4).[33,44] The size of the Q_{PA}-DOPE GUVs produced range from 1–20 μm. GUVs were prepared in 1.40 x 10^{-2} mM sucrose buffered with 10.0 mM TES, pH 7.40 and after centrifugation resuspended in 75 mM KCl buffered with 10.0 mM TES, pH 7.40. The release curve of Q_{PA}-DOPE LUVs (~120 nm) in this buffer system has a 96% contents release at 110 minutes and exhibits deformation prior to release (Figure 3.5).

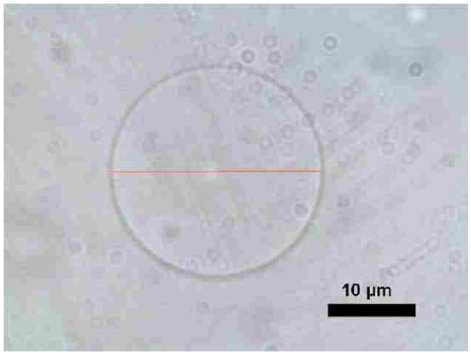

Figure 3.4. A wide-field optical micrograph of Q_{PA}-DOPE GUVs (Bar = 10 μm). The aqueous environment is buffered with 10.0 mM TES and contains 1.40 x 10^{-2} mM sucrose in the encapsulated volume and 75 mM KCl in the exterior space, pH 7.40 in 20% D_2O. The smaller features seen are artifacts from the microscope

Only phospholipid vesicles situated in the RF coil region (~12–18 mm) of the NMR instrument produce signal. In order to obtain an adequate signal-to-noise ratio, it is necessary to concentrate the vesicles into a region of the NMR tube comparable to that of the RF coil region. A 5-mm diameter Shigemi NMR tube made to have the same magnetic susceptibility as D_2O was used to improve the signal-to-noise ratio (Figure 3.5). In traditional NMR tubes, the sample at the bottom of the tube that lies below or above the magnetic coil does not contribute to the acquired signal; however, this loss in efficiency is necessary to provide sample homogeneity in the coil region. A Shigemi NMR tube has a quartz plug at the top and bottom of the sample area so the

entire undiluted sample can be placed inside coil region. Moreover, because the tube is made to have the same magnetic susceptibility as D_2O, there is no effect on the homogeneity of the magnetic field in the coil region.

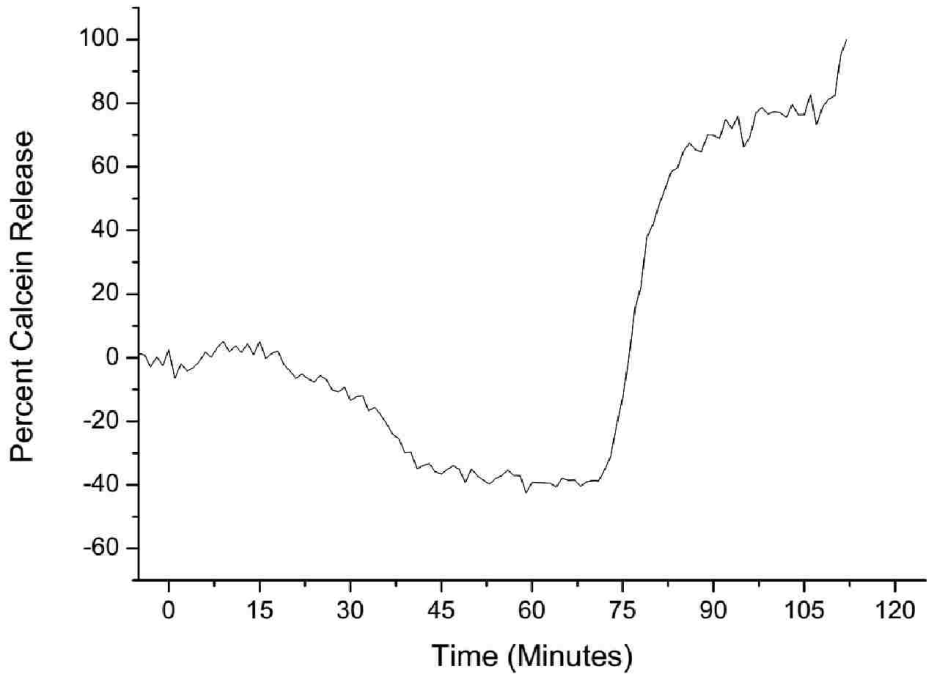

Figure 3.5. Calcein release curve of 100 μM Q_{PA}-DOPE LUVs (~120 nm) buffered in 10.0 mM TES with 1.40 x 10^{-2} mM sucrose in the encapsulated volume and pH 7.40–75 mM KCl with 1.0 mM EDTA in the surrounding volume at 25 °C. The t_{50} for calcein release is 81 min, and 96% total release is observed at 110 min prior to lysis.

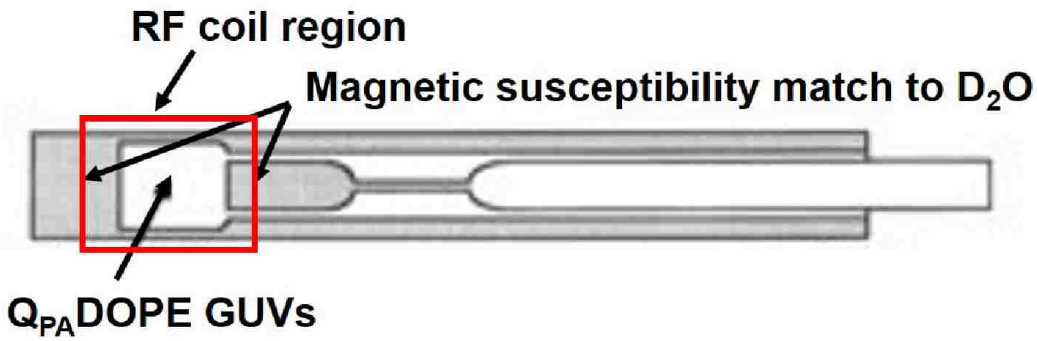

Figure 3.6. A 5-mm Shigemi NMR tube matched to have the same magnetic susceptibility as D_2O. The bottom is plugged to maximize the amount of sample within the radio frequency (RF) coil region (red). The sample region is bored to have a wider diameter, so as to increase the amount of sample in the RF coil region.

3.6 ^{31}P NMR Anisotropy Results and Discussion

To demonstrate the ability to obtain the CSA lineshapes of phospholipid vesicles, ^{31}P NMR spectra of 1-palmitoyl-2-oleoyl-*sn*-glycero-3-phosphatidylethanolamine (POPE) MLVs were obtained at 30, 50, 65 and 80 ºC on a Bruker DPX-400 spectrometer at a frequency of 161.975 MHz with 2048 scans using a proton-decoupled, spin-echo pulse sequence (Figure 3.7). The T_H of POPE is reported to be ~70 ºC.[45] The ^{31}P NMR spectra at 30, 50 and 65 ºC indicate the presence of an L_α phase with $\Delta\sigma_{avg}$= 40.4 ± 2.6 ppm. At 80 ºC, the ^{31}P NMR spectrum of POPE has a mirror image lineshape, in comparison to that of the L_α phase, and the spectrum exhibits $\Delta\sigma$=21.3 ppm, both indicating the presence of an H_{II} phase. Kohler *et al*. modeled the phosphoethanolamine (PE) head group and reported the theoretical values of the chemical shift tensors to be σ_{11}= –67, σ_{22}= –13 and σ_{33}= 69.[22] If the principle axis of the chemical shift tensors coincide with the molecular frame and no Euler rotations are necessary, Equation 3.3 holds true, and the theoretical value of $\Delta\sigma$ for PE is 42 ppm for L_α vesicles, 4.8% difference from the experimental value. This suggests the procedure used for sample preparation and ^{31}P NMR spectra acquisition are accurate.

To validate the GUV preparation method developed with ^{31}P NMR anisotropy lipid phase measurements, 1,2-dioleoyl-*sn*-glycero-3-phosphatidylcholine (DOPC) GUVs were prepared using the method outlined in Chapter 2. DOPC is a bilayer-forming lipid and does not favor the H_{II} phase at any temperature when hydrated. After growth and harvesting of DOPC GUVs, the vesicles were resuspended in pH 7.40 75 mM KCl/10.0 mM TES (20% D_2O). The sample was transferred into a Shigemi NMR tube and analyzed on a Bruker Ascend-400 spectrometer at a frequency of

161.975 MHz with 2,048 scans using a proton-decoupled, spin-echo pulse sequence (Figure 3.8). The acquired linewidth (49.5 ppm) and lineshape agree with previous ^{31}P NMR studies of DOPC MLVs.[11,46]

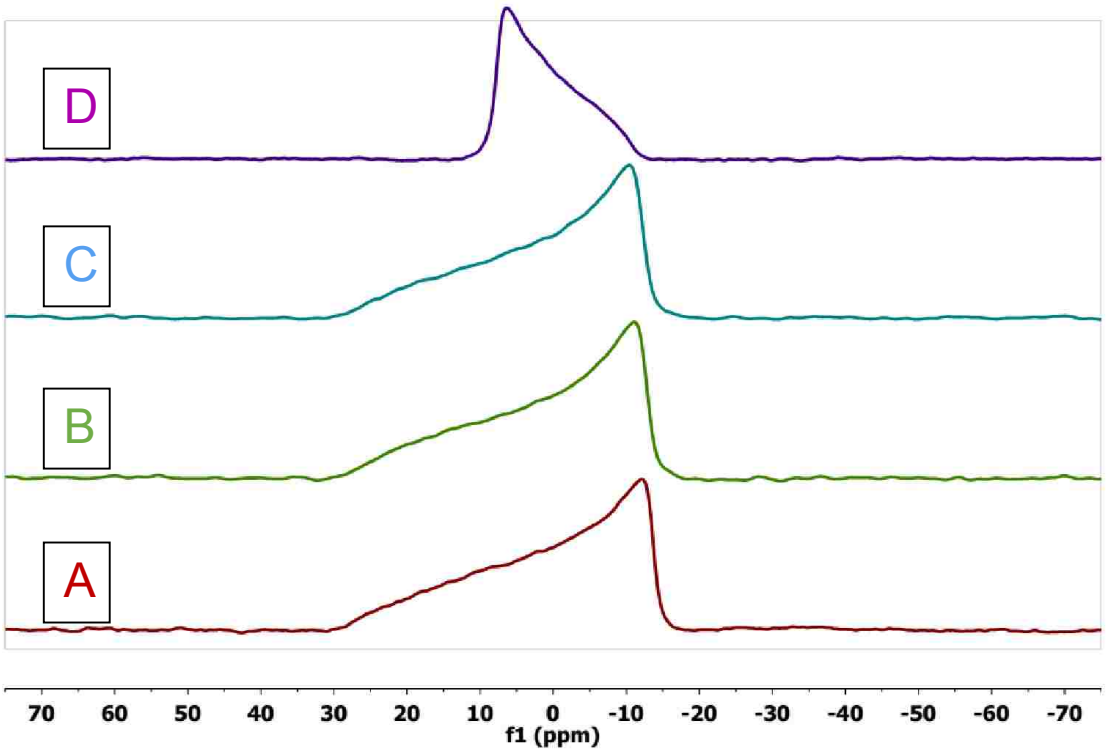

Figure 3.7. ^{31}P NMR lineshapes of POPE MLVs at 30 °C (A), 50 °C (B), 65 °C (C), and 80 °C (D) acquired on a Bruker DPX-400 NMR spectrometer operating at 161.975 MHz with 2048 transient scans. Spectra A, B, and C have lineshapes indicative of a lamellar phase and an average linewidth of 40.4 ± 2.6 ppm. Spectrum D was obtained at a temperature above the transition temperature (T_H =72 °C) of POPE and has a lineshape and linewidth (21.3 ppm) characteristic of an inverted hexagonal phase.

^{31}P NMR spectra of Q_{PA}-DOPE vesicles were obtained on a Bruker DPX-400 spectrometer at a frequency of 161.975 MHz with 40,960 scans using a proton decoupled spin-echo pulse sequence. In an attempt to minimize the isotropic averaging of the signal from vesicle tumbling, the spectrum of the L_α phase was obtained at 5 ºC. Because the T_H of DOPE is reported to be around ~5 ºC, the sample was analyzed at 15 ºC before and after $Na_2S_2O_4$ reduction (Figure 3.9).[47,48] The spectrum of the L_α phase of Q_{PA}-DOPE was $\Delta\sigma$=32.1 ppm and possesses a similar lineshape to the spectrum of

the L_α phase POPE. Akoka et al. investigated the ^{31}P NMR linewidths of *N*-acyl-PE lipids and found that lipid head group modification led to a decrease in the measured linewidth of that lipid.[49] Thayer et al. modeled the effect of altering the torsion angle of the head group and found that bending of the head group can narrow the linewidth of a lipid.[17] A structural change in the polar region of a lipid can generate this torsion angle. Lipids in a bilayer can bend at the point where the polar and non-polar regions meet so as to find a lower free energy for chain packing when the area of the head group is larger than the cross-sectional area of the two hydrocarbon chains.[50] Because Q_{PA}-DOPE GUVs have a shorter linewidth than expected for PE lipids, this latter scenario is most likely the case. The spectrum of Q_{PA}-DOPE at 15 ºC after $Na_2S_2O_4$ reduction had a linewidth of $\Delta\sigma$=22.3 ppm. This is similar to the experimental value obtained for the H_{II} phase of POPE and the theoretical value for PE lipids in the H_{II} phase.[22]

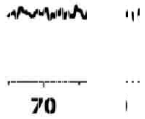

Figure 3.8. ^{31}P NMR spectrum of DOPC GUVs acquired on a Bruker Ascend-400 spectrometer operating at 161.975 MHz with 2048 transient scans at 25 °C. The lineshape is indicative of a lamellar phase and has a linewidth of 49.5 ppm, which is in agreement with previously measured ^{31}P NMR linewidths for DOPC MLVs.

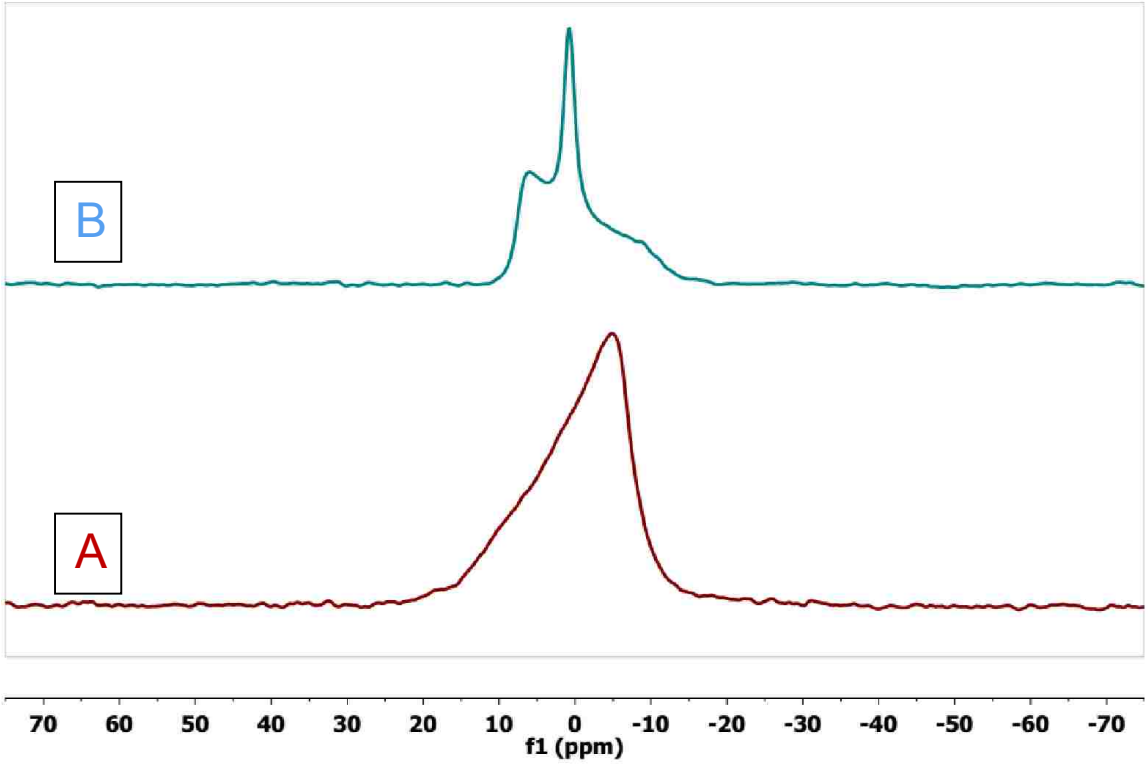

Figure 3.9. ^{31}P NMR spectra of Q_{PA}-DOPE GUVs before (A) and after (B) reduction with NaS_2O_4 acquired on a Bruker DPX-400 NMR spectrometer operating at 161.975 MHz with 40,960 transient scans. (A) Before $S_2O_4^{2-}$ addition, the lineshape is indicative of a lamellar phase and has a linewidth 32.1 ppm; the narrower linewidth is due to Q_{PA} functionalization of the polar region. (B) After reduction, the lineshape and linewidth (22.3 ppm) are indicative of an inverted hexagonal phase. The co-existence of an isotropic state is also observed after reduction. Reprint (adapted) with permission from McCarley, R.L., Forsyth, J.C., Loew, M., Mendoza, M.F., Hollabaugh, N.M., Winter, J.E., Release Rates of Liposomal contents are controlled by Kosmotropes and Chaotropes. *Langmuir*. 2013, 29 (46), 13991-5. Copyright (2013) American Chemical Society.

In addition to the H_{II} line shape, the spectrum of Q_{PA}-DOPE after $Na_2S_2O_4$ reduction has a superimposed isotropic peak. The spectral line shape of the reduced Q_{PA}-DOPE spectrum did not change after being at room temperature for a week. The isotropic state observed in this system can be either micelles, small unilamellar vesicles (SUVs), small lipidic particles, or cubic phase (Q_{II}).[1,2,17] Unfortunately, an inability to further refine the isotropic state of lipid systems is one limitation of ^{31}P NMR spectroscopy. Based on the lipid geometry modeling done by Israelachvill et al., normal micelle vesicles are not probable for DOPE lipids, because the polar region is never

larger than the non-polar region.[51] Recently, two different groups observed an isotropic state for DOPE MLVs with ^{31}P NMR after repetitively cycling the lipid above and below its transition temperature.[52,53] Shyamsunder et al. used X-ray diffraction to investigate the isotropic state of DOPE and found the presence of a cubic phase. This suggests the isotropic peak observed after Q_{PA}-DOPE reduction arises from the co-existence of H_{II} and Q_{II} phases.

3.7 Conclusion

^{31}P NMR was used to probe the phase behavior of Q_{PA}-DOPE liposomes before and after $Na_2S_2O_4$ reduction. A new method to prepare large quantities of concentrated GUVs was successfully developed and implemented for multiple lipids. Both the linewidths and lineshapes confirm that Q_{PA}-DOPE undergoes an $L_\alpha \rightarrow H_{II}$ phase change after reduction. Numerous theoretical models have been published embodying the paths lamellar systems take as they undergo a phase transition to non-lamellar phases.[54-60] The emergence of an isotropic state and possibly a cubic phase in Q_{PA}-DOPE liposomes after reduction is an example of how lipid phases and their transition processes are even more complex. Clearly, the release of contents entrapped by Q_{PA}-DOPE vesicles is due to a reduction-triggered phase change. The role of the cubic phase in this process, and what it means for this system, is still yet to be determined. The only method capable of making this measurement is X-ray diffraction; however, due to the dynamic nature of Q_{PA}-DOPE, a strong radiation source from a synchrotron is needed for the time required for temporal resolution.

3.8 References

(1) Cullis, P. R.; de Kruijff, B., Lipid Polymorphism and the Functional Roles of Lipids in Biological Membranes. *Biochimica et Biophysica Acta* **1979,** *559* (4), 399-420.

(2) Cullis, P. R.; de Kruijff, B., The Polymorphic Phase Behaviour of Phosphatidylethanolamines of Natural and Synthetic Origin. A ^{31}P NMR Study. *Biochimica et Biophysica Acta* **1978,** *513* (1), 31-42.

(3) Tilcock, C. P. S.; Cullis, P. R., The Polymorphic Phase Behaviour and Miscibility Properties of Synthetic Phosphatidylethanolamines. *Biochimica et Biophysica Acta* **1982,** *684* (2), 212-218.

(4) Epand, R. M., High Sensitivity Differential Scanning Calorimetry of the Bilayer to Hexagonal Phase Transitions of Diacylphosphatidylethanolamines. *Chemistry and Physics of Lipids* **1985,** *36* (4), 387-393.

(5) Hui, S. W.; Stewart, T. P.; Boni, L. T., The Nature of Lipidic Particles and Their Roles in Polymorphic Transitions. *Chemistry and Physics of Lipids* **1983,** *33* (2), 113-26.

(6) Boni, L. T.; Hui, S. W., Polymorphic Phase Behaviour of Dilinoleoylphosphatidylethanolamine and Palmitoyloleoylphosphatidylcholine Mixtures: Structural Changes between Hexagonal, Cubic and Bilayer Phases. *Biochimica et Biophysica Acta* **1983,** *731* (2), 177-185.

(7) Mantsch, H. H.; Martin, A.; Cameron, D. G., Characterization by Infrared Spectroscopy of the Bilayer to Nonbilayer Phase Transition of Phosphatidylethanolamines. *Biochemistry* **1981,** *20* (11), 3138-3145.

(8) Chiu, M. H.; Prenner, E. J., Differential Scanning Calorimetry: An Invaluable Tool for a Detailed Thermodynamic Characterization of Macromolecules and Their Interactions. *Journal of Pharmacy and Bioallied Sciences* **2011,** *3* (1), 39-59.

(9) Basanez, G.; Ruiz-Arguello, M. B.; Alonso, A.; Goni, F. M.; Karlsson, G.; Edwards, K., Morphological Changes Induced by Phospholipase C and by Sphingomyelinase on Large Unilamellar Vesicles: a Cryo-Transmission Electron Microscopy Study of Liposome Fusion. *Biophysical Journal* **1997,** *72* (6), 2630-2637.

(10) Siegel, D. P.; Banschbach, J. L., Lamellar/Inverted cubic (L_α/Q_{II}) Phase Transition in *N*-Methylated Dioleoylphosphatidylethanolamine. *Biochemistry* **1990,** *29* (25), 5975-5981.

(11) Cullis, P. R.; Grathwohl, C., Hydrocarbon Phase Transitions and Lpid-Protein Interactions in the Erythrocyte Membrane. A ^{31}P NMR and Fluorescence Study. *Biochimica et Biophysica Acta* **1977,** *471* (2), 213-226.

(12) Gruner, S. M., Non-lamellar Lipid Phases. In *The Structure of Biological Membranes; Yeagle, P.L. Ed.;* CRC Press: Boca Raton, Florida, 2005, pp 173-199.

(13) Luzzati, v.; Mariani, P.; Gulik-Krzywicki, T., Cubic Phases of Lipid-Containing Systems: Physical Structure and Biological Implications. *Physics of Amphiphilic Layers* **1987**, 21, 131-137.

(14) Mariani, P.; Luzzati, V.; Delacroix, H., Cubic Phases of Lipid-Containing Systems. Structure Analysis and Biological Implications. *Journal of Molecular Biology* **1988,** *204* (1), 165-189.

(15) Burnell, E. E.; Cullis, P. R.; de Kruijff, B., Effects of Tumbling and Lateral Diffusion on Phosphatidylcholine Model Membrane ^{31}P-NMR Lineshapes. *Biochimica et Biophysica Acta* **1980,** *603* (1), 63-69.

(16) Thayer, A. M.; Kohler, S. J., Phosphorus-31 nuclear magnetic resonance spectra characteristic of hexagonal and isotropic phospholipid phases generated from phosphatidylethanolamine in the bilayer phase. *Biochemistry* **1981,** *20* (24), 6831-6834.

(17) Thayer, A. M.; Kohler, S. J., Phosphorus-31 Nuclear Magnetic Resonance Spectra Characteristic of Hexagonal and Isotropic Phospholipid Phases Generated from Phosphatidylethanolamine in the Bilayer Phase. *Biochemistry* **1981,** *20* (24), 6831-6834.

(18) Frohlich, M.; Brecht, V.; Peschka-Suss, R., Parameters Influencing the Determination of Liposome Lamellarity by ^{31}P-NMR. *Chemistry and Physics of Lipids* **2001,** *109* (1), 103-112.

(19) Seelig, J., ^{31}P Nuclear Magnetic Resonance and the Head Group Structure of Phospholipids in Membranes. *Biochimica et Biophysica Acta* **1978,** *515* (2), 105-140.

(20) M. Mehring, R. G. G., and J. S. Waugh, ^{19}F Shielding Tensors from Coherently Narrowed NMR Powder Spectra *Journal of Chemical Physics* **1971,** *55 (2)*, 746-755.

(21) Hitchcock, P. B.; Mason, R.; Thomas, K. M.; Shipley, G. G., Structural Chemistry of 1,2 Dilauroyl-DL-Phosphatidylethanolamine: Molecular Conformation and Intermolecular Packing of Phospholipids. *Proceedings of the National Academy of Sciences of The United States of America* **1974,** *71* (8), 3036-3040.

(22) Kohler, S. J.; Klein, M. P., ^{31}P Nuclear Magnetic Resonance Chemical Shielding Tensors of Phosphorylethanolamine, Lecithin, and Related Compounds: Applications to Head-Group Motion in Model Membranes. *Biochemistry* **1976,** *15* (5), 967-974.

(23) Kohler, S. J.; Ellett, J. D.; Klein, M. P., ^{31}P NMR Chemical Shielding Tensors of α-$Ca_2P_2O_7$ *The Journal of Chemical Physics* **1976,** *64* (11), 4451-4458.

(24) Mehring, M.; Griffin, R. G.; Waugh, J. S., ^{19}F Shielding Tensors from Coherently Narrowed NMR Powder Spectra. *The Journal of Chemical Physics* **1971,** *55* (2), 746-755.

(25) Noggle, J. H.; Marecek, J. F.; Mandal, S. B.; van Venetie, R.; Rogers, J.; Jain, M. K.; Ramirez, F., Bilayers of Phosphatidyldiacylglycerol and Phosphatidylcholesterol Give ^{31}P-NMR Spectra Characteristic for Hexagonal and Isotropic Phases. *Biochimica et Biophysica Acta* **1982,** *691* (2), 240-248.

(26) Hauser, H.; Radloff, C.; Ernst, R. R.; Sundell, S.; Pascher, I., The Phosphorus-31 Chemical Shielding Tensor in Phospholipids. *Journal of the American Chemical Society* **1988,** *110* (4), 1054-1058.

(27) Ong, W.; Yang, Y.; Cruciano, A. C.; McCarley, R. L., Redox-Triggered Contents Release from Liposomes. *Journal of the American Chemical Society* **2008,** *130* (44), 14739-14744.

(28) Loew, M.; Forsythe, J. C.; McCarley, R. L., Lipid Nature and Their Influence on Opening of Redox-Active Liposomes. *Langmuir* **2013,** *29* (22), 6615-6623.

(29) Good, N. E.; Winget, G. D.; Winter, W.; Connolly, T. N.; Izawa, S.; Singh, R. M., Hydrogen Ion Buffers for Biological Research. *Biochemistry* **1966,** *5* (2), 467-477.

(30) Alligrant, T. M.; Alvarez, J. C., The Role of Intermolecular Hydrogen Bonding and Proton Transfer in Proton-Coupled Electron Transfer. *The Journal of Physical Chemistry C* **2011,** *115* (21), 10797-10805.

(31) Mendoza, M. F.; Hollabaugh, N. M.; Hettiarachchi, S. U.; McCarley, R. L., Human NAD(P)H:Quinone Oxidoreductase Type I (hNQO1) Activation of Quinone Propionic Acid Trigger Groups. *Biochemistry* **2012,** *51* (40), 8014-8026.

(32) Kresge, A. J.; Keeffe, J.R., Catalysis by Small Molecules in Homogenous Solutions. In: *Investigation of Rates and Mechanisms of Reactions*. (4th ed.), Bernasconi, C.F, Ed., Wiley-Interscience: New York, 1986. p 747

(33) Sanchez-Lopez, V.; Fernandez-Romero, J. M.; Gomez-Hens, A., Evaluation of Liposome Populations Using a Sucrose Density Gradient Centrifugation Approach Coupled to a Continuous Flow System. *Analytica Chimica Acta* **2009,** *645* (1-2), 79-85.

(34) Cullis, P. R., Lateral Diffusion Rates of Phosphatidylcholine in Vesicle Membranes: Effects of Cholesterol and Hydrocarbon Phase Transitions. *FEBS Letters* **1976,** *70* (1), 223-228.

(35) Ellens, H.; Siegel, D. P.; Alford, D.; Yeagle, P. L.; Boni, L.; Lis, L. J.; Quinn, P. J.; Bentz, J., Membrane Fusion and Inverted Phases. *Biochemistry* **1989,** *28* (9), 3692-3703.

(36) Yeagle, P. L.; Hutton, W. C.; Huang, C. H.; Martin, R. B., Headgroup Conformation and Lipid--Cholesterol Association in Phosphatidylcholine Vesicles: a ^{31}P(^{1}H) Nuclear Overhauser Effect Study. *Proceedings of the National Academy of Sciences of The United States of America* **1975,** *72* (9), 3477-3481.

(37) Yeagle, P. L.; Sen, A., Hydration and the Lamellar to Hexagonal Phase Transition of Phosphatidylethanolamine. *Biochemistry* **1986,** *25* (23), 7518-7522.

(38) Barry, J. A.; Lamparski, H.; Shyamsunder, E.; Osterberg, F.; Cerne, J.; Brown, M. F.; O'Brien, D. F., ^{31}P NMR and X-ray Diffraction Study of the Effect of Photopolymerization on Lipid Polymorphism. *Biochemistry* **1992,** *31* (41), 10114-10120.

(39) Boomer, J. A.; Inerowicz, H. D.; Zhang, Z.-Y.; Bergstrand, N.; Edwards, K.; Kim, J.-M.; Thompson, D. H., Acid-Triggered Release from Sterically Stabilized Fusogenic Liposomes via a Hydrolytic DePEGylation Strategy. *Langmuir* **2003,** *19* (16), 6408-6415.

(40) Hub, H. H.; Zimmermann, U.; Ringsdorf, H., Preparation of Large Unilamellar Vesicles. *FEBS Letters* **1982,** *140* (2), 254-256.

(41) Dimitrov, D. S.; Li, J.; Angelova, M.; Jain, R. K., Surface Effects in Preparation of Cell-Size Liposomes. *FEBS Letters* **1984,** *176* (2), 398-400.

(42) Rodriguez, N.; Pincet, F.; Cribier, S., Giant Vesicles Formed by Gentle Hydration and Electroformation: A comparison by Fluorescence Microscopy. *Colloids and Surfaces B: Biointerfaces* **2005,** *42* (2), 125-130.

(43) Staneva, G.; Angelova, M. I.; Koumanov, K., Phospholipase A2 Promotes Raft Budding and Fission from Giant Liposomes. *Chemistry and Physics of Lipids* **2004,** *129* (1), 53-62.

(44) de Kruijff, B.; van den Besselaar, A. M.; Cullis, P. R.; van den Bosch, H.; van Deenen, L. L., Evidence for Isotropic Motion of Phospholipids in Liver Microsomal Membranes. A ^{31}P NMR study. *Biochimica et Biophysica Acta* **1978,** *514* (1), 1-8.

(45) Epand, R. M.; Bottega, R., Determination of the Phase Behaviour of Phosphatidylethanolamine Admixed with Other Lipids and the Effects of Calcium Chloride: Implications for Protein Kinase C Regulation. *Biochimica et Biophysica Acta* **1988,** *944* (2), 144-154.

(46) Holland, G. P.; McIntyre, S. K.; Alam, T. M., Distinguishing Individual Lipid Headgroup Mobility and Phase Transitions in Raft-Forming Lipid Mixtures with ^{31}P MAS NMR. *Biophysical Journal* **2006,** *90* (11), 4248-4260.

(47) Toombes, G. E.; Finnefrock, A. C.; Tate, M. W.; Gruner, S. M., Determination of L(α)-H(II) Phase Transition Temperature for 1,2-dioleoyl-sn-glycero-3-Phosphatidylethanolamine. *Biophysical Journal* **2002,** *82* (5), 2504-2510.

(48) Tate, M. W.; Shyamsunder, E.; Gruner, S. M.; D'Amico, K. L., Kinetics of the Lamellar-Inverse hexagonal Phase Transition Determined by Time-Resolved X-ray Diffraction. *Biochemistry* **1992,** *31* (4), 1081-1092.

(49) Akoka, S.; Tellier, C.; Le Roux, C.; Marion, D., A Phosphorus Magnetic Resonance Spectroscopy and a Differential Scanning Calorimetry Study of the Physical Properties of *N*-acylphosphatidylethanolamines in Aqueous Dispersions. *Chemistry and Physics of Lipids* **1988,** *46* (1), 43-50.

(50) Hanaor, D.; Michelazzi, M.; Leonelli, C.; Sorrell, C. C., The Effects of Carboxylic Acids on the Aqueous Dispersion and Electrophoretic Deposition of ZrO_2. *Journal of the European Ceramic Society* **2012,** *32* (1), 235-244.

(51) Israelachvili, J. N.; Wolfe, J., The Membrane Geometry of the Prolamellar Body. *Protoplasma* **1980,** *102* (3-4), 315-321.

(52) Veiro, J. A.; Khalifah, R. G.; Rowe, E. S., P-31 Nuclear Magnetic Resonance Studies of the Appearance of an Isotropic Component in Dielaidoylphosphatidylethanolamine. *Biophysical Journal* **1990,** *57* (3), 637-641.

(53) Shyamsunder, E.; Gruner, S. M.; Tate, M. W.; Turner, D. C.; So, P. T.; Tilcock, C. P., Observation of Inverted Cubic Phase in Hydrated Dioleoylphosphatidylethanolamine Membranes. *Biochemistry* **1988,** *27* (7), 2332-2336.

(54) Bentz, J.; Ellens, H., Membrane Fusion: Kinetics and Mechanisms. *Colloids and Surfaces* **1987,** *30* (1), 65-112.

(55) Siegel, D. P., Inverted Micellar Intermediates and the Transitions between Lamellar, Cubic, and Inverted Hexagonal lipid phases. I. Mechanism of the L_α-H_{II} Phase Transitions. *Biophysical Journal* **1986,** *49* (6), 1155-1170.

(56) Siegel, D. P., Inverted Micellar Intermediates and the Transitions between Lamellar, Cubic, and Inverted Hexagonal Lipid Phases. II. Implications for Membrane-Membrane Interactions and Membrane Fusion. *Biophysical Journal* **1986,** *49* (6), 1171-1183.

(57) Tate, M. W.; Gruner, S. M., Lipid Polymorphism of Mixtures of Dioleoylphosphatidylethanolamine and Saturated and Monounsaturated Phosphatidylcholines of Various Chain Lengths. *Biochemistry* **1987,** *26* (1), 231-236.

(58) Gruner, S. M., Intrinsic Curvature Hypothesis for Biomembrane Lipid Composition: A Role for Nonbilayer lipids. *Proceedings of the National Academy of Sciences of The United States of America* **1985,** *82* (11), 3665-3669.

(59) Kirk, G. L.; Gruner, S. M.; Stein, D. L., A Thermodynamic Model of the Lamellar to Inverse Hexagonal Phase Transition of Lipid Membrane-Water Systems. *Biochemistry* **1984,** *23* (6), 1093-1102.

(60) Lindblom, G.; Rilfors, L., Cubic Phases and Isotropic sStructures Formed by Membrane Lipids — Possible Biological Relevance. *Biochimica et Biophysica Acta* **1989,** *988* (2), 221-256.

CHAPTER 4
A TRIGGERALBE RAPID CONTENTS RELEASE LIPOSMAL SYSTEM BASED ON A REDOX-SENSITIVE Q_{PA}-DOPE:POPE LIPID MIXTURE

4.1 Introduction

Liposomal delivery systems have potential for site-specific delivery of therapeutic agents to tumor sites. Of recent scientific interest is the development of 3rd-generation liposomes whose contents are released by an endogenous stimulus unique to the targeted site. The McCarley lab has developed a redox-sensitive liposome, composed of a quinone propionic (Q_{PA}) trigger group bound to the polar head group of DOPE, to target NAD(P)H:quinone oxidoreductase type 1 (NQO1). This reductase enzyme is upregulated in numerous cancer cells, and it catalyzes the reduction of quinones to hydroquinones.[1-8] Upon reduction from a quinone to a hydroquinone in Q_{PA}-DOPE liposomes, the outer leaflet Q_{PA} is cleaved from the DOPE lipid, and the liposomal payload is released. Q_{PA}-DOPE liposomes faces two challenges: (1) the contents release of Q_{PA}-DOPE liposomes is lipid concentration dependent, which requires a minimum bioaccumulation concentration threshold to function properly; and (2) the time required for contents release is limited by the kinetics of Q_{PA} cyclization and cleavage. To improve the application potential of Q_{PA}-DOPE liposomes, the mechanism of release must be manipulated by altering the nature of the bilayer.

It is a characteristic of phospholipids to form either a lamellar or inverted hexagonal phase when hydrated in excess water.[9] An intermediate phase that has recently received much attention is the cubic phase, which has isotropic state properties and has been identified as a possible intermediate in the fusion of opposed bilayers.[10-12] The cubic phase is a closely packed spherical micelle existing in one of three possible 3-D arrays: (A) primitive cubic, (B) body-centered cubic, or

(C) face-centered cubic (Figure 4.1).[13] Lipids can be mixed with one another to form a composition having a new phase different from either counterpart.[14-16] Gruner et al. explained the phase identity of a lipid composition in terms of its intrinsic curvature.[17] The radius of curvature (R_o) is large for a bilayer and small for non-bilayer structures. R_o is determined from the geometry of the lipid, which dictates the packing of the non-polar region in the bilayer. As an example, if the temperature of a lipid system were to be increased, the lipid's intrinsic R_o would decrease, due to an increase in the cross-sectional area of the non-polar region. Likewise, if the area of the polar region were increased (e.g., methylation of a PE head group, (PC vs PE), or Q_{PA} functionalization), the lipid's intrinsic R_o would increase.[10,18-20] For a given lipid system where R_o is intermediate between R_o (L_α) and R_o (H_{II}), R_o would be highly sensitive to lipid physical environment (i.e., ions, temperature, pH) or any change on the membrane's surface (i.e., charge, hydration, head group size).[21-24]

The phase exhibited by a lipid or lipid mixture is the one that has the lowest free energy. When the free energy of two phases are equal, both phases can co-exist and be mesomorphic.[13,25] Kirk et al. modeled the free energy of L_α, H_{II}, and inverted cubic (Q_{II}) phases for unsaturated PE lipids using the sum of the local, packing, hydration, and electrostatic free energies.[25] In the model, the L_α, H_{II}, and Q_{II} free energy of a lipid mixture composed of 80% PS and 20% PE lipids exponentially decreased with increasing degrees of hydration ($Q_{II} > H_{II} > L_\alpha$). At no point did the authors observe the Q_{II} phase to have a lower free energy than either the L_α or H_{II} phase. Their reasoning for this was unsaturated PE lipids have a high chain packing energy, forbidding the Q_{II} phase.

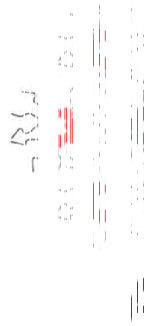

Figure 4.1. (A) The inverted hexagonal phase (H_{II}) is a two-dimensional array of inverted micelle tubes in a hexagonal packing arrangement. The cubic phase is a closely packed spherical micelle in one of three three-dimensional arrays: (B) Primitive cubic, (C) Body-centered cubic, or (D) Face-centered cubic also known as the inverted cubic phase (Q_{II}).

The cubic phase is exhibited by a lipid when it has a lower free energy than either the L_α or H_{II} phase, which is due to competing R_o and packing constraints.[26] In any phase, the hydrocarbon chains must stretch to completely fill the non-polar areas of these geometries, which effects R_o of the lipid mixture.[27] If the lipid is incapable of an increase in its nonpolar cross-sectional area, L_α (R_o) will be favored. Incorporating saturated and/or shorter acyl chains in the hydrocarbon region lowers the packing free energy.[25,26] If this resulting R_o falls between H_{II} (R_o) and L_α (R_o), the free energy of the cubic phase is at its lowest value. Tilcock et al. studied lipid mixtures of 1,2-dioleoyl-*sn*-glycerol-3-phosphatidylethanolamine (DOPE, diacyl-18:1) and 1,2-ditetradecanoyl-*sn*-glycerol-3-phosphatidylethanolamine (DTPE, diacyl-14:0) and found a mesomorphic lamellar-isotropic state in the ^{31}P NMR lineshape over a wide range of temperatures. Both acyl chains in DTPE are unsaturated and are four carbon units shorter than those in DOPE, which suggests the inclusion of the 14:0 chains lowers the packing free energy of the bilayer and promotes the cubic phase.[28]

In the work presented herein, large unilamellar vesicles (LUVs, 100-nm diameter) composed of 1-palmitoyl-2-oleoyl-3-*sn*-glycerol-phosphatidylethanolamine (POPE) and Q_{PA}-DOPE can be readily formed at 40 °C. Furthermore, the time required for

50% release of the encapsulated contents (t_{50}) after Q_{PA}-DOPE reduction was dramatically reduced with increasing molar quantities of POPE and was relatively unaffected at lower lipid concentrations. ^{31}P NMR lineshapes of 20:80 Q_{PA}-DOPE:POPE giant unilamellar vesicles (GUVs, > 1-μm diameter) are characteristic of a mesomorphic lamellar phase (L_α) and isotropic state before chemical reductive activation; a slow transition to an inverted hexagonal phase (H_{II}) is noted after reduction. This work suggests Q_{PA}-DOPE:POPE vesicles undergo a charge destabilized $L_\alpha \rightarrow H_{II}$ transition with isotropic or possibly cubic phase intermediates that is kinetically slower than Q_{PA}-DOPE liposomes. I posit the growth of the observed isotropic state is associated with a bicontinuous cubic intermediate phase in the Q_{PA}-DOPE:POPE bilayer. The mesomorphic cubic-lamellar phase results in extensive and rapid liposomal contents release, caused by stress in the area around the cubic phase nucleation sites, upon the near instantaneous reduction of the Q_{PA} head groups to the hydroquinone (HQ_{PA}) version.

4.2 Results

Q_{PA}-DOPE:POPE LUVs having different molar amounts of Q_{PA}-DOPE were studied for payload release and phase properties. For contents release experiments, each sample came from a freshly prepared stock solution of 100 μM total lipid as LUVs (100-nm diameter) prepared in PBS (pH 7.40) with 40 mM calcein encapsulated. After equilibrating at 40 °C in the fluorometer for no less than 15 min, sodium dithionite (5:1 $S_2O_4^{2-}$:lipid, mol/mol) was added as a reducing agent to cleave the outer leaflet Q_{PA} from its DOPE lipid counterpart. The contents release profiles for the various Q_{PA}DOPE:POPE systems are shown in Figure 4.2. For a quantitative comparison of these systems, the time required for 50% of total calcein release (t_{50}) is used as a tool

for comparison. The t_{50} values and the total percent release of the encapsulated contents are displayed in Table 4.1. There is an inverse correlation between the release rate of the liposome system and the Q_{PA}-DOPE molar concentration, as seen from the t_{50} values of the vesicles containing 100% and 15% Q_{PA}-DOPE; 9.5 ± 0.5 min and 2.5 ± 0.1 min, respectively. Higher sodium dithionite concentrations had no effect on the observed release times and maximum percentage of contents release.

After reduction, Q_{PA}-DOPE LUVs undergo contact-mediated release of opposing vesicle, which can be observed by an increase in light scattering. The single-trial light scattering profiles for varying ratios of Q_{PA}-DOPE:POPE LUVs are shown in Figures 4.3A-E overlaid with their respective contents release curves. An increase in light scattering is strongly correlated with an increase in fluorescent signal from calcein release for 100% Q_{PA}-DOPE LUVs after reduction.

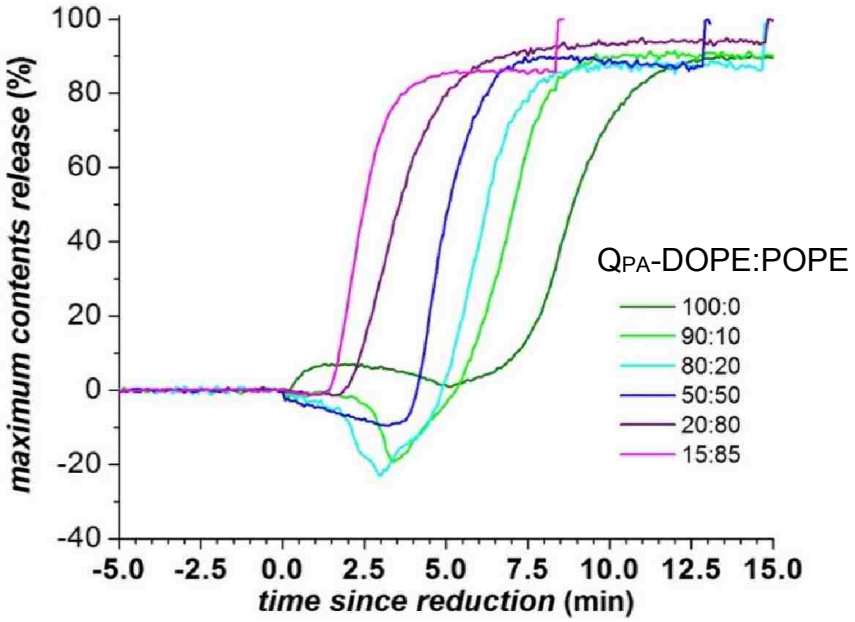

Figure 4.2. Contents release curves of Q_{PA}-DOPE:POPE (mol%) large unilamellar vesicles (LUVs, 100-nm diameter) prepared in 100 mM KCl and 0.1 mM EDTA buffered with 50 mM phosphate, pH 7.4 with 40 mM calcein encapsulated inside the vesicles at 40 °C. A 5:1 molar ratio of sodium dithionite:lipid was injected at t=0 min. After no additional increase in fluorescent signal occurred, the remaining vesicles were lysed by the addition of 1.0% TritonX-100 detergent to determine the maximum fluorescent signal from encapsulated calcein

Table 4.1. The time required for 50% of the encapsulated contents to release (t_{50}) and percent of total content release for the various Q_{PA}-DOPE vesicle systems at 40 °C.

Q_{PA}-DOPE:POPE	t_{50}(min)	Contents Release (%)	DLS Diameter (nm)
100:0	9.5 ± 0.5	86.7 ± 5.8	114 ± 2
90:10	7.3 ± 0.2	88.3 ± 2.5	96.7 ± 3
80:20	6.4 ± 0.1	89.1 ± 0.3	100. ± 1
50:50	5.8 ± 0.6	88.3 ± 2.6	109 ± 1
20:80	3.0 ± 0.9	90.3 ± 3.4	108 ± 1
15:85	2.5 ± 0.1	85.4 ± 1.1	118 ± 1

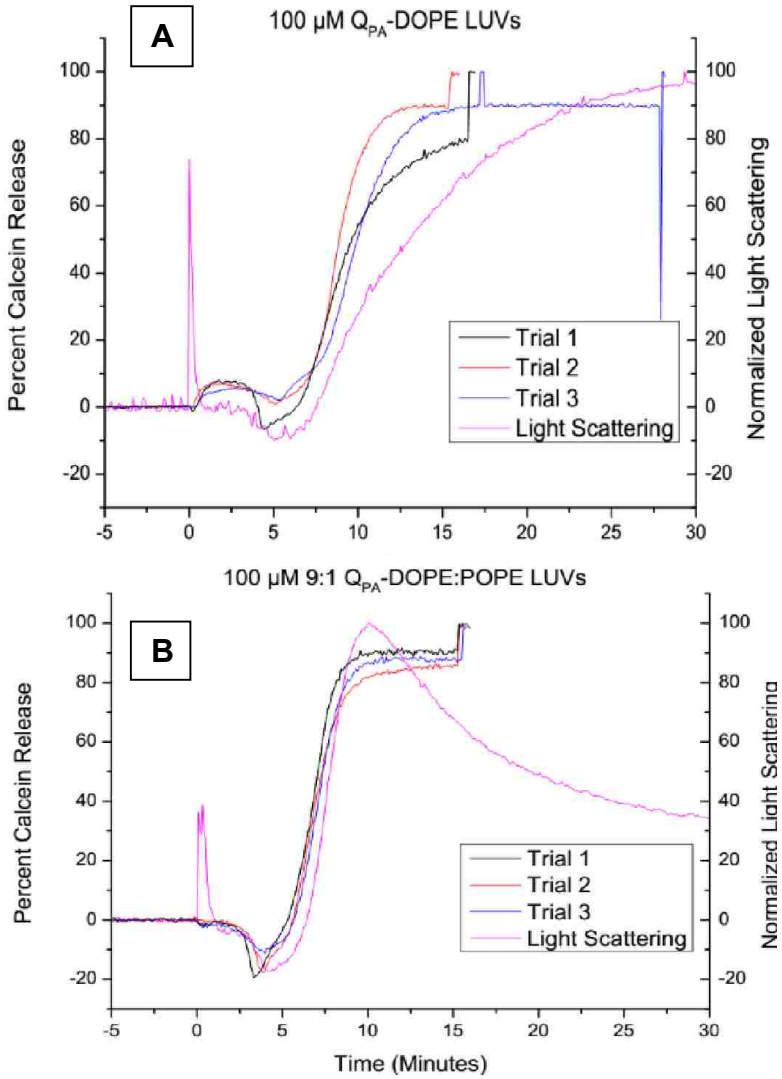

Figure 4.3A-E Q_{PA}-DOPE:POPE Contents release curves overlaid with light scattering curves for 100:0 (A), 90:10 (B), 80:20 (C), 50:50 (D), and 20:80 (E) ratios at 40 °C are displayed. The 20:80 mixture shows the onset of light scattering after contents release is observed.

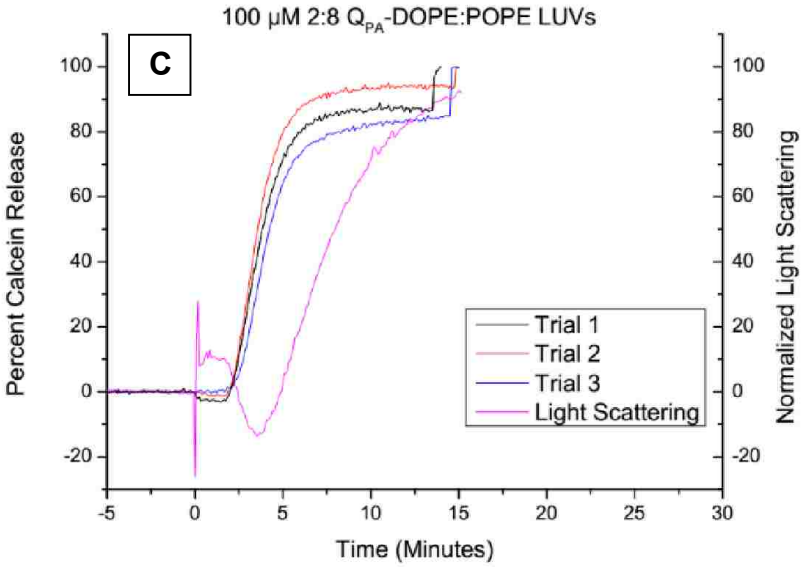

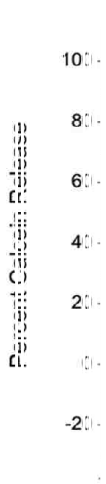

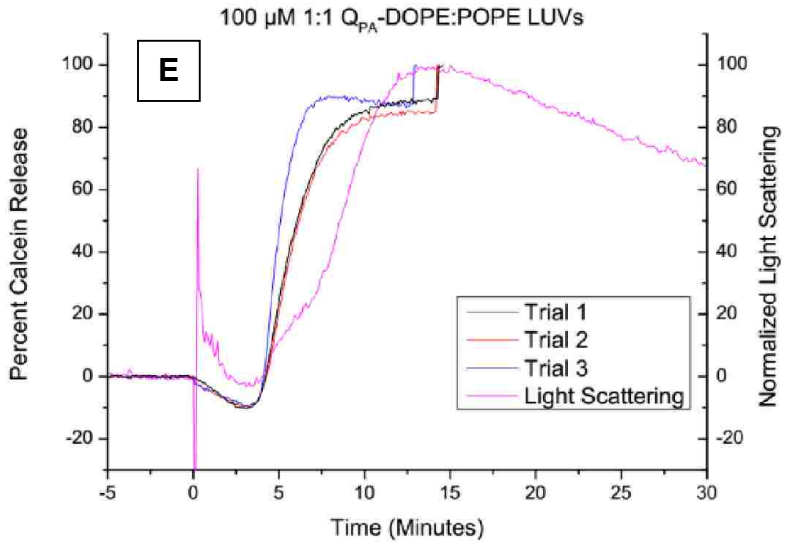

Figure 4.3 Continued

This property is also observed for Q_{PA}-DOPE:POPE lipid mixtures when Q_{PA}-DOPE is the more abundant lipid. In the 20:80 Q_{PA}-DOPE:POPE lipid mixture, an increase in light scattering is also observed, but its onset occurs after the encapsulated contents has already released (Figure 4.3E). This suggests that the vesicles begin to release their contents prior to significantly aggregating. In such a case, the observed contents release time would be independent of vesicle concentration.

To test this, the contents release properties of 100% Q_{PA}-DOPE and 20:80 Q_{PA}-DOPE:POPE LUVs were assessed as a function of vesicle concentration (Figure 4.4A-B). The McCarley group has previously reported on the lipid concentration dependence of contents release from Q_{PA}-DOPE LUVs and found the ability of this system to release its contents after reduction was significantly hindered at lower concentrations; this evidence was used to support the argument that the release mechanism for 100% Q_{PA}-DOPE liposomes is based on contact-mediated process.[23] In that study, 100% Q_{PA}-DOPE LUVs showed a decrease in both the rate of release and total contents release with lower lipid concentrations, having < 10% release over 40 min for 12.5 μM lipid.

In the work at hand, this trend was not seen with 20:80 Q_{PA}-DOPE:POPE LUVs. At 12.5 μM, the 20:80 Q_{PA}-DOPE:POPE vesicles had a t_{50}=3.3 min and 88.7% contents release, which is within the standard deviation reported in Table 4.1. There appears to be a threshold for which contents release is observed, namely, 7.5 μM 20:80 Q_{PA}-DOPE:POPE. This suggests that while the number of contact events from opposed bilayers does not affect the release kinetics, a low amount of bilayer contact is needed. This is supported by the light scattering measurement in Figure 4.3E, where, it is found 20:80 Q_{PA}-DOPE:POPE LUVs are not dependent on extensive aggregation

in order to release their contents after reduction; the latter is the driving force for contents release from 100% Q_{PA}-DOPE liposomes.

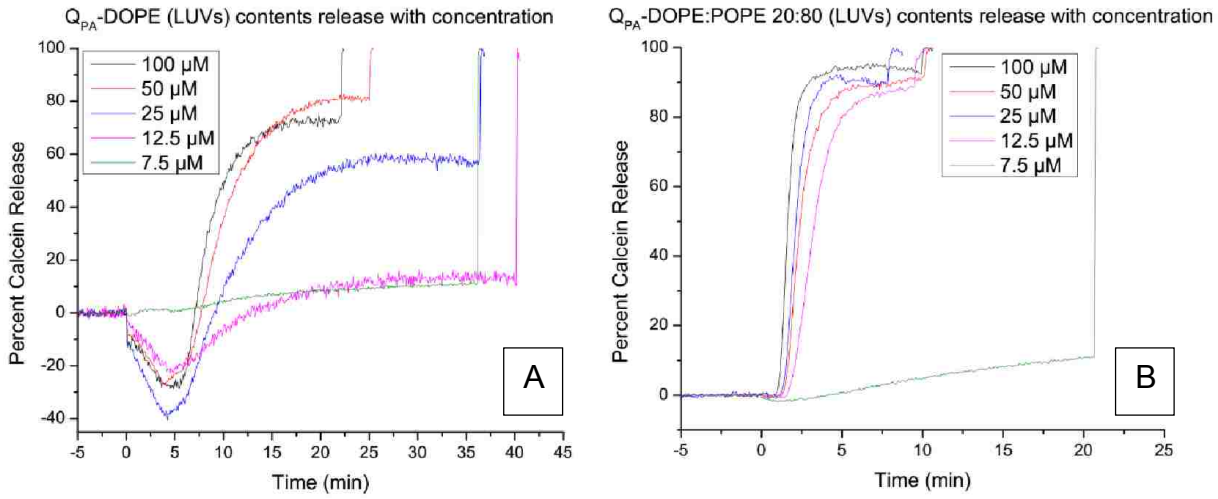

Figure 4.4A-B. Contents release curves for 100% Q_{PA}-DOPE (A) and a 20:80 (mol) mixture of Q_{PA}DOPE:POPE LUVs at 40 °C (B) as a function of lipid concentration. Q_{PA}-DOPE LUVs are contact dependent and require aggregation to release their contents. The contents release profile of 20:80 Q_{PA}-DOPE:POPE LUVs does not show a significant dependence on lipid concentration; however, it does have a minimum threshold concentration (7.5 μM) necessary for release.

We have previously shown that the Q_{PA}-DOPE system undergoes an $L_\alpha \rightarrow H_{II}$ phase change upon reduction, with the final phase being a mesospheric inverted hexagonal-isotropic state.[23] This is driven by the affinity of DOPE to exist in an inverted hexagonal phase above 5 °C; however, to our knowledge, the phase effect of mixing POPE with DOPE has yet to be studied. Differential scanning calorimetry (DSC) measurements I performed are in agreement with the reported POPE T_M and T_H values of 24 °C and 72 °C, respectively (Figure 4.5).[16] ^{31}P NMR anisotropy measurements of POPE MLVs at temperatures below and above the T_H of POPE reveal lineshapes and linewidths characteristic of an L_α and H_{II} phase, respectively (see Chapter 3).

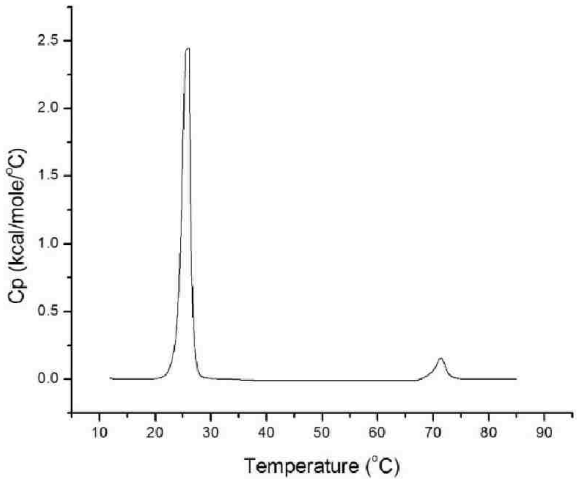

Figure 4.5. Differential scanning calorimetry (DSC) spectrum of 18 mM POPE in 140 mM sucrose buffered with 10 mM TES, pH 7.4. The heat capacity profile of POPE reveals two peaks at 24 °C and 72 °C, corresponding to the $L_\beta \rightarrow L_\alpha$ phase transition (T_M) and the $L_\alpha \rightarrow H_{II}$ (T_H) phase transition, respectively.

^{31}P NMR anisotropy was also used to determine the phase behavior of 20:80 Q_{PA}-DOPE:POPE vesicles after reduction (Figure 4.6A-E). Before reduction, 20:80 Q_{PA}-DOPE:POPE GUVs had a linewidth of 44 ppm and a lineshape profile supporting the presence of an L_α phase. This is in agreement with the predicted linewidth of a PE lipid in the L_α phase (see Chapter 3).[29,30] Unlike pure Q_{PA}-DOPE GUVs, which showed complete conversion from the L_α phase within such and such time after reduction, conversion of 20:80 Q_{PA}-DOPE:POPE GUVs was significantly slower, taking 84 hours for completion. Its final linewidth was 22.6 ppm, with a lineshape indicative of an H_{II} phase. The spectra at intermediate times reveal the presence of both L_α and H_{II} phases, in addition to an isotropic state. The co-existence of an isotropic state with a lamellar phase prior to reduction could arise from contact of opposed bilayers during centrifugation or multi-lamellar structures. DSC measurements of 20:80 Q_{PA}-DOPE:POPE and 20:80 DOPE:POPE lipid mixtures exhibit a decrease in T_H from 64 °C to 55 °C when the Q_{PA} group is not attached to DOPE (Figure 4.7A-B).

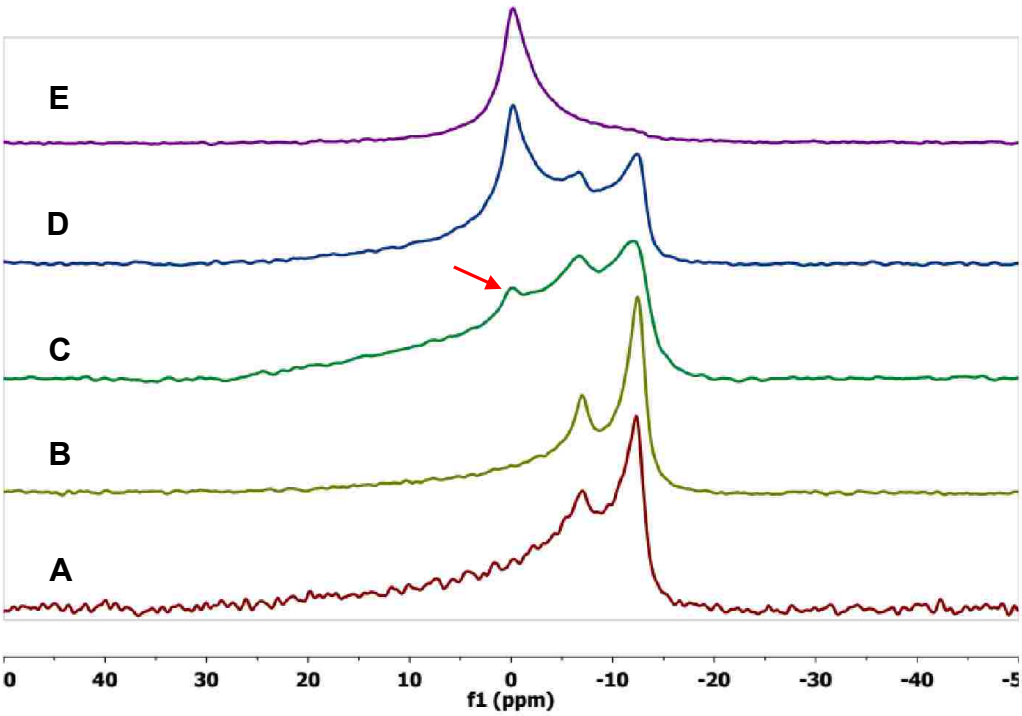

Figure 4.6A-E. ^{31}P NMR anisotropy spectra of Q_{PA}-DOPE:POPE GUVs (2:8 mol/mol) in 100 mM KCl buffered with 10 mM TES, pH 7.4 before and after the addition of $S_2O_4^{2-}$ at 25 °C. (A, bottom) Q_{PA}-DOPE:POPE GUVs (2:8 mol/mol) before reduction, (B) 1 h, (C) 36 h, (D) 60 h, and (E) 84 hours after $S_2O_4^{2-}$ reduction. An L_α phase is present in spectra A-E as evident by the lineshape and an average linewidth of 43.5 ppm. The appearance of an H_{II} phase is first indicated by its lineshape in spectrum C (red arrow) and is co-existent with both an L_α phase and isotropic state until spectrum E, having a linewidth of 22.6 ppm and lineshape characteristic of only a H_{II} phase. An isotropic state is seen in A-D, as evident by the signal at –6.5 ppm.

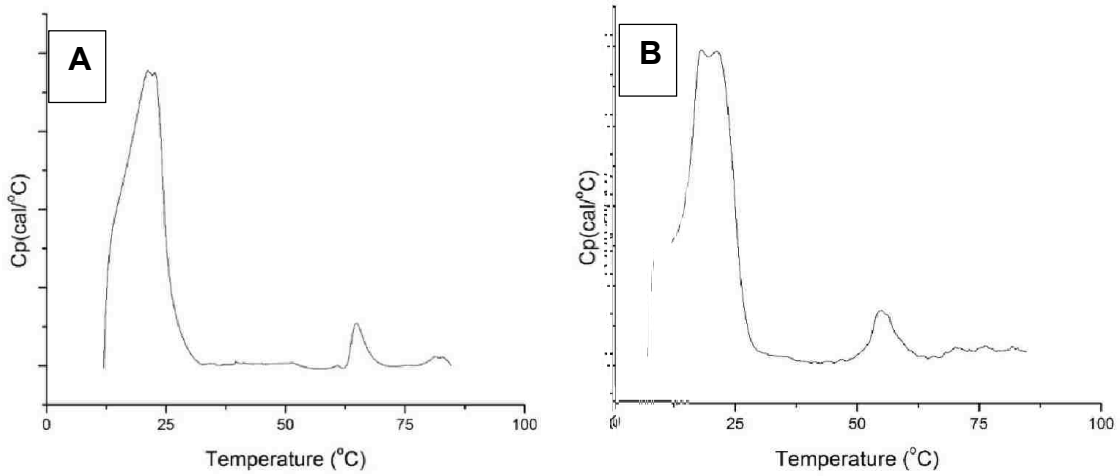

Figure 4.7A-B. (A) The heat capacity profile of 20:80 Q_{PA}DOPE:POPE MLVs reveals two peaks at 21 °C and 64 °C, corresponding to the $L_\beta \rightarrow L_\alpha$ phase transition (T_M) and the $L_\alpha \rightarrow H_{II}$ (T_H) phase transition, respectively. (B) The heat capacity profile of 20:80 DOPE:POPE reveals two peaks at 21 °C and 55 °C, corresponding to the T_M and T_H, respectively.

4.3 Discussion

The contents release from reduced 20:80 Q_{PA}-DOPE:POPE LUVs occurs after a slight increase in light scattering, but before extensive aggregation, and its mode of contents release is not dependent on the concentration of liposomes present. The rate of release is a function of the ratio of unsaturated POPE to Q_{PA}-DOPE in the bilayer. Moreover, ^{31}P NMR data is indicative of a mesomorphic lamellar-isotropic state after reduction that diminishes as a H_{II} phase is formed. DSC measurements of Q_{PA}-DOPE:POPE and DOPE:POPE MLVs demonstrate a 9 °C decrease in T_H from 64 °C to 55 °C when Q_{PA} is not attached to DOPE. From these results, it is proposed the mechanism of contents release for 20:80 Q_{PA}-DOPE:POPE liposomes differs from that of pure Q_{PA}-DOPE LUVs, which relies on a contact mediated $L_\alpha \rightarrow H_{II}$ transition of opposed bilayers. Based on observation here and prior literature, the mechanistic difference arises from a difference in the packing free energy of the mixed acyl bilayer.

An isotropic lipid state is complex, and it can be composed of micelles, small lamellar particles (<< 1-μm diameter), or a cubic phase. In Q_{PA}-DOPE:POPE GUVs, the isotropic state signal decreases over time with the rise of a hexagonal phase. With this in mind, a more probable explanation of the isotropic signal is the temporal existence of a cubic phase. The cubic phase is an intermembrane intermediate (IMI) that gives rise to isotropic ^{31}P NMR signal and has been observed in various lipid systems at temperatures between T_M and T_H.[31,32] Two different research groups independently found an isotropic state in hydrated DOPE and DEPE membranes with ^{31}P NMR spectroscopy.[33,34] Also, Shyamsunder et al. used X-ray diffraction to investigate the isotropic state of DOPE, and they found an inverted cubic phase when they repeatedly cycled the lipid above and below its T_H.[33]

It is known that rapid formation of IMIs in a bilayer drives the lytic pathway of liposomal contents release, ($L_\alpha \rightarrow H_{II}$), while fewer IMIs formed in a bilayer in a given time results in a kinetically slower contents release process from liposomes with cubic phase intermediates playing a major role; the latter path has been associated with vesical fusion.[11,12,35-37] As the most stable phase is the one that has the lowest free energy, the cubic phase will only form when it has a lower free energy than either the L_α or H_{II} phases, and this can only occur upon competition of intrinsic radius of curvature and packing constraints.[25,26] Saturated lipids, such as POPE, can elastically stretch in the non-polar region of a lipid phase to fill the cross sectional areas, thereby lowering the packing free energy.

No contents release or vesicle aggregation was observed for 100% Q_{PA}-POPE LUVs after Q_{PA} reduction (Appendix 23); therefore, the mechanism of contents release in 80:20 Q_{PA}-DOPE:POPE LUVs stems from mixed acyl chains in the bilayer. DOPE is an unsaturated lipid favoring the H_{II} phase at temperatures above its T_H of 8 °C.[38,39] POPE is a mixed acyl lipid that favors the L_α phase below 72 °C. The DSC measurement of DOPE:POPE mixtures suggests the single 16:0 acyl chain in POPE lowers the packing free energy of the bilayer, in turn lowering the T_H of the bilayer to 55 °C by relaxing the packing stress in the bilayer. Gruner and co-workers studied the change in H_{II} free energy of PE and PC mixtures upon inclusion of tetradecane (14:0) and found three effects: (1) the spontaneous radius of curvature of the membrane was lowered; (2) the work necessary to dehydrate the polar head groups was decreased; and (3) the hydrocarbon stress in the non-polar bilayer was relaxed.[40] Tate et al. explored the lipid polymorphism of PE lipid mixtures with other PE lipids having varying chain lengths and saturation and confirmed the same effect.[27]

An identical light scattering profile to that of 20:80 Q_{PA}-DOPE:POPE (Figure 4.2E) was reported by Wilschut et al. when studying Ca^{2+}-induced fusion of phosphatidylserine (PS) LUVs.[41] After inducing fusion, the authors observed a small initial increase in light scattering quickly followed by a subsequent decrease in light scattering that preceded a dramatic increase in light scattering. The initial increase followed by a decrease in light scattering correlates to contact of opposing vesicles that results in fewer particles scattering light. The large increase in light scattering that occurred after PS vesicles achieve maximum fusion suggests the signal increase arises from collapse of the internal aqueous space before extensive aggregation.

The only chemical difference in 20:80 Q_{PA}-DOPE:POPE LUVs after $S_2O_4^{2-}$ addition and prior to contents release is the reduction of the quinone head groups in the outer leaflet of Q_{PA}-DOPE to hydroquinones (HQ_{PA}-DOPE). Therefore, it is proposed the contents release is triggered by a decrease in the repulsive hydration force of the outer leaflet polar region. Akoka et al. studied the hydrogen-bonding effects of various *N*-acyl-PE lipids and noted that functional groups attached to the polar head of PE lipids may fold back into the membrane and hydrogen-bond with either the NH or phosphate oxygen in the polar region of the PE lipid.[42] An increase in hydrogen-bonding in the polar region of PE lipids decreases the overall hydration force.[43]

It is proposed the HQ_{PA}-DOPE formed in the outer LUV leaflet leads to changes in hydration that allow opposed bilayer surfaces to come into contact with each other so as to form isotropic IMIs. The unsaturated chain in POPE lowers the packing free energy in the bilayer by its stretching to fill the empty space in the non-polar region around IMI spaces. This results in deformation of the bilayer, which generates local stress in the bilayer at the deformation areas around the IMIs. Stress can be relieved

near these localized points in the bilayer in two ways: (1) fusion of the opposed bilayers occurs, resulting in contents and lipid mixing; and/or (2) fracturing of the bilayer occurs at the lipid-stress site, resulting in LUVs contents release into the interstitial volume (Scheme 4.1).

Gruner et al. characterized the polymorphic phase behavior and properties of mono-, di-, and tri-methylated POPE lipids (DOPE, DOPE-Me, DOPE-Me_2) mixed with DOPC.[18] Functionalizing the polar head group of DOPE raised the T_H of the lipid from ~8 °C to ~65 °C for a single methylation (DOPE-Me).[28] The authors also observed a cubic phase in the DOPE-Me system upon raising its temperature to a definitive point below its measured T_H. A similar hydration effect is observed with Q_{PA}-DOPE; functionalizing the DOPE head group with Q_{PA} lowered the free energy of the lamellar phase, as observed by Q_{PA}-DOPE forming LUVs at temperatures above the T_H of DOPE.

Gangné et al. investigated the lipid mixing of opposed PS bilayers from Ca^{2+}-induced fusion.[32] They studied PS:DEPE-Me and PS:DEPE-Me_2 liposomes and found that the more hydrated DEPE-Me_2 lipids mixed better than DEPE-Me lipid.[32] This suggests the degree of hydration affects fusion (both contents and lipid mixing). It is worth mentioning that Gagné et al. also observed an isotropic ^{31}P NMR lineshape for mono-methylated DOPE at temperatures above its T_M; using freeze-fracture electron microscopy, they confirmed the isotropic state was associated with a cubic phase. After the internal contents of the 20:80 Q_{PA}-DOPE:POPE LUVs were released, massive aggregation of opposed bilayer membranes was observed by light scattering. At this point, the internal contents of the liposomes have mixed with the exterior volume, allowing $S_2O_4^{2-}$ to reduce the inner leaflet Q_{PA}-DOPE lipids to HQ_{PA}-DOPE. Eventually,

the hydroquione cyclizes to form a lactone, which cleaved from DOPE, resulting in massive aggregation of opposed bilayers, as seen in the light scattering measurements of Figure 4.3. Rapid aggregation and IMI formation drive the lytic pathway and result in formation of the H_{II} phase (Scheme 4.2).

Scheme 4.1.

Scheme 4.1. Formation of a leaky mesomorphic bicontinuous cubic–lamellar bilayer structure. (1) Upon reduction of the outer leaflet Q_{PA}-DOPE lipids in the 20:80 Q_{PA}-DOPE:POPE vesicles, opposed bilayers approach one another and come into contact due to a change in hydration force. (2) At the contact site, cubic intermembrane intermediates (IMIs) form at the contact site and can have the geometry of a (A) primitive, (B) body-centered, or (C) face-centered cubic phase (see Figure 4.1). This cubic-isotropic phase is bicontinuous and co-exists with the lamellar-liquid crystal phase as a fusogenic system. (3) The acyl chains in the non-polar region around the cubic phase IMI stretch to fill the entire volume, causing deformation in the bilayer (red arrows). In a traditional fusion pathway (4a), the cubic phase IMI facilitate fusion of the opposed bilayers and mixing of both their encapsulated volumes and lipid bilayers. In the proposed lysis pathway (4b), the deformation sites stress the intrinsic curvature of the bilayer and serve as a nucleation site, which results in membrane lysis, extensive contents leakage, and eventually mixing of the internal contents with the exterior volume (contents release).

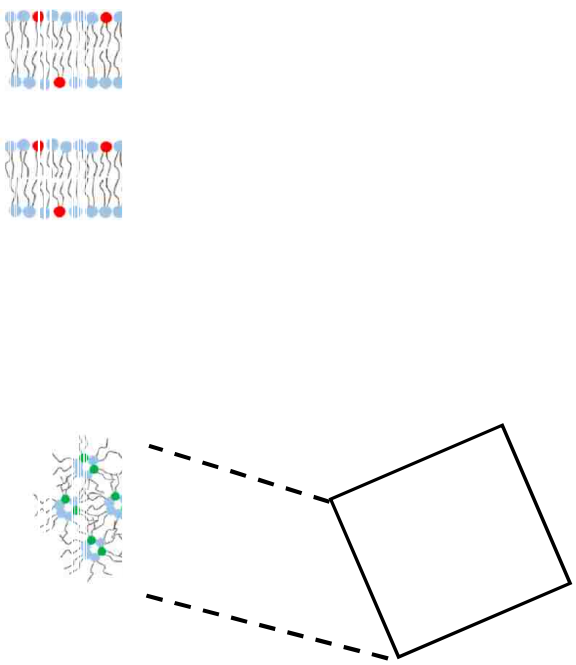

Scheme 4.2. Formation of the inverted hexagonal phase from a mesomorphic cubic-lamellar bilayer after contents release. (1) Upon reduction of the outer leaflet Q_{PA}-DOPE lipids in the 20:80 Q_{PA}-DOPE:POPE lipid mixture, opposed bilayers approach one another and come into contact due to a change in the hydration force (Scheme 4.1). (2) After lysis of the membrane, the external volume mixes with the internal volume of the vesicle, allowing reduction of Q_{PA}-DOPE in the inner leaflet of the bilayer membrane. (3) After the hydroquinone forms a lactone and is cleaved from the DOPE lipid, the bilayer membranes become charge neutral. The charge repulsion force is lost and the opposed PE bilayers aggregate extensively. (4) There is rapid IMI formation between opposed bilayers, following the lytic pathway reported by Ellens et. al. (*Biochemistry* 1989). (5) The lytic path phase change from the mesomorphic lamellar-cubic bilayers into the inverted hexagonal phase.

4.4 Conclusion

20:80 Q_{PA}-DOPE:POPE LUVs are chemically unique from other liposomal systems exhibiting inverted cubic (Q_{II}) phase properties, in that they require a redox stimulus to chemically trigger contents release rather than pH, temperature, or water content. The contents release mechanism for reduced Q_{PA}-DOPE:POPE LUVs is triggered by a change in surface structure of the outer membrane, which results in a

lowering of the repulsive hydration force of the outer membrane surface. The physical driving force responsible for rapid contents release is in the inclusion of an unsaturated lipid that lowers the packing free energy in the non-polar region surrounding the IMI. It is quite notable that the simple structural change of a quinone to a hydroquinone in 20% of lipids on the outer leaflet of a liposome membrane can initiate rapid and extensive contents leakage. Because of the time improvement in contents release and its relative independence on liposome concentration, the 20:80 Q_{PA}-DOPE liposomal system has much potential as a carrier for drug delivery.

The use of a reduction process to trigger rapid contents release based on altering the surface hydration force and not Q_{PA} cleavage (as is the case with 100% Q_{PA}-DOPE) is a significant advance in the realm of 3rd-generation liposomes.[23] While more work is needed to further investigate the isotropic state and suspected cubic phase, an exciting future path for similar systems is the engineering of new head groups that are sensitive to a larger array of chemical stimuli characteristic of various cancers or diseases.

4.5 References

(1) Ong, W.; Yang, Y.; Cruciano, A. C.; McCarley, R. L., Redox-Triggered Contents Release from Liposomes. *Journal of the American Chemical Society* **2008,** *130* (44), 14739-14744.

(2) Awadallah, N. S.; Dehn, D.; Shah, R. J.; Russell Nash, S.; Chen, Y. K.; Ross, D.; Bentz, J. S.; Shroyer, K. R., NQO1 Expression in Pancreatic Cancer and its Potential use as a Biomarker. *Applied Immunohistochemistry and Molecular Morphology* **2008,** *16* (1), 24-31.

(3) Rooseboom, M.; Commandeur, J. N.; Vermeulen, N. P., Enzyme-Catalyzed Activation of Anticancer Prodrugs. *Pharmacological Reviews* **2004,** *56* (1), 53-102.

(4) Fitzsimmons, S. A.; Workman, P.; Grever, M.; Paull, K.; Camalier, R.; Lewis, A. D., Reductase Enzyme Expression Across the National Cancer Institute Tumor Cell Line Panel: Correlation with Sensitivity to Mitomycin C and EO9. *Journal of the National Cancer Institute* **1996,** *88* (5), 259-269.

(5) Cresteil, T.; Jaiswal, A. K., High Levels of Expression of the NAD(P)H:Quinone Oxidoreductase (NQO1) Gene in Tumor Cells Compared to Normal Cells of the Same Origin. *Biochemical Pharmacology* **1991,** *42* (5), 1021-1027.

(6) Siegel, D.; Franklin, W. A.; Ross, D., Immunohistochemical Detection of NAD(P)H:Quinone Oxidoreductase in Human Lung and Lung Tumors. *Clinical Cancer Research* **1998,** *4* (9), 2065-2070.

(7) Ross, D.; Beall, H.; Traver, R. D.; Siegel, D.; Phillips, R. M.; Gibson, N. W., Bioactivation of Quinones by DT-diaphorase, Molecular, Biochemical, and Chemical Studies. *Oncology Research* **1994,** *6* (10-11), 493-500.

(8) Monks, T. J.; Hanzlik, R. P.; Cohen, G. M.; Ross, D.; Graham, D. G., Quinone Chemistry and Toxicity. *Toxicology and Applied Pharmacology* **1992,** *112* (1), 2-16.

(9) Gruner, S. M., Non-lamellar Lipid Phases. In *The Structure of Biological Membranes; Yeagle, P.L. Ed.;* CRC Press: Boca Raton, Florida, 2005, pp 173-199.

(10) Ellens, H.; Siegel, D. P.; Alford, D.; Yeagle, P. L.; Boni, L.; Lis, L. J.; Quinn, P. J.; Bentz, J., Membrane Fusion and Inverted Phases. *Biochemistry* **1989,** *28* (9), 3692-3703.

(11) Siegel, D. P., Inverted Micellar Intermediates and the Transitions between Lamellar, Cubic, and Inverted Hexagonal Lipid Phases. I. Mechanism of the L_{α}–H_{II} Phase Transitions. *Biophysical Journal* **1986,** *49* (6), 1155-1070.

(12) Siegel, D. P., I Inverted Micellar Intermediates and the Transitions between Lamellar, Cubic, and Inverted Hexagonal Lipid Phases. II. Implications for Membrane-Membrane Interactions and Membrane Fusion. *Biophysical Journal* **1986,** *49* (6), 1171-1183.

(13) Lindblom, G.; Rilfors, L., Cubic Phases and Isotropic Structures Formed by Membrane Lipids — Possible Biological Relevance. *Biochimica et Biophysica Acta* **1989,** *988* (2), 221-256.

(14) Boni, L. T.; Hui, S. W., Polymorphic Phase Behaviour of Dilinoleoyl-Phosphatidylethanolamine and Palmitoyl-oleoyl-phosphatidylcholine Mixtures: Structural Changes between Hexagonal, Cubic and Bilayer Phases. *Biochimica et Biophysica Acta* **1983,** *731* (2), 177-185.

(15) Lerche, D.; Fuller, N. L.; Rand, R. P., Membrane Curvature and Structural Transitions for Charged/Uncharged Phospholipid Mixtures. *Springer Proccedings in Physics* **1992,** *66*, 226-229.

(16) Epand, R. M.; Bottega, R., Determination of the Phase Behaviour of Phosphatidylethanolamine Admixed with Other Lipids and the Effects of Calcium Chloride: Implications for Protein Kinase C Regulation. *Biochimica et Biophysica Acta* **1988,** *944* (2), 144-154.

(17) Gruner, S. M., Intrinsic Curvature Hypothesis for Biomembrane Lipid Composition: A Role for Nonbilayer Lipids. *Proceedings of the National Academy of Sciences of the United States of America* **1985,** *82* (11), 3665-3669.

(18) Gruner, S. M.; Tate, M. W.; Kirk, G. L.; So, P. T. C.; Turner, D. C.; Keane, D. T.; Tilcock, C. P. S.; Cullis, P. R., X-ray Diffraction Study of the Polymorphic Behavior of *N*-methylated Dioleoylphosphatidylethanolamine. *Biochemistry* **1988,** *27* (8), 2853-2866.

(19) Gagne, J.; Stamatatos, L.; Diacovo, T.; Hui, S. W.; Yeagle, P. L.; Silvius, J. R., Physical Properties and Surface Interactions of Bilayer Membranes Containing *N*-Methylated Phosphatidylethanolamines. *Biochemistry* **1985,** *24* (16), 4400-4408.

(20) Israelachvili, J. N.; Marcelja, S.; Horn, R. G., Physical Principles of Membrane Organization. *Quarterly Reviews of Biophysics* **1980,** *13* (2), 121-200.

(21) Lewis, R. N., and McElhaney, R. N., Calorimetric and Spectroscopic Studies of the Thermotropic Phase Behavior of Lipid Bilayer Model Membranes Composed of a Homologous Series of Linear Saturated Phosphatidylserines. *Biophysical Journal* **2000,** *79* (4), 2043-2055.

(22) McCarley, R. L.; Forsythe, J. C.; Loew, M.; Mendoza, M. F.; Hollabaugh, N. M.; Winter, J. E., Release Rates of Liposomal Contents are Controlled by Kosmotropes and Chaotropes. *Langmuir* **2013,** *29* (46), 13991-13995.

(23) Loew, M.; Forsythe, J. C.; McCarley, R. L., Lipid Nature and Their Influence on Opening of Redox-Active Liposomes. *Langmuir* **2013,** *29* (22), 6615-6623.

(24) LeNeveu, D. M.; Rand, R. P.; Parsegian, V. A., Measurement of Forces between Lecithin Bilayers. *Nature* **1976,** *259* (5544), 601-603.

(25) Kirk, G. L.; Gruner, S. M.; Stein, D. L., A Thermodynamic Model of the Lamellar to Inverse Hexagonal Phase Transition of Lipid Membrane-Water Systems. *Biochemistry* **1984,** *23* (6), 1093-1102.

(26) Anderson, D. M.; Gruner, S. M.; Leibler, S., Geometrical Aspects of the Frustration in the Cubic Phases of Lyotropic Liquid Crystals. *Proceedings of the National Academy of Sciences of the United States of America* **1988,** *85* (15), 5364-5368.

(27) Tate, M. W.; Gruner, S. M., Lipid Polymorphism of Mixtures of Dioleoylphosphatidylethanolamine and Saturated and Monounsaturated Phosphatidylcholines of Various Chain Lengths. *Biochemistry* **1987,** *26* (1), 231-236.

(28) Tilcock, C. P. S.; Cullis, P. R., The Polymorphic Phase Behaviour and Miscibility Properties of Synthetic Phosphatidylethanolamines. *Biochimica et Biophysica Acta* **1982,** *684* (2), 212-218.

(29) Kohler, S. J.; Klein, M. P., ^{31}P Nuclear Magnetic Resonance Chemical Shielding Tensors of Phosphorylethanolamine, Lecithin, and Related Compounds: Applications to Head-Group Motion in Model Membranes. *Biochemistry* **1976,** *15* (5), 967-974.

(30) Thayer, A. M.; Kohler, S. J., Phosphorus-31 Nuclear Magnetic Resonance Spectra Characteristic of Hexagonal and Isotropic Phospholipid Phases Generated from Phosphatidylethanolamine in the bilayer phase. *Biochemistry* **1981,** *20* (24), 6831-6834.

(31) Rilfors, L.; Lindblom, G.; Wieslander, Å.; Christiansson, A., Lipid Bilayer Stability in Biological Membranes. In *Membrane Fluidity*, Kates, M., and Manson, L., (Eds.) Springer:USA 1984; Vol. 12, pp 205-245.

(32) Gagne, J.; Stamatatos, L.; Diacovo, T.; Hui, S. W.; Yeagle, P. L.; Silvius, J. R., Physical Properties and Surface Interactions of Bilayer Membranes Containing N-Methylated Phosphatidylethanolamines. *Biochemistry* **1985,** *24* (16), 4400-4408.

(33) Shyamsunder, E.; Gruner, S. M.; Tate, M. W.; Turner, D. C.; So, P. T.; Tilcock, C. P., Observation of Inverted Cubic Phase in Hydrated Dioleoylphosphatidylethanolamine Membranes. *Biochemistry* **1988,** *27* (7), 2332-2336.

(34) Veiro, J. A.; Khalifah, R. G.; Rowe, E. S., P-31 Nuclear Magnetic Resonance Studies of the Appearance of an Isotropic Component in Dielaidoylphosphatidylethanolamine. *Biophysical Journal* **1990,** *57* (3), 637-641.

(35) Ellens, H.; Bentz, J.; Szoka, F. C., Fusion of Phosphatidylethanolamine-Containing Liposomes and Mechanism of L_{α}–H_{II} Phase Transition. *Biochemistry* **1986,** *25* (14), 4141-4147.

(36) Siegel, D. P.; Epand, R. M., The Mechanism of Lamellar-to-Inverted Hexagonal Phase Transitions in Phosphatidylethanolamine: Implications for Membrane FusionMechanisms. *Biophysical Journal* **1997,** *73* (6), 3089-3111.

(37) Bentz, J.; Ellens, H., Membrane Fusion: Kinetics and Mechanisms. *Colloids and Surfaces* **1987,** *30* (1), 65-112.

(38) Epand, R. M., High Sensitivity Differential Scanning Calorimetry of the Bilayer to Hexagonal Phase Transitions of Diacylphosphatidylethanolamines. *Chemistry and Physics of Lipids* **1985,** *36* (4), 387-393.

(39) Aurell Wistrom, C.; Rand, R. P.; Growe, L. M.; Spargo, B. J.; Crowe, J. H., Direct Transition of Dioleoylphosphatidylethanolamine from Lamellar Gel to Inverted Hexagonal Phase Caused by Trehalose. *Biochimica et Biophysica Acta* **1989,** *984* (2), 238-242.

(40) Gruner, S. M.; Parsegian, V. A.; Rand, R. P., Directly Measured Deformation Energy of Phospholipid H_{II} Hexagonal Phases. *Faraday Discussions of the Chemical Society* **1986,** *81* (0), 29-37.

(41) Wilschut, J.; Duzgunes, N.; Fraley, R.; Papahadjopoulos, D., Studies on the Mechanism of Membrane Fusion: Kinetics of Calcium Ion Induced Fusion of Phosphatidylserine Vesicles Followed by a New Assay for Mixing of Aqueous Vesicle Contents. *Biochemistry* **1980,** *19* (26), 6011-6021.

(42) Akoka, S.; Tellier, C.; Le Roux, C.; Marion, D., A Phosphorus Magnetic Resonance Spectroscopy and a Differential Scanning Calorimetry Study of the Physical Properties of *N*-acylphosphatidylethanolamines in Aqueous Dispersions. *Chemistry and Physics of Lipids* **1988,** *46* (1), 43-50.

(43) Browning, J. L., Motions and Interactions of Phospholipid Head Groups at the Membrane Surface. Three Dynamic Properties of Amine-Containing Head Groups. *Biochemistry* **1981,** *20* (25), 7144-7151.

CHAPTER 5
SUMMARY, CONCLUSIONS, AND OUTLOOK

5.1 Summary and Conclusions

The overall goal of this research was to develop analytical methods to study the phase properties of Q_{PA}-DOPE LUVs upon reduction and use this knowledge to manipulate the phase behavior of Q_{PA}-DOPE in order to improve its application potential. The outcomes presented here have provided new insights into the nature of Q_{PA}-DOPE liposomes and have equipped the McCarley lab with a robust set of analytical methods to investigate this unique lipid. Moreover, the results I obtained with Q_{PA}-DOPE:POPE lipid mixture-based LUVs is progressive in context of the field of 3rd-generation liposomes, and they have significantly improved the application potential of Q_{PA}-DOPE. The scientific significance of this system both in real-world applications and in understanding the nature of the lipid bilayers will provide a new area of sustainable research in the McCarley lab.

In the second chapter, the protocols for a wide-array of analytical methods used to study Q_{PA}-DOPE liposomes were exhaustively reported. My hope in writing Chapter 2 in this manner was to provide future researchers with a set of methods that reproducibly work for Q_{PA}-DOPE and other lipids. Personally, two of the greatest challenges in working with Q_{PA}-DOPE were finding and/or modifying existing methods that were compatible with Q_{PA}-DOPE liposomes, and more often than not, reproducing methods previously reported for traditional lipids. To solve these problems, often the best approach was to break down the method and focus on the chemical role of each individual component. As an example, the first reproducibility challenge I faced in this research was that of acquiring calcein release curves for Q_{PA}-DOPE LUVs.

Prior to this work, EDTA was not a component in the buffer media used to study Q_{PA}-DOPE liposomes. Calcein is an anionic fluorescent dye that can be quenched by forming chelation complexes with various transition metals.[1] Upon my surveying liposomal systems in the literature, realizing that most of these aqueous systems contained EDTA, and then understanding its role, the calcein release curves of Q_{PA}-DOPE vesicles were obtained in a reproducible fashion.

By far, the greatest challenge overcome in this work was consistently synthesizing Q_{PA}-DOPE that functioned properly (contents release upon $Na_2S_2O_4$ addition). When starting this project, I was given a procedure to synthesize Q_{PA}-DOPE; however, I would frequently obtain a Q_{PA}-DOPE product that had a correct ^{1}H NMR spectrum and mass spectrum, but not the expected contents release after $Na_2S_2O_4$ addition. This was a problem that had occurred several times before in the McCarley lab, and the origin of this was never fully understood. It was not until I considered the influence of impurities on the nature of the lipid, and worked with organic chemists in the McCarley lab to break down the basics of the synthetic steps, that two impurities were being neglected in the synthetic protocol of Q_{PA}-DOPE: (1) hydrocarbon impurities and (2) the urea byproduct in Q_{PA}-NHS synthesis. Hydrocarbon impurities appear at 0.09 (s) and 0.88 (m) ppm in the ^{1}H NMR spectra of all products not containing Q_{PA}-DOPE, corresponding to silicon oil and vacuum-line grease, respectively. Hydrocarbon chain impurities intercalate into the non-polar regions of the bilayer and stabilize the lamellar phase; however, vacuum-line grease cannot be observed in the ^{1}H NMR spectrum of Q_{PA}-DOPE because the terminal acyl-chain methyl groups of DOPE overlap in this region. This impurity must be removed prior to Q_{PA}-NHS DOPE coupling. The second impurity, dicyclohexylurea, is a byproduct of coupling NHS to Q_{PA}-Acid.

Dicyclohexylurea is hydrophobic, and like hydrocarbon impurities, it stabilizes the non-polar region of lipid membranes. Prior to this work, multiple filtrations were used to collect and remove this impurity; however, trace amounts remained. To improve this method, and remove the urea impurity, normal-phase chromatography was used successfully to purify Q_{PA}-NHS with much success.

In Chapter 3, the phase behavior of Q_{PA}-DOPE after $Na_2S_2O_4$ addition was discussed. By developing a new method to prepare GUVs at high concentrations, I was able to confirm our hypothesis that Q_{PA}-DOPE undergoes an $L_\alpha \rightarrow H_{II}$ phase transition after $Na_2S_2O_4$ reduction. To my knowledge, this is the first and only instance that triggered phase studies of GUVs were used with ^{31}P NMR spectroscopy. GUVs have high void volumes, thus they are of inherently lower lipid concentration than those of other MLVs of comparable diameters. 3rd-generation, phase-sensitive liposomes relying on a chemical stimulus are a growing niche in liposomal DDS research. This method could prove to be a significant analytical asset that is applicable to other chemically unique liposomal systems.

A new liposomal system, composed of Q_{PA}-DOPE:POPE lipid mixtures, was discussed in Chapter 4. The goal of this work was to improve the application potential of Q_{PA}-DOPE as a drug delivery system. The mechanism of contents release for Q_{PA}-DOPE LUVs is dependent on contact from opposed bilayers triggered from reduction and cleavage of the outer leaflet Q_{PA} head groups from DOPE. Concentration-dependent release is not an ideal property for a liposomal DDS due to an intrinsically lower therapeutic index and the adverse side-effects at high doses of liposomes in the body.

In a serendipitous discovery, Q_{PA}-DOPE liposomes containing POPE released their contents faster than Q_{PA}-DOPE LUVs alone. This was a surprising discovery, because POPE favors the lamellar phase at the temperatures being investigated. Conventional wisdom would suggest lipids that favor the lamellar phase would stabilize liposomes instead of promoting rapid destabilization. The result of this work was new insight into the nature of bilayer mixtures and the role of chain length and saturation of bilayers stabilized by the hydration force of Q_{PA}-DOPE. The mechanism for contents release of Q_{PA}-DOPE:POPE LUVs is unique from Q_{PA}-DOPE in that cyclization and cleavage of the head group is not necessary for contents release. Instead, the reduction of the outer leaflet quinones to hydroquinones lowers the hydration force and initiates destabilization and rupturing of the bilayer prior to the head group leaving DOPE. Moreover, this mechanism does not show a dependence on concentration like Q_{PA}-DOPE LUVs. This exciting development in the McCarley lab will provide a sustainable avenue for future research (5.2.1).

5.2 Outlook

5.2.1 New Class of PE-functionalized Lipids

The Q_{PA}-DOPE:POPE rapid release liposome developed in this project has potential for growth and is a sustainable research area. Both this Q_{PA}-DOPE:POPE and pure Q_{PA}-DOPE GUVs exhibited an isotropic state that is believed to be caused by an inverted cubic phase. The only analytical method capable of elucidating this state is X-ray diffraction. In Figure 4.1, the geometries of three more common cubic phases were depicted: primitive-body cubic, body-centered cubic, and bicontinuous face-centered cubic, which have a crystallographic space group of Im3m, Ia3d, and Pn3m, respectively.[2,3] Seddon and Templer have authored an excellent book chapter

on lipid polymorphism and the cubic phase as it relates to intrinsic curvature, geometry, and crystalline space groups.[4] Because of the temporal nature of the isotropic state observed in both Q_{PA}-DOPE and Q_{PA}-DOPE:POPE GUVs, a high energy X-ray source will be necessary to resolve the isotropic state.

An new era of 3rd-generation liposomal DDSs can be built utilizing the mechanism of Q_{PA}-DOPE:POPE LUVs. While the Q_{PA} derivative used in this work is ideal for Q_{PA}-DOPE because it has faster kinetics of forming the lactone species (i.e., cyclization and cleavage of the head group from DOPE), the mechanism of Q_{PA}-DOPE:POPE only requires reduction. A possible route to expand this system is derivatizing new quinone propionic functional groups that undergo a kinetically faster reduction or that are more easily reduced. Mendoza et al. reported the kinetics of various hNQO1-activated quinone propionic acid functional groups that reduced faster than the tri-methyl Q_{PA} group used in this work (Table 5.1).[5] Any one of these head groups should theoretically decrease the t_{50} of contents release for this liposomal system.

5.2.2 Redox-triggered Liposomal Nanoreactors

Opposed phosphatidylserine (PS) liposomes aggregate and fuse in the presence of Ca^{2+}, undergoing mixing of both lipid membranes and entrapped volumes.[7,8] Düzgünes et al. investigated liposomal mixtures of PS, PE, and PC lipids and found that PS:PE liposomes fused upon Ca^{2+} addition, and less so in PS:PE:PC mixtures, with no fusion being observed in PS:PC mixtures.[7]

(Fusion) PS > PS:PE > 2PS:PE:PC >> PS:PC (No Fusion)

Table 5.1 Kinetic parameters for the reduction of quinone propionic acid derivatives by hNQO1. Reprint (adapted) with permission from (Mendoza, M.F., Hollabaugh, N.M., Hettiarachi, S.U, and McCarley, R.L., Human NAD(P)H:Quinone Oxidoreductase Type 1 (hNQO1) Activation of Quinone Propionic Trigger Groups. *Biochemistry* **2012**, 51 (40), 8014-26) Copyright (2012) American Chemical Society.

Quinone	V_{max} (μmol·min^{-1}·mg^{-1})	K_m (μM)	k_{cat} (s^{-1})	k_{cat}/K_m (M^{-1}·s^{-1})	$E_{1/2}$ vs. SHE (V)	van der Waals volume (Å^3)
Q_{Br}-COOH	88 ±7	41 ±8	45 ±4	1.1±0.2 × 10^6	0.095 ±0.001	251
Q_H-COOH	83 ±8	50 ±11	43 ±4	8.5±2.0 × 10^5	0.117 ±0.002	232
Q_{MeO}-COOH	42 ±5	447 ±102	22 ±3	4.8±1.2 × 10^4	0.098 ±0.001	258
Q_{Me}-	38 ±5	158 ±41	20. ±3	1.2±0.4 × 10^5	0.047 ±0.002	249
Q_{Me}-ETA	60 ±7	132 ±32	31 ±4	2.3±0.6 × 10^5	0.041 ±0.001	295
Q_{diMeO}-COOH	14 ±1	376 ±87	7.2 ±0.5	1.9±0.5 × 10^4	0.128 ±0.001	282
Q'-COOH	78 ±3	20 ±3	40. ±2	2.0±0.3 × 10^6	0.144 ±0.001	232

Table 5.1 Continued

Quinone	V_{max} (μmol·min^{-1}·mg^{-1})	K_m (μM)	k_{cat} (s^{-1})	k_{cat}/K_m (M^{-1}·s^{-1})	$E_{1/2}$ vs. SHE (V)	van der Waals volume (Å^3)
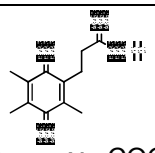 $Q_{nogemMe}$-COOH	66 ±4	5 ±1	34 ±2	6.8±1.4 × 10^6	0.143 ±0.002	215

[a]Values reported are the mean ± one standard deviation for three independent determinations. [NADH] = 1.00 X 10^{-4} M in all cases. The van der Waals volumes were calculated according to the literature.[6]

I had formulated a hypothesis based on these results that Q_{PA}-DOPE lipids could be utilized to inhibit fusion in mixtures with PS lipids and permit fusion after reduction and cleavage of the Q_{PA} head group. This hypothesis was based on Q_{PA}-DOPE having a similar hydration nature to PC lipids, and as a result, its repulsive hydration force would inhibit fusion. Once DOPE was expressed in the outer leaflet, the system would behave like PS:PE mixtures and fuse. To test this hypothesis, liposomes having a 1:1 (mol/mol) lipid mixture of Q_{PA}-DOPE and Brain PS (Avanti Polar Lipids, Birmingham, AL) were prepared in the method outlined in Section 2.5. It is believed that Q_{PA}-DOPE:PS LUVs fused in the presence of Ca^{2+} before reduction and that these liposomes fused at a higher efficiency than PS:PE lipid mixtures (Figure 5.1). Moreover, pure Q_{PA}-DOPE liposomes appear to have fused upon Ca^{2+} addition. This suggests that Ca^{2+} was able to charge screen opposed Q_{PA}-DOPE liposomes, forming dehydrated intermembrane complexes and inducing fusion. The reproducibility of this fusion assay has been problematic. Düzgünes et al. have shown many fusion assays disagree and should be interpreted with caution, because the rise in signal of

these assays could be due to simple aggregation.[9] Based on signal similarity in Figure 5.1 to light scattering previously observed (Figure 4B-D), this may very well be the case.

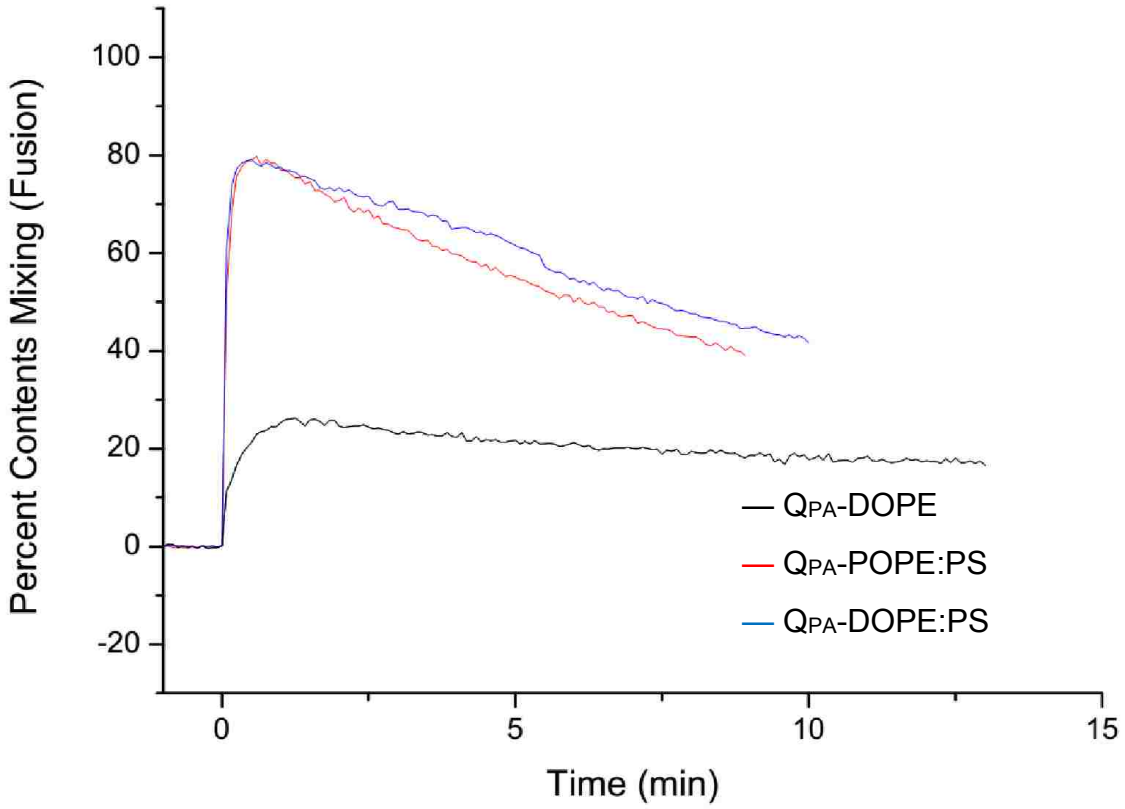

Figure 5.1. The conditions of Tb^{3+}/DPA^{2-} fusion assay can be found in Section 2.5. Briefly, 50 μM of liposomes containing 5 mM Tb^{3+} were added into a 3.0-mL fluorescent cuvette containing 50 μM of liposomes containing 20 mM DPA^{2-} (100 μM total lipid concentration) in pH 7.40 100 mM KCl/10.0 mM TES buffer medium. 10.0 mM Ca^{2+} was added at *t*=0 min and fluorescence of $Tb(DPA)_3^{3-}$ observed (Excitation/Emission 276/545 nm). The data was normalized by lysing 50 μM of liposomes Tb^{3+} in a pH 7.40 20.0 mM DPA^{2-}/80 mM KCl buffer medium, absent EDTA.

A control experiment in this study consisted of liposomes having 1:1 (mol/mol) lipid mixtures of Q_{PA}-DOPE:POPE. These liposomes exhibited an unexpected behavior of releasing their contents faster than pure Q_{PA}-DOPE LUVs. Investigation of this phenomenon afforded the work discussed in Chapter 4; however, investigations of the fusion behavior of Q_{PA}-DOPE were not continued. One potential application of these findings is engineering a new class of liposomal nanoreactor that responds to a redox

stimulus. Like Brain PS liposomes, Q_{PA}-DOPE LUVs may have fused in the presence of Ca^{2+} because of the anionic charge on the bilayer surface. Theoretically, a lipid that was anionic in nature, but is zwitterionic when functionalized with Q_{PA} would not fuse in the presence of Ca^{2+} but would fuse after $Na_2S_2O_4$ reduction (Figure 5.2).

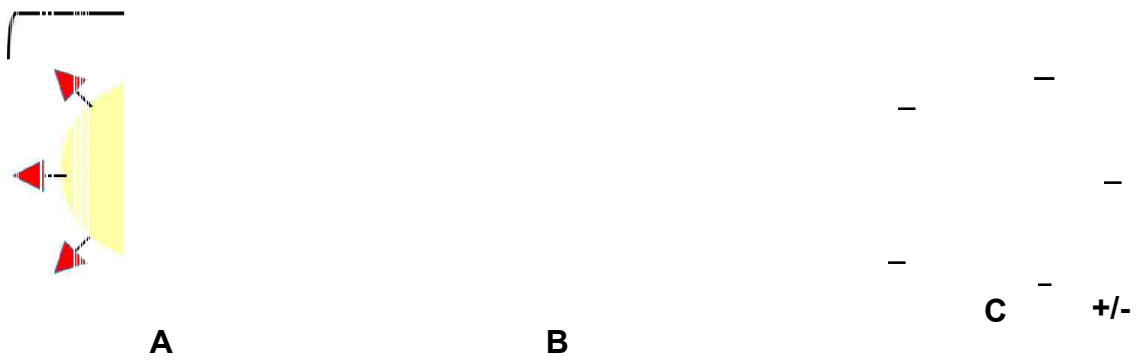

Figure 5.2. The principle of the redox-triggered liposomal nanoreactor is to synthesize a Q_{PA} functionalized lipid that is zwitterionic when bound to the polar head group of the lipid (A and B) and anionic after the Q_{PA} headgroup has been cleaved after $Na_2S_2O_4$ reduction. The system should be stable in a Ca^{2+} environment so that upon a change in surface charge results in trans-membrane Ca^{2+} complexes that fuse opposed liposomes (C).

5.2.3 Second Harmonic Generation Studies

Second harmonic generation (SHG) is a surface sensitive technique that can determine the surface electrostatic potential and surface charge density of colloidal particles.[10-14] In SHG, incident electric field frequency $E(\omega)$ excites an atom from its ground state to an excited state. During this process two photons absorb simultaneously. The electric field surrounding these atoms then emits energy $E(2\omega)$, Figure 5.3.[15] SHG measurements of particle surface potential are possible, because there are two contributions to the SHG signal. In terms of charge density, the intensity of SHG signal (I_{SHG}) observed arises from two non-linear polarizabilties: (1) a second-order susceptibility from oriented chemical species that are hyperpolarizable,

χ^2; and (2) a third-order susceptibility from chemical species in the bulk solution that are aligned by the electric field of the charged particle, χ^3 (Equation 5.1).[15] The χ^3 contributions to I_{SHG} are a function of particle electric field, which decays with distance from the surface.[15,16]

Figure 5.3. The principle of SHG. Incident light having frequency ω polarizes the atoms at the surface of a particle and their electric fields coherently add with each other and the emitted light from this electric field has a frequency of 2ω. The intensity of 2ω light emitted is a function of the non-linear susceptibility tensor of the particle itself (χ^2) and the non-linear susceptibility tensor of the water-surface interface (χ^3).

Equation 5.1 $I_{SHG} = E_\omega E_\omega \chi^2 + E_\omega E_\omega \chi^3 \int E(r)\, dr$

Liu et al. investigated the surface potential of charged DOPG liposomes dispersed in a sucrose medium with SHG.[17] By titrating in different salts (i.e., NaCl and $MgSO_4$), the authors were able to fit the decay curve of I_{SHG} with salt concentration and calculate the charge density of the surface (Å^2/charge). The goal of this work was to collaborate with Raju Kumal in Professor Louis Haber's Lab to study SHG signal from Q_{PA}-DOPE liposomes and measure the change charge density with time. This would be the first direct *in situ* measurement of the reduction and lactonization of the Q_{PA} head group in a Q_{PA}-DOPE liposome. It was discovered that this was not possible as χ^3 goes to zero at salt concentrations > 10 mM, and the I_{SHG} from χ^2 alone did not produce

adequate signal. Because Q_{PA}-DOPE lipids require salt to form LUVs and $Na_2S_2O_4$ to reduce and cleave Q_{PA}, a different quinone propionic acid derivatized DOPE was synthesized, Q_{Br}-DOPE (8a); however, the non-ionic reducing agents used (dithiothreitol, hydrazine, and glutathione) were not capable of triggering contents release from Q_{Br}-DOPE LUVs.

Malachite green (MG) is a cationic dye that can increase $E\chi^3$ in the presence of large salt concentrations.[18-20] We attempted to use MG to investigate the reduction mechanism of Q_{PA}-DOPE LUVs in pH 7.4 PBS; however, we discovered that MG is reduced by $Na_2S_2O_4$. In a second publication, Liu et al. investigated transport kinetics of MG across POPG and POPE:POPC bilayers and found that the transport rate increased linearly with the percentage of charged lipid in the bilayer.[21] Yan et al. studied the effect of cholesterol in the bilayer on the transport kinetics of MG and found that as the concentration of the cholesterol increased, the rate of transport decreased.[22] The decrease in diffusion rates of MG was significantly slower in 50:50 (mol/mol) mixtures of DOPG:Cholesterol then POPG:POPC, which suggests that more rigid bilayers slow MG diffusion.

Similarly, I prepared Q_{PA}-DOPE, DOPG, and DOPG:Cholesterol (80:20 mol/mol) LUVs in pH 7.4 PBS to study the diffusion of kinetics of MG with SHG. MG diffusion decay curves were measured by adding 100 μM of the lipid system (LUVs) into 1.5 mL (total volume) of 8 μM MG in pH 7.40 PBS, which SHG signal was actively being measured (Figure 5.4). After the SHG signal had decayed and approached an asymptote, 100 μM $Na_2S_2O_4$ was added to the cuvette to quench MG that had not diffused into the bilayer. My collaborator fit the decay curve to Equation 5.2, where a_0 is a baseline correction, a_1 is a weighting parameter, t is the experimental time in min,

and τ is a rate constant in min. The diffusion time and zeta potential measurements for the lipid systems studied are given in Table 5.2. The measured diffusion times of MG for DOPG/Cholesterol LUVs were 6x longer than DOPG LUVs, which agrees with the results published by Yan et al.[22] Moreover, there was no significant change in zeta potential between these two systems; therefore, the longer diffusion time in DOPG:Cholesterol LUVs was due to bilayer effects and not surface charge. Q_{PA}-DOPE LUVs have a slightly larger zeta potential than DOPG, but a longer diffusion time than DOPG. This suggests that the Q_{PA} headgroup plays a role at inhibiting molecular transport across the bilayer.

Equation 5.2 $I_{SHG} = a_0 + a_1 \exp(-t / \tau)$

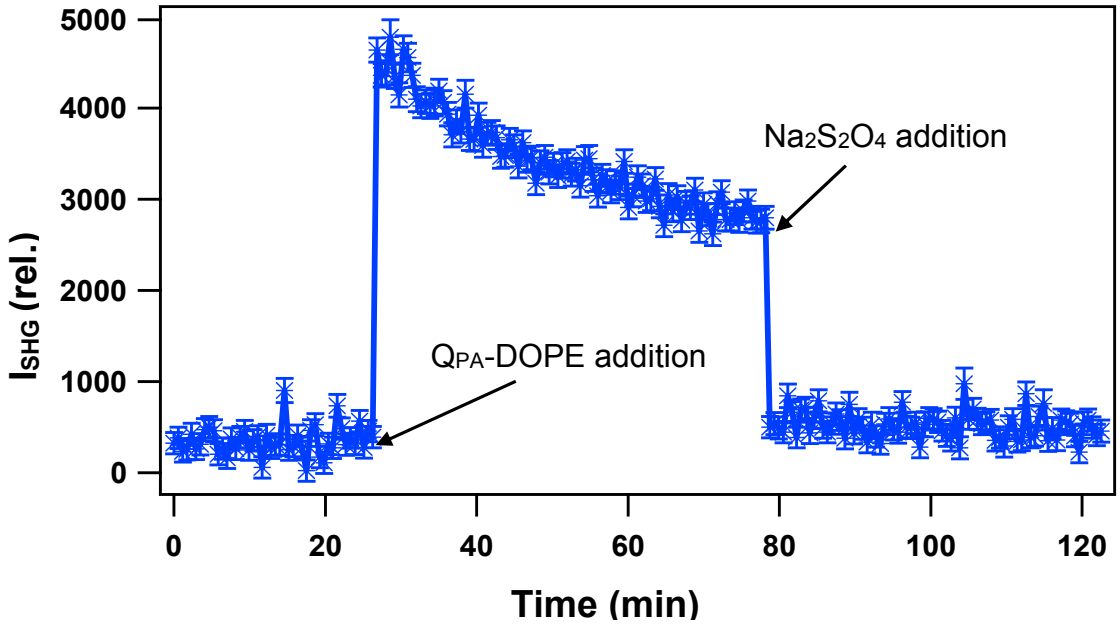

Figure 5.4. The SHG decay of MG signal in 100 μM Q_{PA}-DOPE LUVs added to 1.5 mL of PBS (pH 7.4) containing 8 μM MG. After no significant change in ISHG had occurred, 100 μM $Na_2S_2O_4$ was added to quench exterior MG.

Table 5.2. Zeta potentials and fitted molecular diffusion rates for the three lipid systems investigated using SHG at 25 °C.

Lipid (LUV)	Zeta Potential (mV)			Diffusion rate (min)		
DOPG	-52.0	±	2.57	6.8	±	0.92
DOPG/Cholesterol (8:2, mol/mol)	-53.9	±	2.83	36.8	±	N/A
Q_{PA}-DOPE	-58.7	±	2.30	23.9	±	1.15

The preliminary SHG-diffusion rate data suggesting the Q_{PA} head group hinders molecular diffusion through the bilayer is significant progress not only in the development of new analytical method to study Q_{PA}-DOPE, but also in understanding the nature of Q_{PA}-DOPE liposomes. The unique chemistry of Q_{PA}-DOPE has made SHG studies challenging, and this preliminary data must be investigated further. Recent work in the McCarley lab suggests that $Na_2S_2O_4$ does not cross the bilayer, thus the remaining I_{SHG} signal after MG diffusion and subsequent $Na_2S_2O_4$ addition is due to MG inside the liposome. Shang et al. determined the remaining I_{SHG} from MG does not diffuse to zero because of counter ion electrostatic effects.[23] MG is transported into the liposomes without its counter ion (Cl^-), and therefore there is an increasing electrostatic potential across the bilayer that opposes the additional transport of MG. This does not explain why the signal is near its original after $Na_2S_2O_4$ addition if indeed the reducing agent does not cross the bilayer. One possible explanation is that some I_{SHG} signal from MG contains hyper-Rayleigh scattering, which is incoherent addition of $E_a(2\omega,\chi^3)$ and $E_b(2\omega,\chi^3)$.[15,20] Knowing this, the contribution of I_{SHG} from MG's enhancement of $E\chi^3$ should be investigated.

5.3 References

(1) Breuer, W.; Epsztejn, S.; Millgram, P.; Cabantchik, I. Z., Transport of Iron and other Transition Metals into Cells as Revealed by a Fluorescent Probe. *The American Journal of Physiology* **1995,** *268* (6 Pt 1), C1354-C1361.

(2) Seddon, J. M.; Squires, A. M.; Conn, C. E.; Ces, O.; Heron, A. J.; Mulet, X.; Shearman, G. C.; Templer, R. H., Pressure-Jump X-ray Studies of Liquid Crystal Transitions in Lipids. *Philisophical Transactions of the Royla Society* **2006**. 364, 2635-2655.

(3) Luzzati, V.; Vargas, R.; Mariani, P.; Gulik, A.; Delacroix, H., Cubic Phases of Lipid-containing Systems: Elements of a Theory and Biological Connotations. *Journal of Molecular Biology* **1993,** *229* (2), 540-551.

(4) Seddon, J. M.; Templer, R. H., Polymorphism of Lipid-Water Systems. In *Handbook of Biological Physics*, Lipowsky, R., and Sackmann, E., (Ed. North-Holland: 1995; Vol. 1, pp 97-160.

(5) Mendoza, M. F.; Hollabaugh, N. M.; Hettiarachchi, S. U.; McCarley, R. L., Human NAD(P)H:Quinone Oxidoreductase Type I (hNQO1) Activation of Quinone Propionic Acid Trigger Groups. *Biochemistry* **2012,** *51* (40), 8014-8026.

(6) Zhao, Y. H.; Abraham, M. H.; Zissimos, A. M., Fast Calculation of van der Waals Volume as a Sum of Atomic and Bond Contributions and Its Application to Drug Compounds. *The Journal of Organic Chemistry* **2003,** *68* (19), 7368-7373.

(7) Düzgünes, N.; Wilschut, J.; Fraley, R.; Papahadjopoulos, D., Studies on the Mechanism of Membrane Fusion. Role of Head-Group Composition in Calcium- and Magnesium-Induced Fusion of Mixed Phospholipid Vesicles. *Biochimica et Biophysica Acta* **1981,** *642* (1), 182-195.

(8) Salis, A.; Ninham, B. W., Models and Mechanisms of Hofmeister Effects in Electrolyte Solutions, and Colloid and Protein Systems Revisited. *Chemical Society Reviews* **2014,** *43* (21), 7358-7377.

(9) Duzgunes, N.; Allen, T. M.; Fedor, J.; Papahadjopoulos, D., Lipid Mixing During Membrane Aggregation and Fusion: Why Fusion Assays Disagree. *Biochemistry* **1987,** *26* (25), 8435-8442.

(10) Kumal, R. R.; Karam, T. E.; Haber, L. H., Determination of the Surface Charge Density of Colloidal Gold Nanoparticles Using Second Harmonic Generation *The Journal of Physical Chemistry C* **2015** *119* (28), 16200-16207

(11) Yan, E. C. Y.; Liu, Y.; Eisenthal, K. B., New Method for Determination of Surface Potential of Microscopic Particles by Second Harmonic Generation. *The Journal of Physical Chemistry B* **1998,** *102* (33), 6331-6336.

(12) Zhao, X.; Ong, S.; Eisenthal, K. B., Polarization of Water Molecules at a Charged Interface. Second Harmonic Studies of Charged Monolayers at the Air/Water Interface. *Chemical Physics Letters* **1993,** *202* (6), 513-520.

(13) Ong, S.; Zhao, X.; Eisenthal, K. B., Polarization of Water Molecules at a Charged Interface: Second Harmonic Studies of the Silica/Water Interface. *Chemical Physics Letters* **1992,** *191* (3–4), 327-335.

(14) Zhao, X.; Ong, S.; Wang, H.; Eisenthal, K. B., New Method for Determination of Surface pKa Using Second Harmonic Generation. *Chemical Physics Letters* **1993,** *214* (2), 203-207.

(15) Eisenthal, K. B., Second Harmonic Spectroscopy of Aqueous Nano- and Microparticle Interfaces. *Chemical Reviews* **2006,** *106* (4), 1462-1477.

(16) Giordmaine, J. A., Nonlinear Optical Properties of Liquids. *Physical Review* **1965,** *138* (6A), A1599-A1606.

(17) Liu, Y.; Yan, C. Y.; Zhao, X. L.; Eisenthal, K. B., Surface Potential of Charged Liposomes Determined by Second Harmonic Generation. *Langmuir* **2001,** *17* (7), 2063-2066.

(18) Haber, L. H.; Kwok, S. J. J.; Semeraro, M.; Eisenthal, K. B., Probing the Colloidal Gold Nanoparticle/Aqueous Interface with Second Harmonic Generation. *Chemical Physics Letters* **2011,** *507* (1–3), 11-14.

(19) Kikteva, T.; Star, D.; Leach, G. W., Optical Second Harmonic Generation Study of Malachite Green Orientation and Order at the Fused-Silica/Air Interface. *The Journal of Physical Chemistry B* **2000,** *104* (13), 2860-2867.

(20) Wang, H.; Yan, E. C. Y.; Borguet, E.; Eisenthal, K. B., Second Harmonic Generation from the Surface of Centrosymmetric Particles in Bulk Solution. *Chemical Physics Letters* **1996,** *259* (1–2), 15-20.

(21) Liu, Y.; Yan, E. C.; Eisenthal, K. B., Effects of Bilayer Surface Charge Density on Molecular Adsorption and Transport Across Liposome Bilayers. *Biophysical Journal* **2001,** *80* (2), 1004-1012.

(22) Yan, E. C.; Eisenthal, K. B., Effect of Cholesterol on Molecular Transport of Organic Cations Across Liposome Bilayers Probed by Second Harmonic Generation. *Biophysical Journal* **2000,** *79* (2), 898-903.

(23) Shang, X.; Liu, Y.; Yan, E.; Eisenthal, K. B., Effects of Counterions on Molecular Transport Across Liposome Bilayer: Probed by Second Harmonic Generation. *The Journal of Physical Chemistry B* **2001,** *105* (51), 12816-12822.

APPENDIX A LETTERS OF PERMISSION

Appendix A-1. Reprint Permission Figure 3.3

Rightslink® by

PER

Thus
feel

If yo
from

Copy
Corr

1 of 1

Appendix A-2. Reprint Permission Figure 3.9

Appendix A-3. Reprint Permission Table 5.1

APPENDIX B LIPID CONCENTRATION ASSAYS

Appendix B-4. Q_{PA}-DOPE UV-Vis Absorption Assay

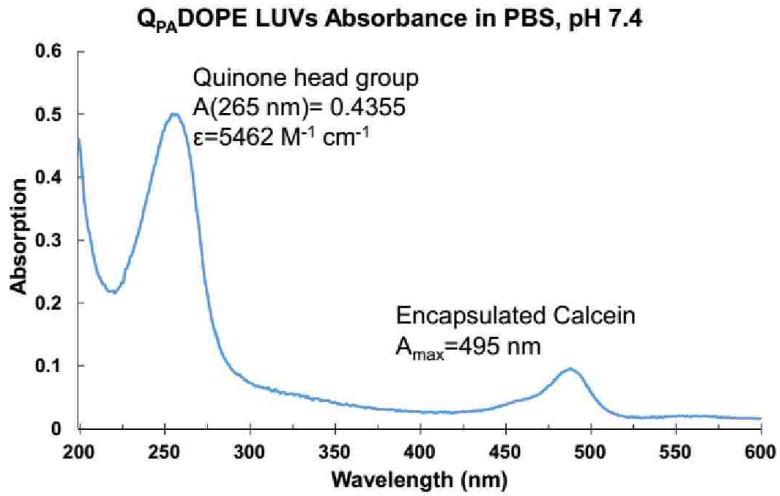

Beer-Lambert law
$A=\varepsilon b C_{cuvette}$
A(265 nm)= 0.4355
b= 1 cm
ε=5462 M^{-1} cm^{-1}
$C_{cuvette}= M_2 = 7.973 \times 10^{-5}$ M

$M_1V_1=M_2V_2$
M_1=3.987 mM
V_1= 10 µL
$M_2= 7.973 \times 10^{-5}$ M
V_2= 500 µL

Where M_1 is the concentration of lipid in the post-spin column eluant

***10 µL of liposome solution post spin column**
****490 µL of 100 mM KCl and 0.1 mM EDTA buffered with 50 mM phosphate, pH 7.4**

Appendix B-5. Bartlett Assay

	Absorbance (820 nm)					
x (µmol)	trial 1	trial 2	trial 3	A. Abs.	A. Std. Dev.	% Std. Dev.
0	-	-	-	0	-	-
0.01	0.0313	0.0442	0.0323	0.03593	0.0059	16.31
0.025	0.0845	0.0680	0.0792	0.07723	0.0069	8.91
0.05	0.1406	0.1616	0.1331	0.14510	0.0121	8.31
0.075	0.2324	0.2292	0.2343	0.23197	0.0021	0.91
0.1	0.3607	0.3202	0.3353	0.33873	0.0167	4.93
DOPG	0.5744	0.5394	0.5524	0.55540	0.0144	2.60

Molar Extinction (μmol^{-1} cm^{-1})		Absolute Std. Dev.	Percent Std. Dev.
3.283	±	0.6883	20.96

Con. (mM)		Absolute Std. Dev.	Percent Std. Dev.
16.8870	±	3.5674	21.12

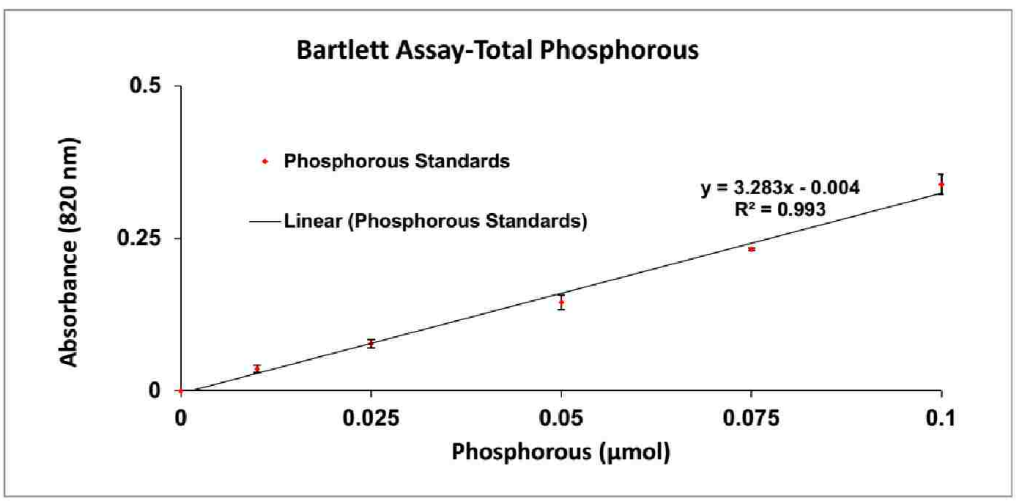

Appendix B-6. Stewart Assay

	Absorbance (485 nm)					
x (µmol)	trial 1	trial 2	trial 3	A. Abs.	A. Std. Dev.	% Std. Dev.
0	-0.009	-0.014	-0.013	-0.01187	0.00236	-19.91
0.013937	0.026	0.0274	0.0265	0.02663	0.00071	2.66
0.027874	0.0781	0.0843	0.077	0.07980	0.00394	4.93
0.055748	0.183	0.175	0.1818	0.17993	0.00431	2.40
0.083622	0.2863	0.2877	0.2841	0.28603	0.00181	0.63
0.111496	0.4008	0.4027	0.3909	0.39813	0.00634	1.59
0.13937	0.4806	0.4731	0.4769	0.47687	0.00375	0.79
Q_{PA}-DOPE	0.1158	0.1017	0.0956	0.1044	0.0104	9.93

Molar Extinction (μmol^{-1} cm^{-1})		Absolute Std. Dev.	Percent Std. Dev.
3.6157	±	0.0003	0.01

Con. (mM)		Absolute Std. Dev.	Percent Std. Dev.
4.7718	±	0.0007	0.01

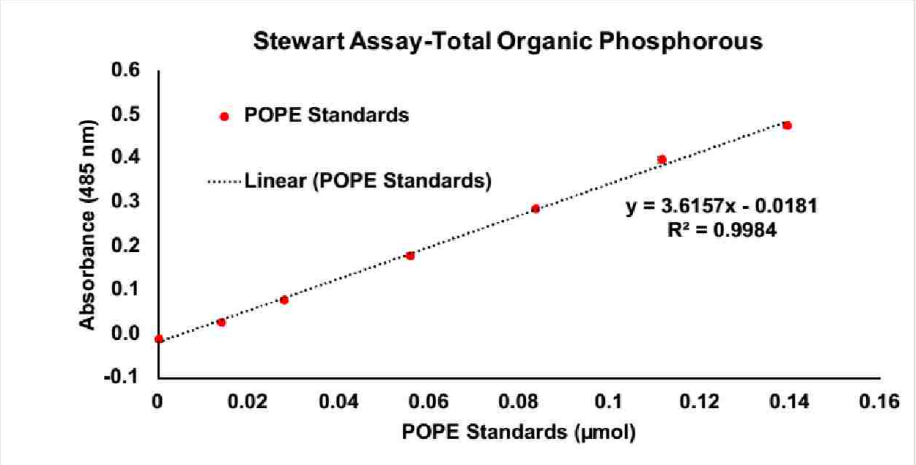

APPENDIX C ^{1}H NMR, ^{13}C NMR, AND ESI-MS

Appendix C-7. ^{1}H and ^{13}C NMR Spectra of Lactone (1c)

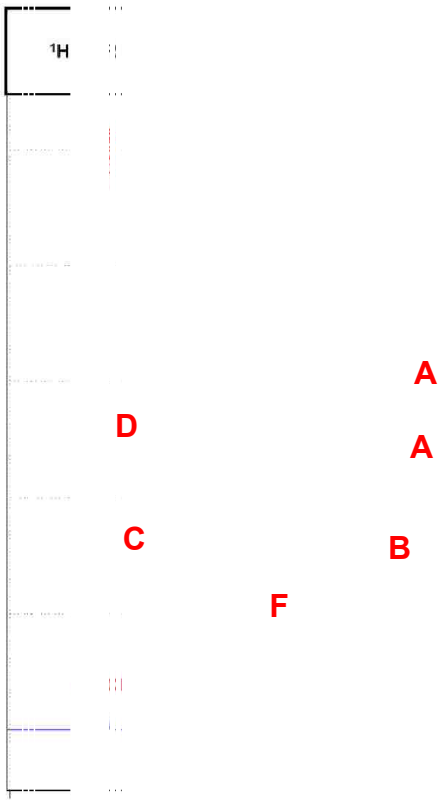

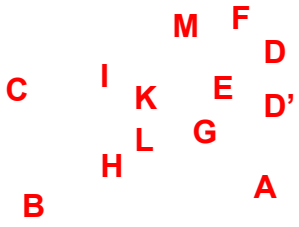

Appendix C-8. ESI-MS of Lactone (1c)

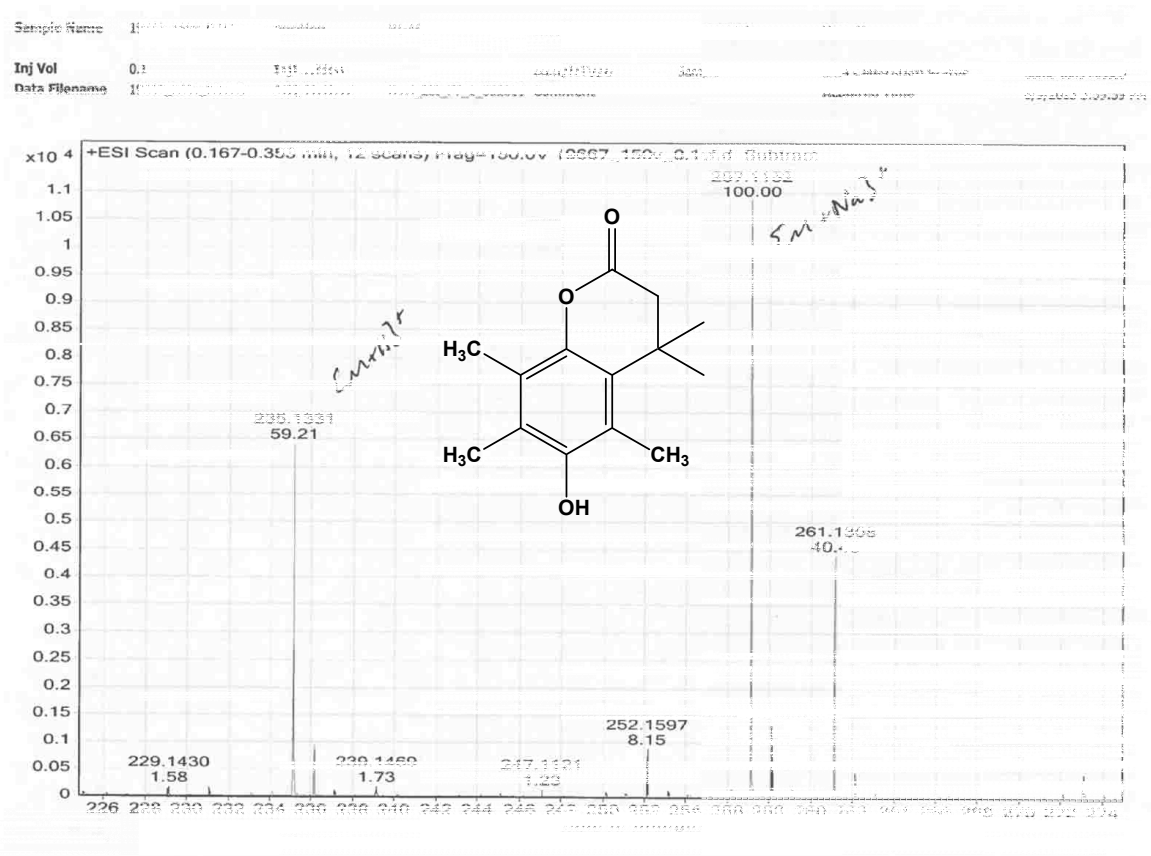

Appendix C-9. ^{1}H and ^{13}C NMR Spectra of Tri-methyl Q_{PA} (2b)

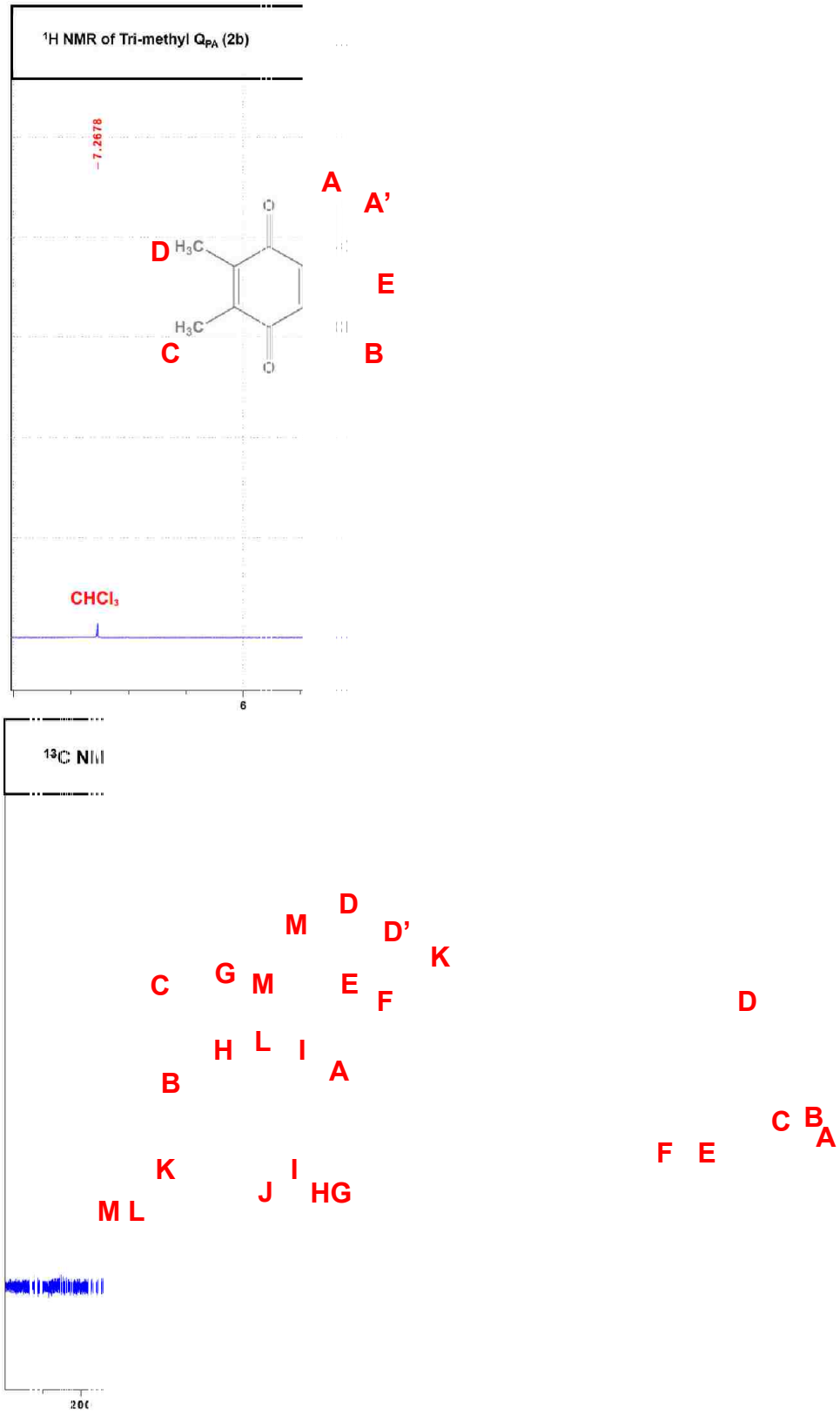

Appendix C-10. ESI-MS of Tri-methyl Q_{PA} (2b)

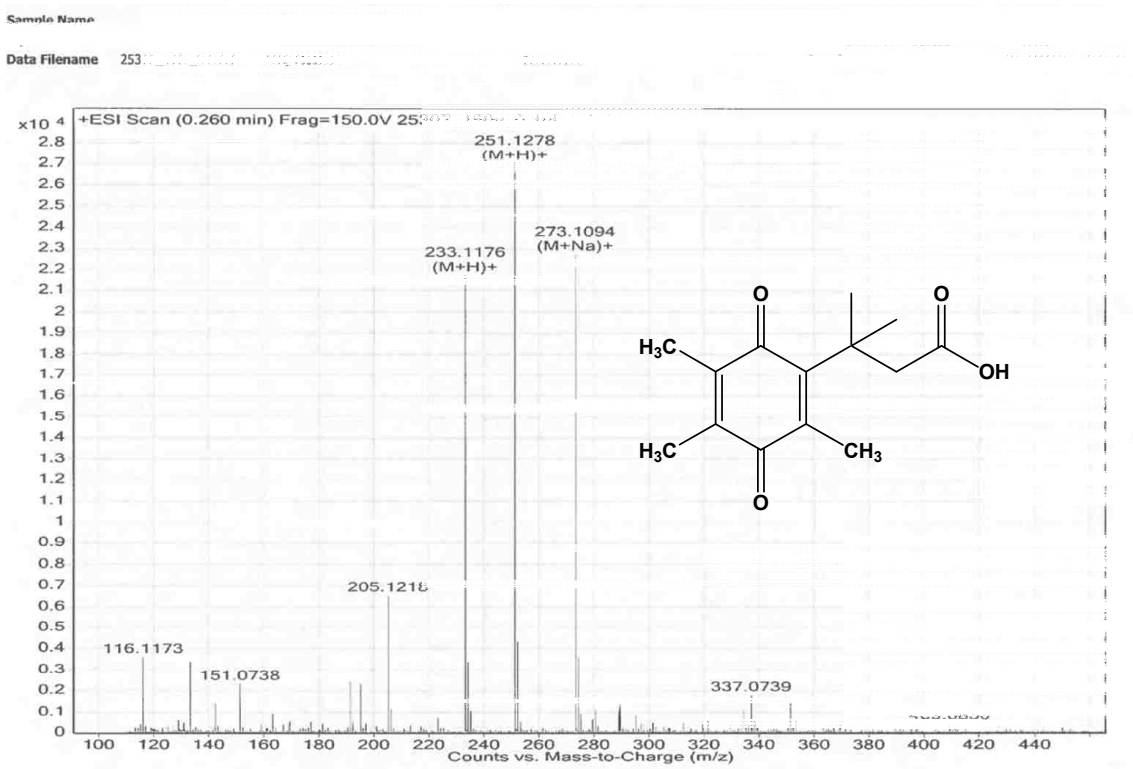

Appendix C-11. ^{1}H and ^{13}C NMR Spectra of Q_{PA}-NHS (3b)

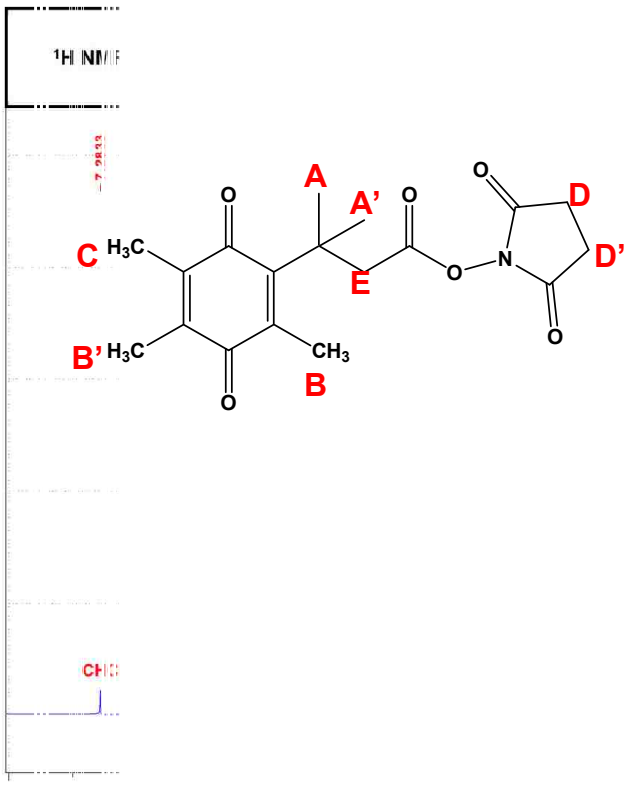

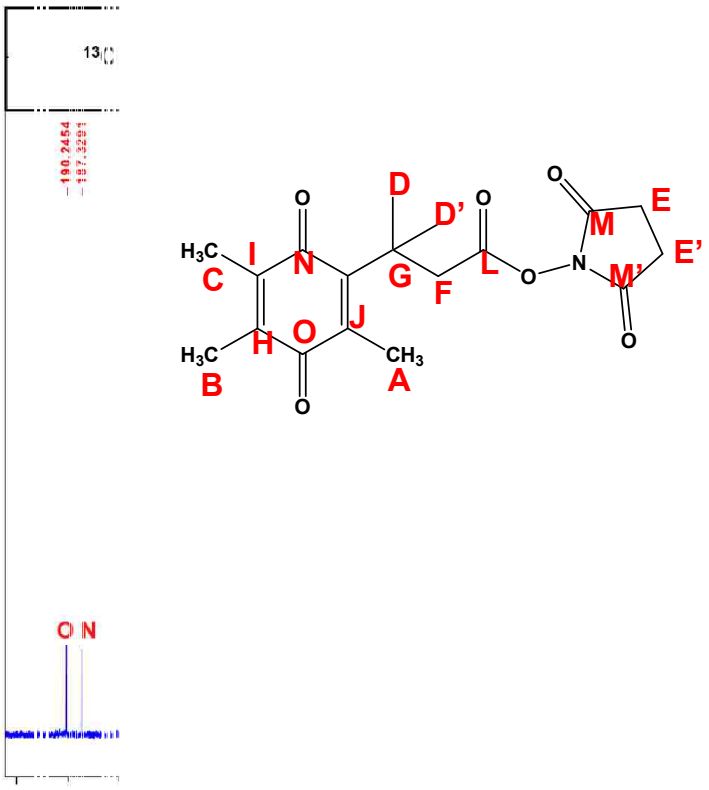

Appendix C-12. ESI-MS of Q_{PA}-NHS (3b)

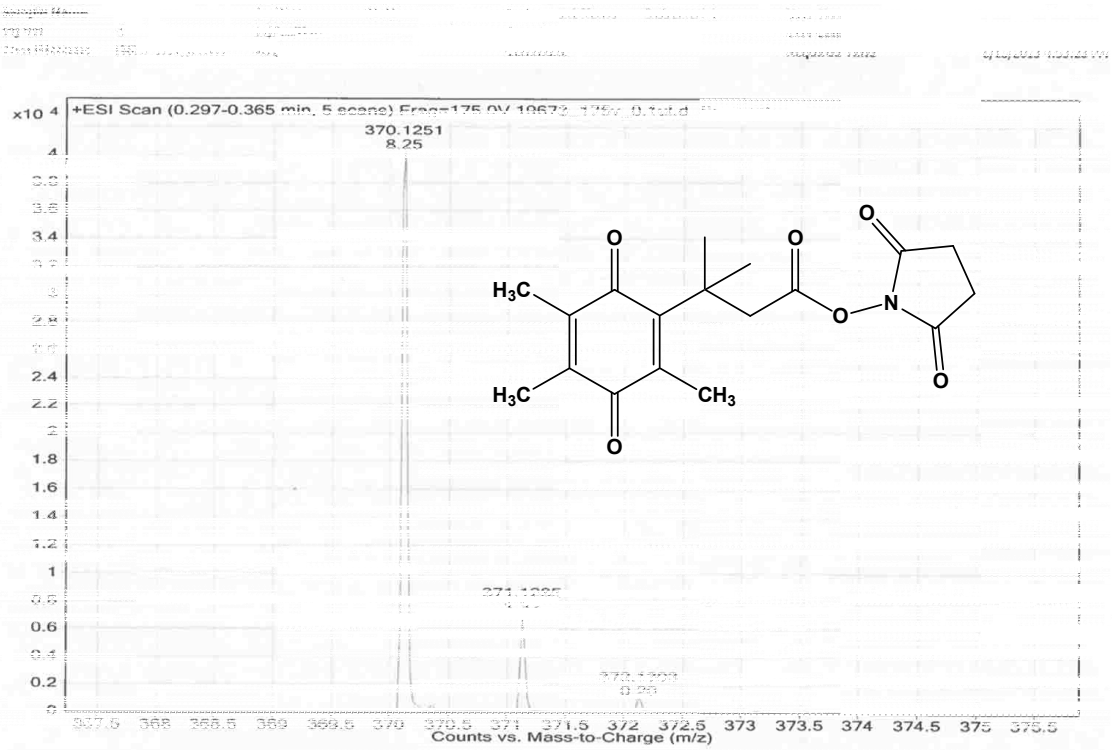

Appendix C-13. ^{1}H NMR Spectra of Q_{PA}-DOPE (4b)

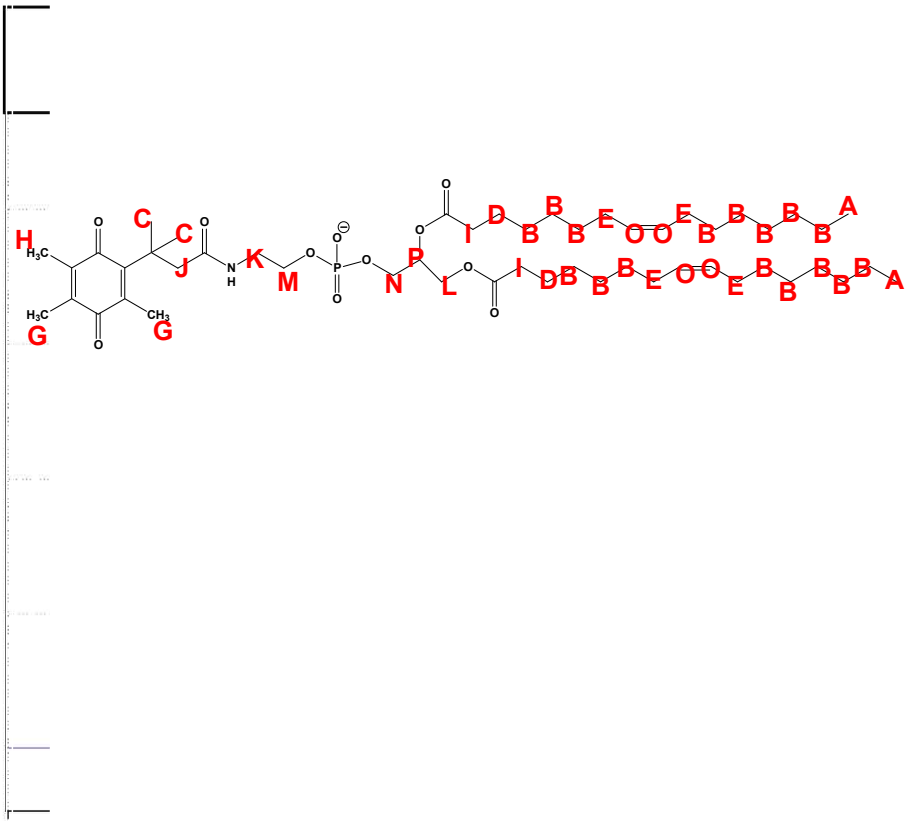

Appendix C-14. ESI-MS of Spectra of Q_{PA}-DOPE (4b)

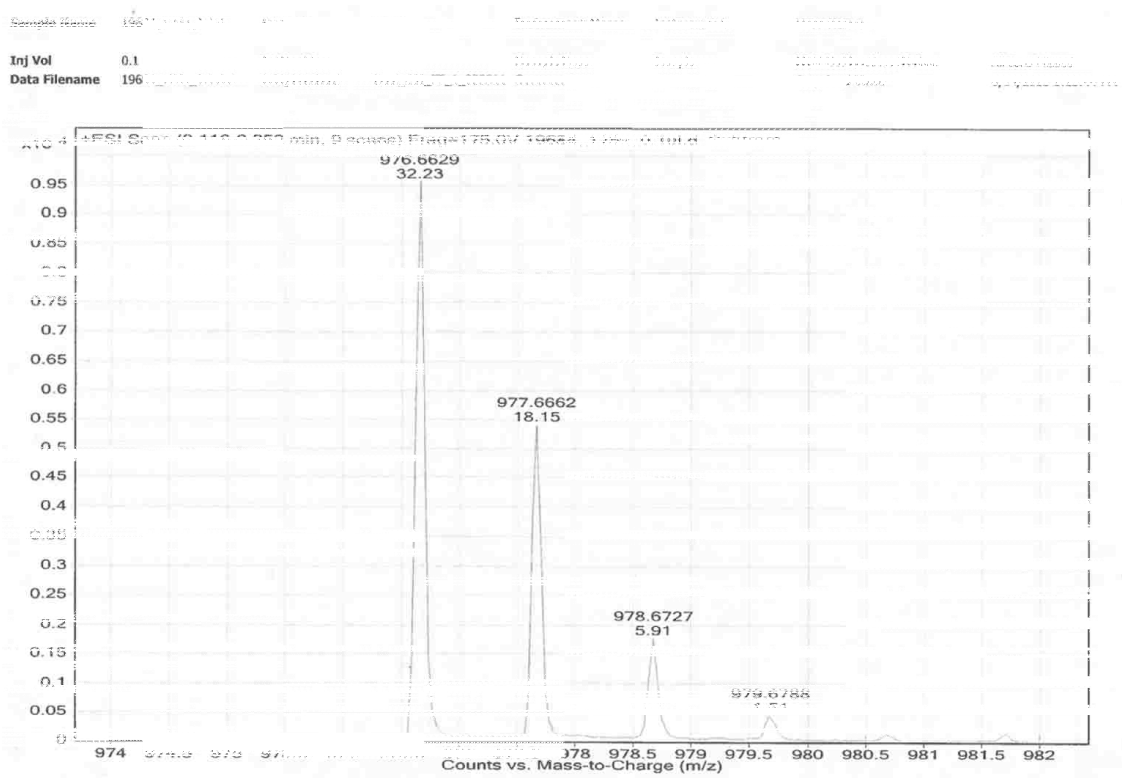

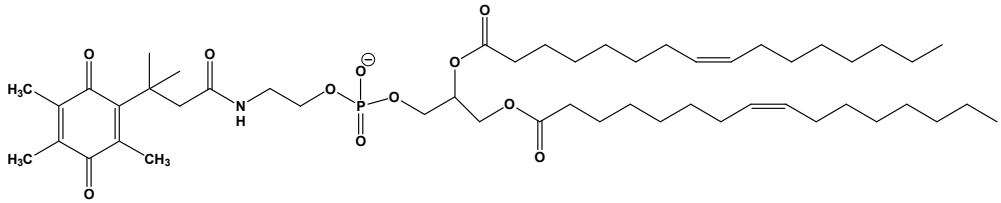

Appendix C-15. ^{1}H NMR and ^{13}C Spectra of di-methyl Lactone (5c)

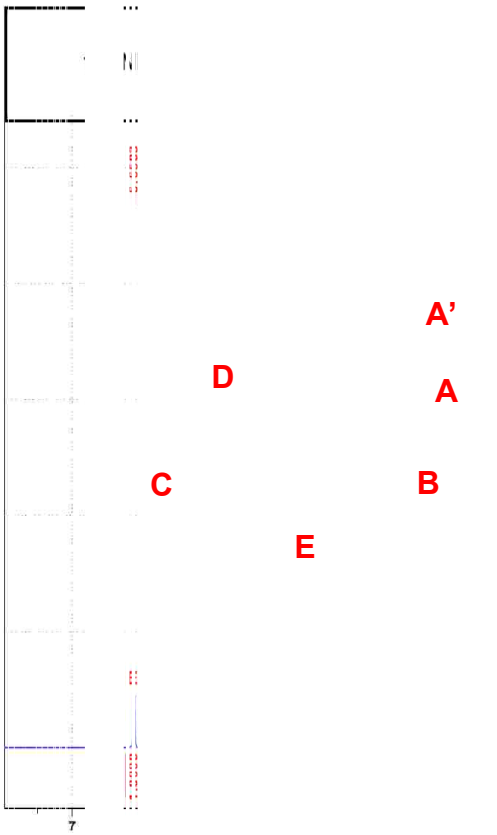

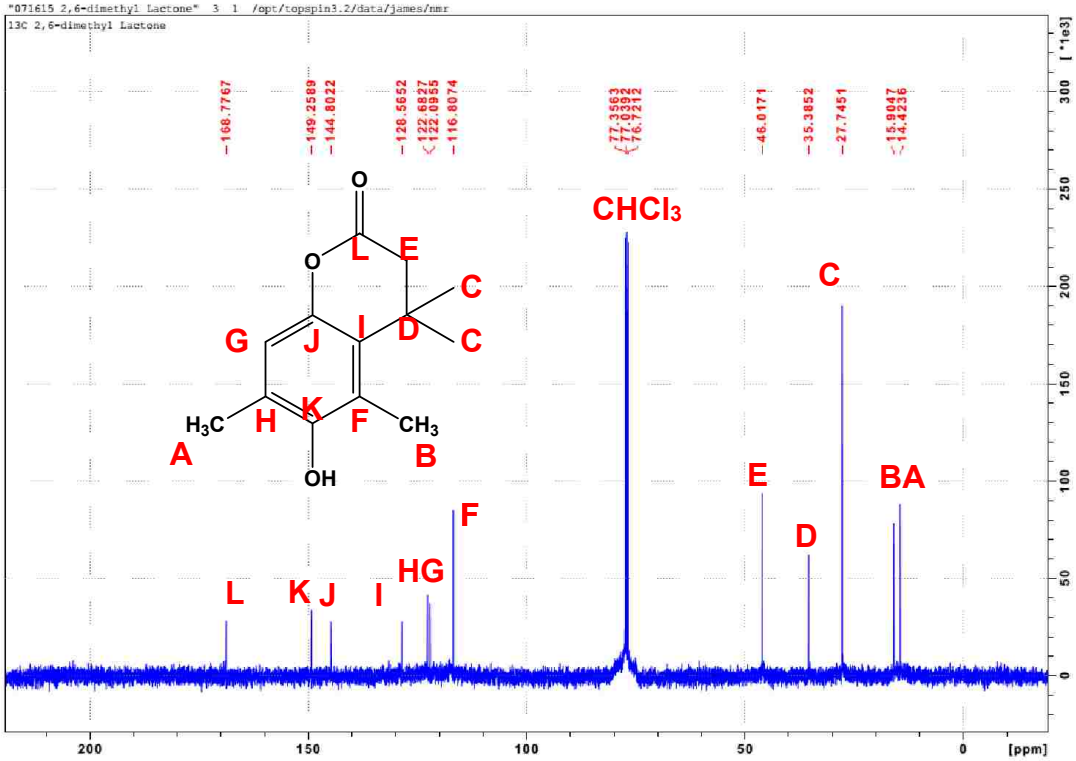

Appendix C-16. ESI-MS of di-methyl Lactone (5c)

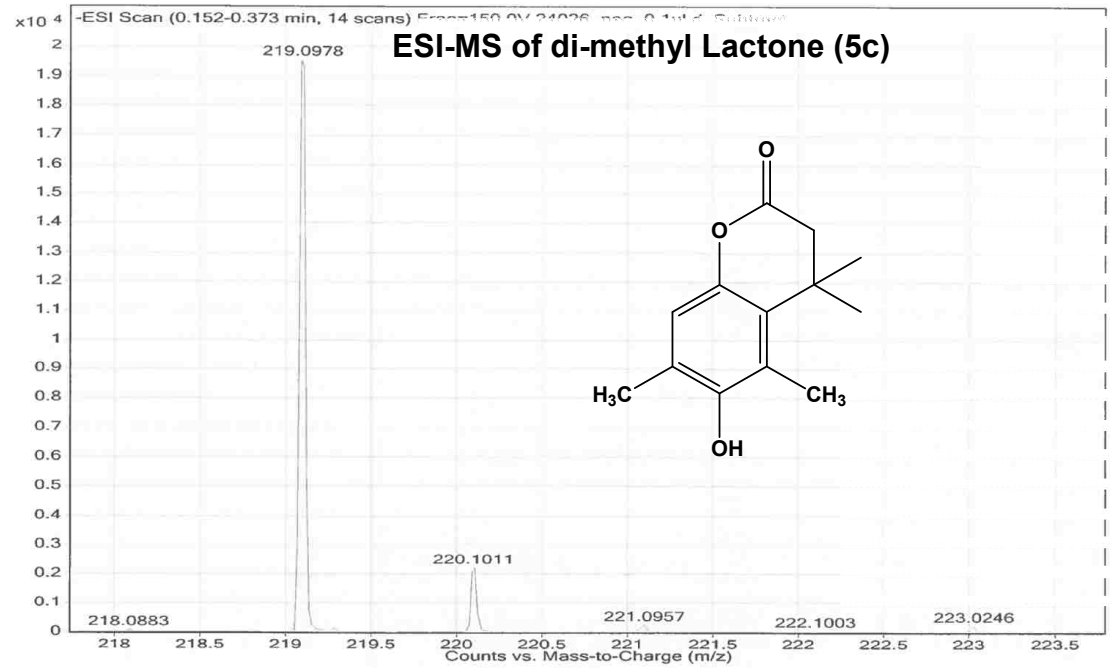

Appendix C-17. ^{1}H NMR and ESI-MS of Q_{Br}-Acid (6b)

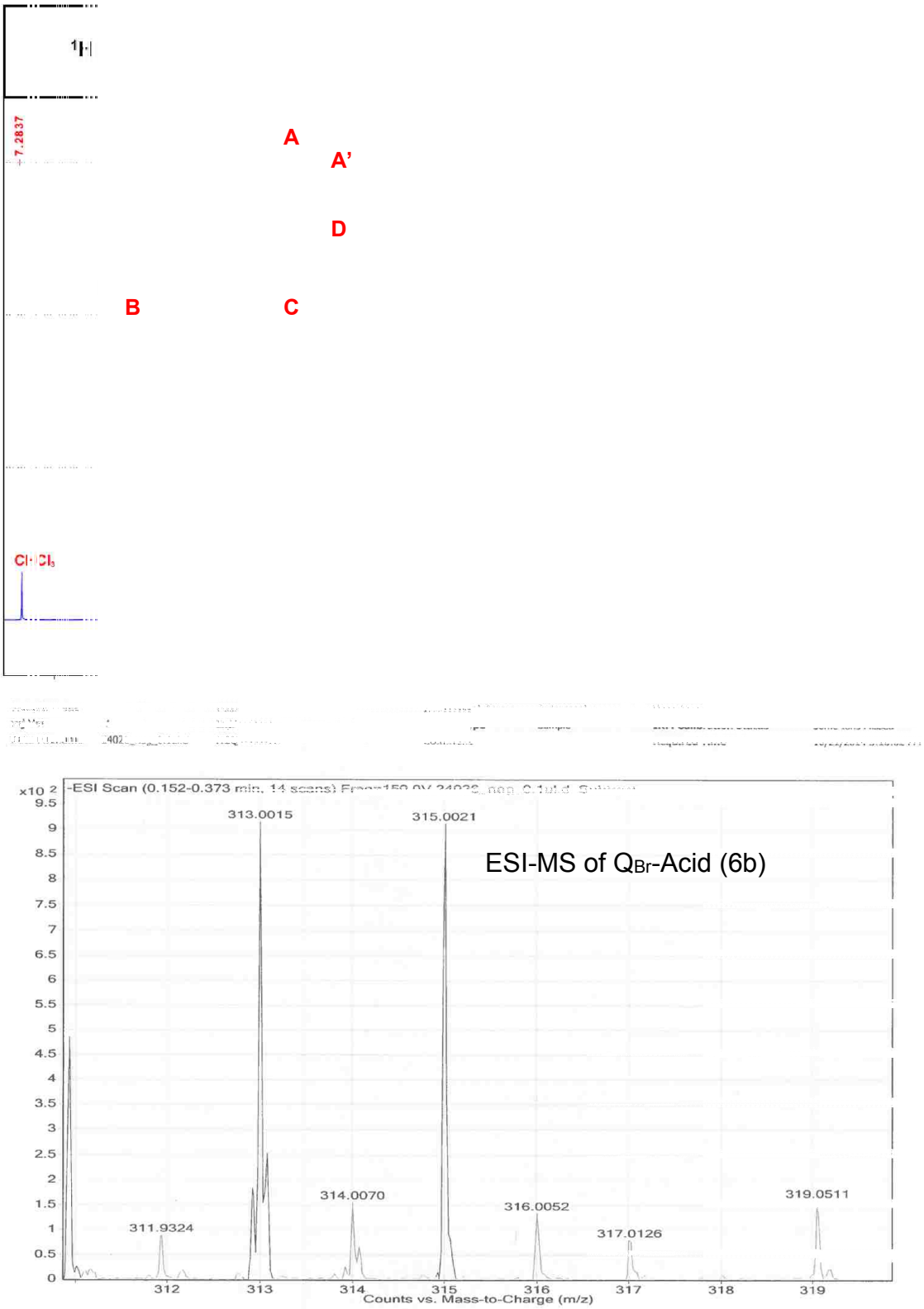

Appendix C-18. ^{1}H and ^{13}C NMR Spectra of Q_{Br}-NHS (7a)

^{1}H NMR Q_{Br}-NHS (7a)

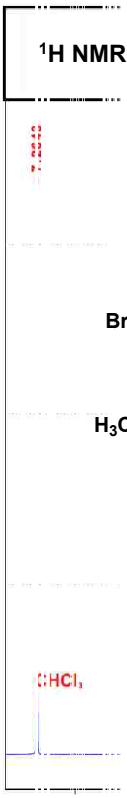

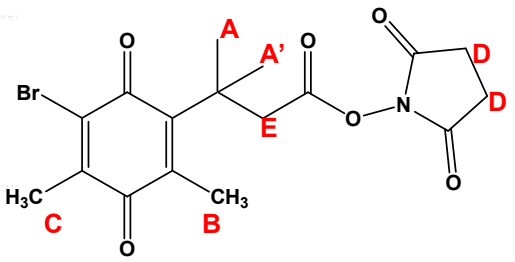

^{13}C DEPTQ135 NMR Q_{Br}-NHS (7a)

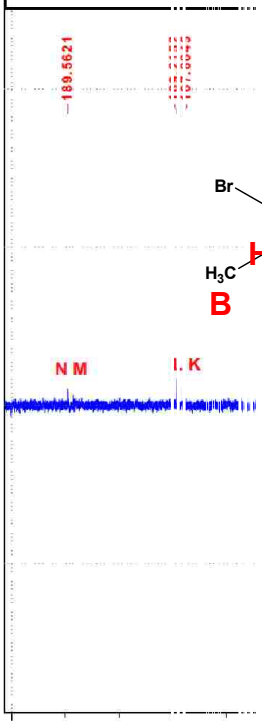

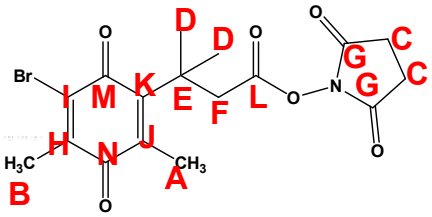

Appendix C-19. ESI-MS of Q_{Br}-NHS (7a)

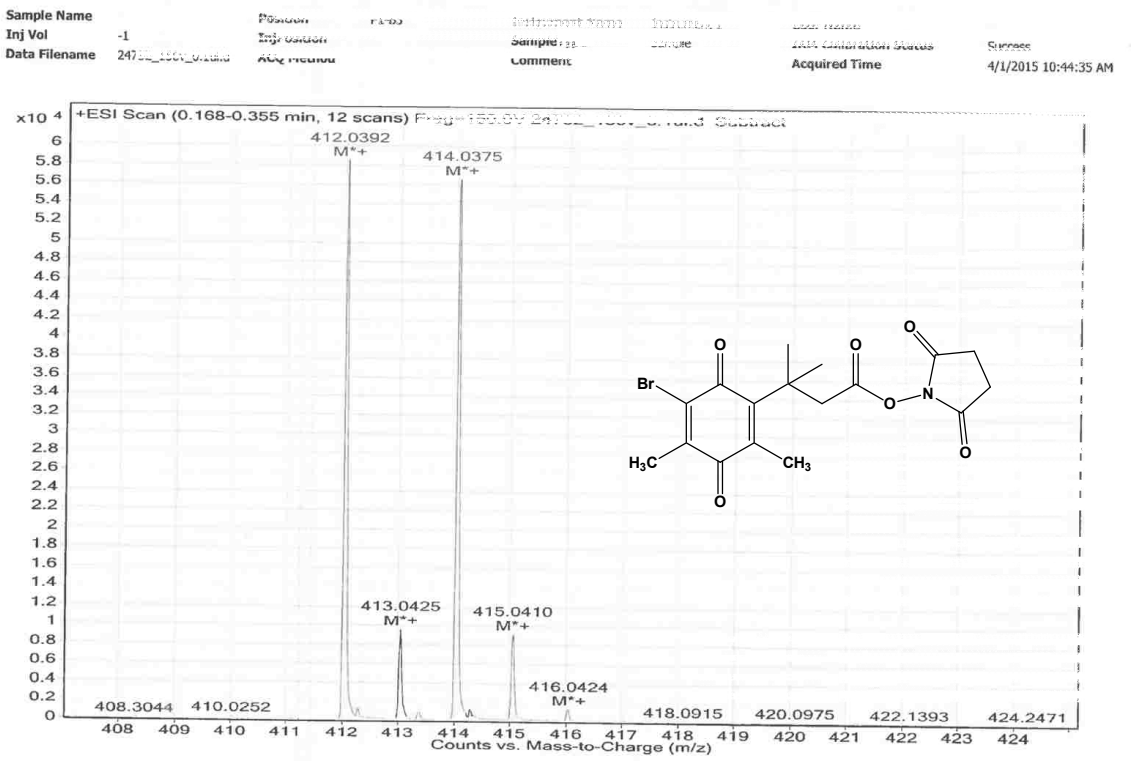

Appendix C-20. ^{1}H NMR Spectrum and ESI-MS of Q_{Br}-DOPE (8a)

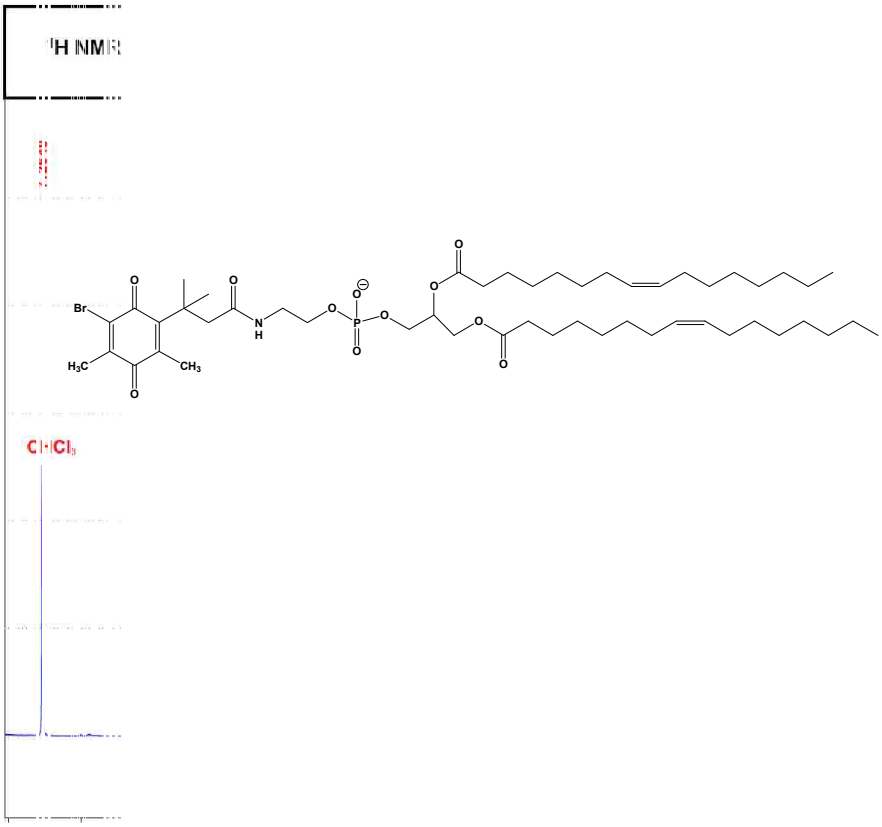

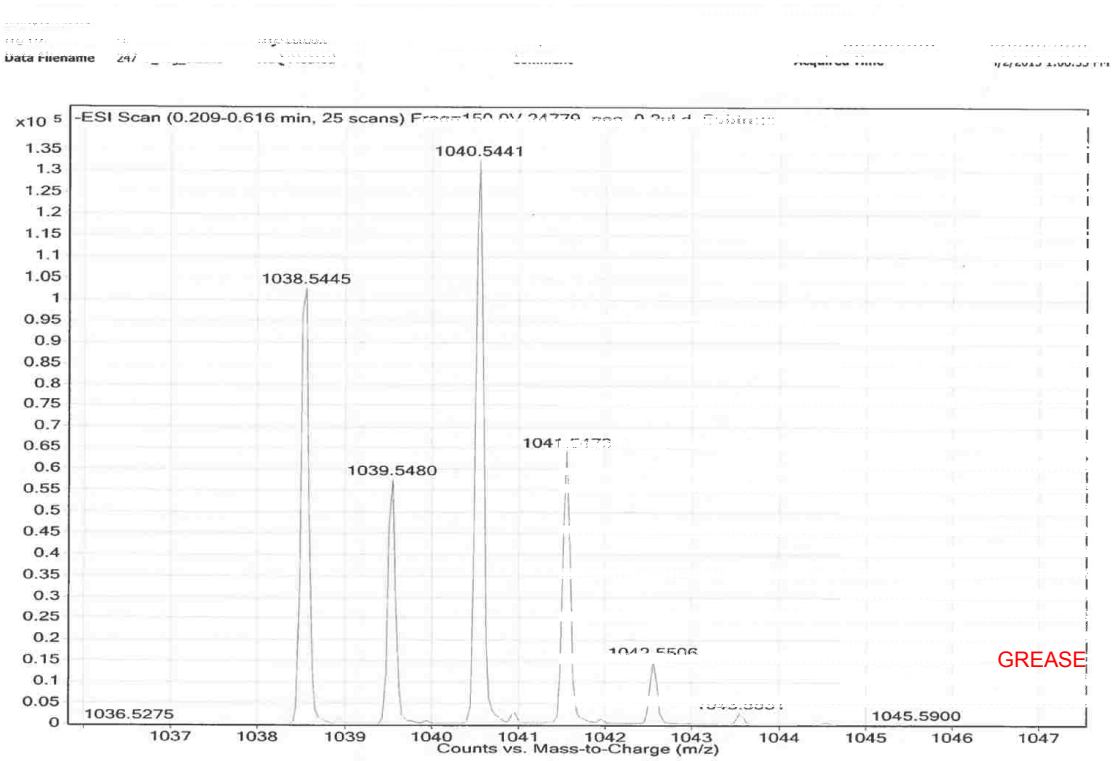

APPENDIX D DLS and ZETA POTENTIAL

Appendix D-21. DLS

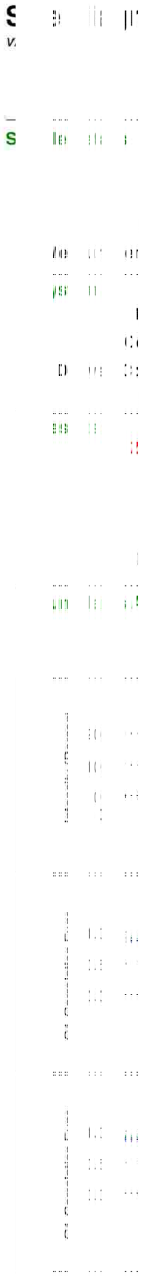

DLS						Mean		Area		
Type	Sample Name	T	Z-Ave	PdI	Diff. Coeff.	Pk 1	Pk 2	Pk 1 %	Pk 2 %	A. Count Rate
		°C	d.nm		μ²/s	d.nm	d.nm			kcps
Size	50 uM DOPG in PBS w/ EDTA	25	96.73	0.254	5.1	125.6	0	100	0	292
Size	50 uM DOPG in PBS w/ EDTA	25	106.4	0.188	4.64	128.1	0	100	0	251.4
Size	50 uM DOPG in PBS w/ EDTA	25	96.66	0.256	5.1	127.4	0	100	0	300
	Mean 1-3	25	99.93	0.233	4.95	127	0	100	0	281.1
	Std Dev	0	5.603	0.039	0.266	1.29	0	0	0	26.1
	RSD %	0	5.61	16.6	5.37	1.02	0	0	0	9.27
	Attenuator	8								
	Duration (s)	10								
	Duration Used (s)	60								
	Measurement Position	3								

Appendix D-22. Zeta Potential

APPENDIX E Q_{PA}-POPE

Appendix E-23. Q_{PA}-POPE LUVs: Content Release and Light Scattering

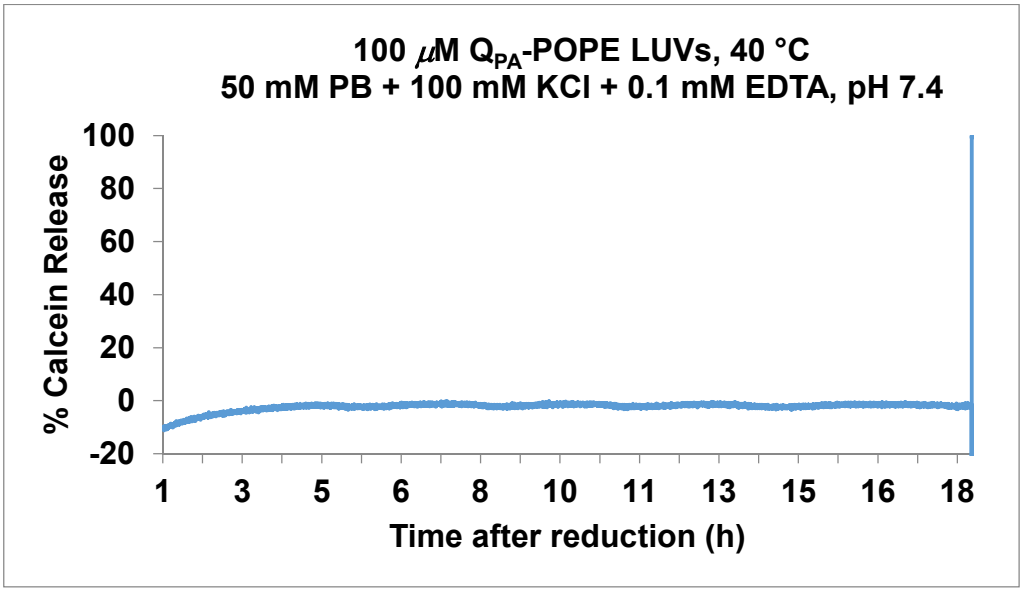

Q_{PA}-POPE Contents Release. Contents release curve of Q_{PA}-POPE LUVs dispersed in 100 mM KCl and 0.1 mM EDTA buffered with 50 mM phosphate pH 7.4 with calcein (40 mM) encapsulated inside.

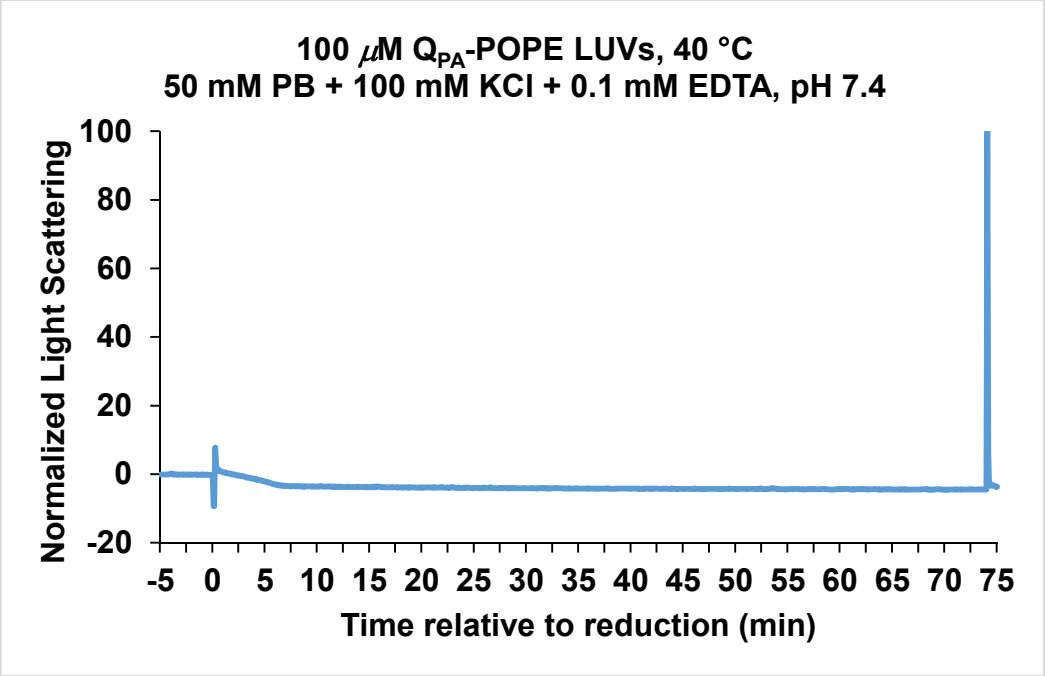

Q_{PA}-POPE Light Scattering. Light scattering of Q_{PA}-POPE LUVs dispersed in 100 mM KCl and 0.1 mM EDTA buffered with 50 mM phosphate pH 7.4 with calcein (40 mM) encapsulated inside.

VITA

James Winter was born in Dalton, Georgia. He received his Associate of Science from Dalton State College in 2008 and a Bachelor of Science in chemistry from The University of Georgia in 2010. He enrolled in the doctoral program in the Department of Chemistry at Louisiana State University in 2010 where he researched under the direction of Professor Robin L. McCarley. James is a candidate for the degree of Doctor of Philosophy to be conferred at the Winter 2015 Commencement.